ACS OMEGA

Article

Cite This: ACS Omega 2019, 4, 15255−15264

http://pubs.acs.org/journal/acsodf

Highlighting Thermodynamic Coupling Effects in Alcohol/Water Pervaporation across Polymeric Membranes

Rajamani Krishna*

Van 't Hoff Institute for Molecular Sciences, University of Amsterdam, Science Park 904, 1098 XH Amsterdam, The Netherlands

Supporting Information

ABSTRACT: The pervaporation of binary alcohol/water mixtures across polymeric membranes is modeled by combining the Maxwell−Stefan (M-S) diffusion formulation with the Flory−Huggins (F-H) description of sorption equilibrium. The combined M-S/F-H model shows that the flux of each penetrant species is coupled to the driving force of its partner penetrant. Two types of coupling contributions can be distinguished: (i) coupling arising out of correlated motions of penetrants in the polymer matrix and (ii) thermodynamic coupling. The focus of this article is on the contribution of thermodynamic coupling, which is quantified by the set of coefficients $\Gamma_{ij} = \frac{\phi_i}{\phi_j}\frac{\partial \ln a_i}{\partial \ln \phi_j}$, where a_i, the activity of species i, is dependent on the volume fractions ϕ_i,ϕ_j, of both penetrants in the polymeric membrane. Detailed analyses of published experimental data for pervaporation of ethanol/water feed mixtures of varying compositions in both hydrophobic (poly(dimethylsiloxane)) and hydrophilic (cellulose acetate, polyimide, and polyvinyl alcohol/polyacrylonitrile composite) membranes show that in all cases, the cross-coefficients Γ_{ij} $(i \neq j)$ are negative and may attain large magnitudes in relation to the diagonal elements Γ_{ii}. The net result is that the permeation fluxes of each penetrant are suppressed by its partner, resulting in mutual slowing down of permeation fluxes. If thermodynamic coupling effects are ignored, significantly higher fluxes are anticipated than those that are experimentally observed.

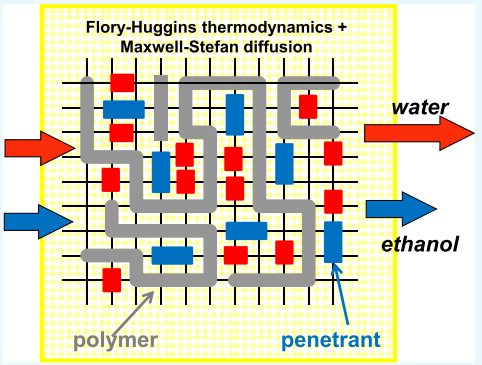

INTRODUCTION

Separations of alcohol/water mixtures by pervaporation across polymeric membranes are of industrial interest because of the high separation selectivities that are achievable.[1−9] Alcohol-selective separations are achievable with hydrophobic membranes such as poly(dimethylsiloxane) (PDMS).[3−5,10] With hydrophilic membranes (e.g., cellulose acetate (CA), polyimide, and poly(vinylalcohol)/polyacrylonitrile (PVA/PAN) composites), the separations are selective to water.[9,11−13] Water-selective separations are also achieved by exploiting size exclusion in hydrophobic perfluorinated polymer membranes.[14,15] For process development and design purposes, robust and accurate models are necessary for calculation of the permeation fluxes.

Chemical potential gradients, $d\mu_i/dz$, are the fundamentally correct driving forces for transport of penetrants across polymeric membranes.[6,16−18] The chemical potentials of the penetrants in the polymer matrix are most conveniently described by the Flory−Huggins (F-H) model that relates the component activities a_i to the volume fractions, ϕ_i.[8,19−21] For ternary mixtures of two penetrants (1, 2), and the polymer matrix (m), there are three interaction parameters in the F-H description of phase equilibrium: χ_{12}, χ_{1m}, and χ_{2m}. The F-H model for the component activities of the penetrants is written as follows[2,8,19,21]

$$\begin{aligned}\ln a_1 &= \ln(\phi_1) + (1-\phi_1) - \phi_2\frac{\overline{V}_1}{\overline{V}_2} - \phi_m\frac{\overline{V}_1}{\overline{V}_m} + (\chi_{12}\phi_2 + \chi_{1m}\phi_m)\\ &(\phi_2 + \phi_m) - \chi_{2m}\frac{\overline{V}_1}{\overline{V}_2}\phi_2\phi_m - u_1u_2\phi_2\frac{\partial\chi_{12}}{\partial u_2} - u_1u_2\phi_m\frac{\partial\chi_{1m}}{\partial u_2} - \phi_1\phi_m^2\frac{\partial\chi_{1m}}{\partial\phi_m}\\ &+ \frac{\overline{V}_1}{\overline{V}_2}u_2^2\phi_m\frac{\partial\chi_{2m}}{\partial u_1} - \frac{\overline{V}_1}{\overline{V}_2}\phi_2\phi_m^2\frac{\partial\chi_{2m}}{\partial\phi_m}\\ \ln a_2 &= \ln(\phi_2) + (1-\phi_2) - \phi_1\frac{\overline{V}_2}{\overline{V}_1} - \phi_m\frac{\overline{V}_2}{\overline{V}_m} + \left(\chi_{12}\phi_1\frac{\overline{V}_2}{\overline{V}_1} + \chi_{2m}\phi_m\right)\\ &(\phi_1 + \phi_m) - \chi_{1m}\frac{\overline{V}_2}{\overline{V}_1}\phi_1\phi_m + \frac{\overline{V}_2}{\overline{V}_1}u_1^2\phi_2\frac{\partial\chi_{12}}{\partial u_2} + \frac{\overline{V}_2}{\overline{V}_1}u_1^2\phi_m\frac{\partial\chi_{1m}}{\partial u_2}\\ &- \frac{\overline{V}_2}{\overline{V}_1}\phi_1\phi_m^2\frac{\partial\chi_{1m}}{\partial\phi_m} - u_1u_2\phi_m\frac{\partial\chi_{2m}}{\partial u_1} - \phi_2\phi_m^2\frac{\partial\chi_{2m}}{\partial\phi_m}\end{aligned} \tag{1}$$

In eq 1, $\overline{V}_i$ are the partial molar volumes, and we define

$$u_2 = \frac{\phi_2}{\phi_1+\phi_2};\quad u_1 = 1-u_2 = \frac{\phi_1}{\phi_1+\phi_2};\quad \phi_m = 1-(\phi_1+\phi_2)$$

In the Maxwell−Stefan (M-S) diffusion formulation, which is firmly rooted in the theory of irreversible thermodynamics,

Received: July 21, 2019
Accepted: August 22, 2019
Published: September 5, 2019

the volumetric permeation fluxes, N_i^V, expressed in $m^3\ m^{-2}\ s^{-1}$, are related to the chemical potential gradients as[16−18]

$$-\frac{\phi_1}{RT}\frac{d\mu_1}{dz} = \frac{(\phi_2 N_1^V - \phi_1 N_2^V)}{Đ_{12}^V} + \frac{\phi_m N_1^V}{Đ_{1m}^V}$$
$$-\frac{\phi_2}{RT}\frac{d\mu_2}{dz} = \frac{(\phi_1 N_2^V - \phi_2 N_1^V)}{Đ_{21}^V} + \frac{\phi_m N_2^V}{Đ_{2m}^V} \quad (2)$$

Detailed derivations of eq 2 are provided in the Supporting Information. Essentially, in the M-S model, the chemical potential driving force acting on a penetrant species (left member) is balanced by (i) friction with partner penetrant (first right member = 1−2 friction) and (ii) friction between the penetrant and the polymer matrix (second right member).[18] The molar flux of component i, expressed in mol $m^{-2}\ s^{-1}$, is $N_i^{molar} = \frac{N_i^V}{\overline{V_i}}$. The mass flux of component i, expressed as kg $m^{-2}\ s^{-1}$, is $N_i^{mass} = \rho_i^L N_i^V = M_i N_i^{molar}$, where ρ_i^L is the liquid-phase mass density of the pure component i, with molar mass M_i.

The M-S diffusivities for penetrant−membrane interactions, $Đ_{im}^V$, are often strongly influenced by the volume fractions of penetrants due to swelling[1,3,6,16]

$$Đ_{1m}^V = Đ_{1m}^V(0)\exp(\varepsilon_{11}\phi_1 + \varepsilon_{12}\phi_2);$$
$$Đ_{2m}^V = Đ_{2m}^V(0)\exp(\varepsilon_{21}\phi_1 + \varepsilon_{22}\phi_2) \quad (3)$$

In eq 3, ε_{11}, ε_{12}, ε_{21}, ε_{22} are termed plasticization coefficients. More detailed discussions on the interpretation of the magnitude, and signs, of ε_{ij} are available in the literature.[2,3,22,23]

The M-S diffusivities $Đ_{12}^V$ and $Đ_{21}^V = Đ_{12}^V\frac{\overline{V_1}}{\overline{V_2}}$ quantify the extent to which the mobilities of the penetrants are *correlated* to each other; correlation effects have the effect of slowing down the transport of the more mobile partners due to correlation motions with tardier partners in the polymer matrix.[17,18]

Let us define a 2 × 2 dimensional matrix $[\Lambda]$ whose elements are given by

$$\begin{bmatrix}\Lambda_{11} & \Lambda_{12}\\ \Lambda_{21} & \Lambda_{22}\end{bmatrix} = \frac{\begin{bmatrix} Đ_{1m}^V\left(\phi_m + \frac{\phi_1 Đ_{2m}^V}{Đ_{21}^V}\right) & Đ_{1m}^V\frac{\phi_1 Đ_{2m}^V}{Đ_{21}^V}\\ Đ_{2m}^V\frac{\phi_2 Đ_{1m}^V}{Đ_{12}^V} & Đ_{2m}^V\left(\phi_m + \frac{\phi_2 Đ_{1m}^V}{Đ_{12}^V}\right)\end{bmatrix}}{\phi_m\left(\frac{\phi_1 Đ_{2m}^V}{Đ_{21}^V} + \frac{\phi_2 Đ_{1m}^V}{Đ_{12}^V} + \phi_m\right)} \quad (4)$$

The ratios $\frac{Đ_{1m}^V}{Đ_{12}^V}$ and $\frac{Đ_{2m}^V}{Đ_{21}^V}$ quantify the *degrees of correlations*; only one of these is independent because $\frac{Đ_{1m}^V}{Đ_{12}^V} = \frac{Đ_{2m}^V}{Đ_{21}^V}\frac{Đ_{1m}^V}{Đ_{2m}^V}\frac{\overline{V_1}}{\overline{V_2}}$. We may estimate $Đ_{12}^V$ using the Vignes interpolation formula[24] for diffusion in binary liquid mixtures, adapted as follows[17]

$$(Đ_{12}^V/\overline{V_2}) = (Đ_{21}^V/\overline{V_1})$$
$$= (Đ_{1m}^V/\overline{V_2})^{\phi_1/(\phi_1+\phi_2)}(Đ_{2m}^V/\overline{V_1})^{\phi_2/(\phi_1+\phi_2)} \quad (5)$$

with the limiting scenarios

$$\phi_2 \to 0,\ Đ_{12}^V = Đ_{1m}^V; \quad \phi_1 \to 0,\ Đ_{21}^V = Đ_{2m}^V \quad (6)$$

Alternatively, the degree of correlations $\frac{Đ_{2m}^V}{Đ_{21}^V}$ may be fitted to match experimental data on mixture permeation.[18]

In the limiting scenario in which correlation effects are considered to be of negligible importance, i.e., $\frac{Đ_{1m}^V}{Đ_{12}^V} \to 0$; $\frac{Đ_{2m}^V}{Đ_{21}^V} \to 0$, the matrix $[\Lambda]$ simplifies to yield

$$\begin{bmatrix}\Lambda_{11} & \Lambda_{12}\\ \Lambda_{21} & \Lambda_{22}\end{bmatrix} = \frac{1}{\phi_m}\begin{bmatrix} Đ_{1m}^V & 0\\ 0 & Đ_{2m}^V\end{bmatrix} \quad (7)$$

Strictly speaking, we should expect eq 7 to hold when the volume fractions of both penetrants in the membrane are negligibly small.

The parameters on the left-hand side of eq 2 may be expressed in terms of gradients in the volume fractions by introducing a 2 × 2 dimensional matrix of thermodynamic correction factors $[\Gamma]$

$$\frac{\phi_i}{RT}\frac{d\mu_i}{dz} = \phi_i\frac{d\ln a_i}{dz} = \sum_{j=1}^{2}\Gamma_{ij}\frac{d\phi_j}{dz}; \quad \Gamma_{ij} = \frac{\phi_i}{\phi_j}\frac{\partial \ln a_i}{\partial \ln \phi_j};$$
$$i, j = 1, 2 \quad (8)$$

The four elements Γ_{ij} can be determined by the analytic differentiation of eq 1.

Combining eqs 2, 4, and 8, we derive an explicit expression for the volumetric fluxes as functions of the gradients in the volume fractions

$$\begin{pmatrix}N_1^V\\ N_2^V\end{pmatrix} = -\begin{bmatrix}\Lambda_{11} & \Lambda_{12}\\ \Lambda_{21} & \Lambda_{22}\end{bmatrix}\begin{bmatrix}\Gamma_{11} & \Gamma_{12}\\ \Gamma_{21} & \Gamma_{22}\end{bmatrix}\begin{pmatrix}\frac{d\phi_1}{dz}\\ \frac{d\phi_2}{dz}\end{pmatrix} \quad (9)$$

Under steady-state conditions, and assuming that the volume fraction profiles for both penetrants across the membrane layer are linear, the permeation fluxes across a membrane of thickness δ may be calculated explicitly as follows[17,18]

$$\begin{pmatrix}N_1^V\\ N_2^V\end{pmatrix} = \frac{\begin{bmatrix}\Lambda_{11} & \Lambda_{12}\\ \Lambda_{21} & \Lambda_{22}\end{bmatrix}}{\delta}\begin{bmatrix}\Gamma_{11} & \Gamma_{12}\\ \Gamma_{21} & \Gamma_{22}\end{bmatrix}\begin{pmatrix}\Delta\phi_1\\ \Delta\phi_2\end{pmatrix} \quad (10)$$

In eq 10, $\Delta\phi_i = \phi_{i0} - \phi_{i\delta}$; i = 1,2, where ϕ_{i0} and $\phi_{i\delta}$ are, respectively, the volume fractions at the upstream (subscript 0) and downstream (subscript δ) faces of the membrane; the volume fractions are in equilibrium with the bulk fluid mixtures in the contiguous compartments, determined from solution of the F-H equations as detailed in the Supporting Information. In the linearized approach, the elements of each of the two matrices $[\Lambda]$, and $[\Gamma]$ are evaluated at the arithmetic averaged volume fractions $\phi_{i,av} = \frac{(\phi_{i0} + \phi_{i\delta})}{2}$. The accuracy of the linearized eq 10 has been established in an earlier work.[18]

Except in the scenario in which the volume fractions of both penetrants are vanishingly small, i.e., $\phi_i \to 0$, each of the two square matrices $[\Lambda]$ and $[\Gamma]$ on the right-hand side of eq 10 will have significant off-diagonal elements; consequently, the flux of a penetrant is *coupled* to the driving force of its partner species. From eq 10, it is evident that there are two distinct and

DOI: 10.1021/acsomega.9b02255
ACS Omega 2019, 4, 15255−15264

separate contributions to coupled transports: (i) correlation effects, embodied in the off-diagonal elements of $[\Lambda]$ and (ii) thermodynamic coupling engendered by the off-diagonal elements of $[\Gamma]$. The significance of correlation effects has been highlighted in earlier published works.[3,13,16−18] The main focus of this article is on the significance of thermodynamic coupling effects in alcohol/water pervaporation.

As an illustration, Figure 1a presents calculations of Γ_{ij} for the ternary mixture ethanol(1)/water(2)/PDMS(m) at 313 K

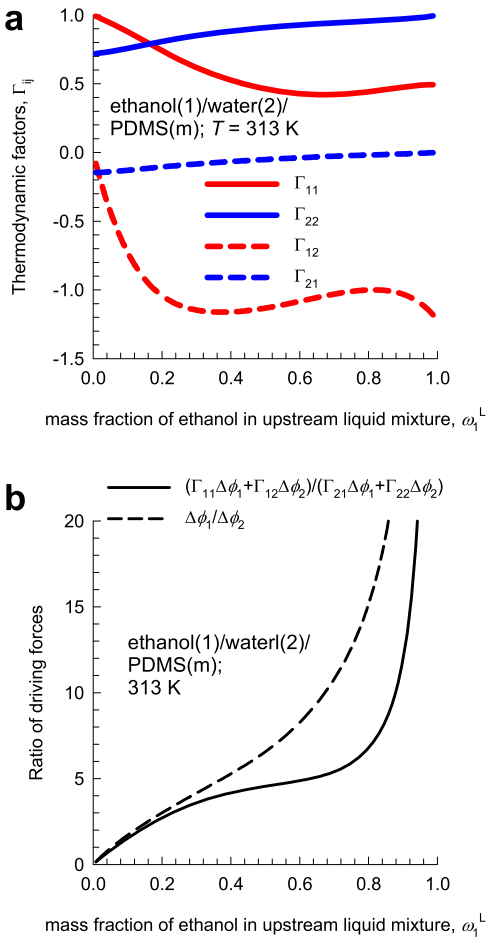

Figure 1. (a) Flory−Huggins calculations of the thermodynamic correction factors, Γ_{ij} for sorption equilibrium of ethanol (1) and water (2) in PDMS (m) at 313 K, plotted as a function of the mass fraction of ethanol in the liquid feed mixture in the upstream compartment ω_1^L. (b) The ratio of driving forces $(\Gamma_{11}\Delta\phi_1 + \Gamma_{12}\Delta\phi_2)/(\Gamma_{21}\Delta\phi_1 + \Gamma_{22}\Delta\phi_2)$, and $\Delta\phi_1/\Delta\phi_2$ plotted as a function of ω_1^L. For the calculations in (b), the elements Γ_{ij} are calculated at the averaged volume fractions $\phi_{i,av} = (\phi_{i0} + \phi_{i\delta})/2$, taking $\phi_{i\delta} \approx 0$. The F-H parameters and calculation details are provided in Table S2 of the Supporting Information.

for varying mass fractions of ethanol in the liquid feed mixture in the upstream compartment of the membrane, ω_1^L. Both the off-diagonal elements are negative; particularly noteworthy are the large negative values of Γ_{12}. The effective driving forces for membrane transport of penetrants ethanol, and water are, respectively, $\Gamma_{11}\Delta\phi_1 + \Gamma_{12}\Delta\phi_2$ and $\Gamma_{21}\Delta\phi_1 + \Gamma_{22}\Delta\phi_2$. The large negative value of Γ_{12} implies that the flux of ethanol, N_1^V, is strongly influenced, i.e., suppressed, by the driving force for water transport, $\Delta\phi_2 = (\phi_{20} - \phi_{2\delta})$. Although the off-diagonal element Γ_{21} has a small negative value, the flux of water, N_2^V, is also significantly influenced by the driving force for ethanol because $\Delta\phi_1 \gg \Delta\phi_2$ for hydrophobic PDMS. As an illustration of the strong influence of thermodynamic coupling, Figure 1b plots the ratio of driving forces $(\Gamma_{11}\Delta\phi_1 + \Gamma_{12}\Delta\phi_2)/(\Gamma_{21}\Delta\phi_1 + \Gamma_{22}\Delta\phi_2)$ as a function of ω_1^L. Also plotted in Figure 1b is the corresponding ratio if thermodynamic coupling effects are ignored, $\Delta\phi_1/\Delta\phi_2$. Neglect of thermodynamic coupling should be expected to have the effect of severely overestimating the ethanol/water permeation selectivity.

This article has threefold objectives. First, we aim to demonstrate that thermodynamic coupling effects are the root cause of mutual slowing-down effects that have been observed in the published experimental studies of Hietaharju et al.,[3] and Nasiri and Aroujalian[4] for ethanol/water pervaporation across PDMS membrane. The second objective is to show that the off-diagonal elements Γ_{12} and Γ_{21} also engender mutual slowing-down effects in hydrophilic (CA,[6,7] polyimide,[13] and PVA/PAN composite[11]) membranes. The third objective is to offer deeper physicochemical insights into membrane permeation fluxes and selectivities by delineating the separate influences of diffusion and thermodynamic coupling for each of the case studies that are analyzed.

To meet the set objectives of this article, we analyze ethanol/water pervaporation across four different polymeric membranes: PDMS, CA, polyimide, and PVA/PAN composite. The Supporting Information accompanying this publication provides: (i) the F-H model parameters used in the phase equilibrium calculations and (ii) input data on the M-S diffusivities.

RESULTS AND DISCUSSION

Analysis of Ethanol/Water/PDMS Permeation Data of Nasiri. Nasiri and Aroujalian[4] report experimental data for pervaporation of ethanol(1)/water(2) mixtures across PDMS membrane, measured at three different temperatures: T = 313, 323, and 333 K. In eqs 19 and 20 of Nasiri and Aroujalian,[4] used to model their own experiments, the M-S diffusivities are modified in the following manner to explicitly account for cluster formation leading to mutual slowing-down effects observed in their experiments:

$$Đ_{1m}^V = Đ_{1m}^V(0)\exp(\varepsilon_{11}\phi_1)\exp(-b_{11}\phi_1^2 - b_{12}\phi_1\phi_2)$$
$$Đ_{2m}^V = Đ_{2m}^V(0)\exp(\varepsilon_{21}\phi_1)\exp(-b_{22}\phi_2^2 - b_{21}\phi_1\phi_2) \quad (11)$$

The set of plasticization, and clustering, coefficients, along with the zero-occupancy diffusivities are fitted for each of the three experiment sets; see Table 2 of their paper. Below, we adopt a different approach for modeling their three sets of experiments, using the linearized eq 10, invoking the Vignes interpolation formula 5, along with eq 3 to describe the penetrant−membrane interactions. From sorption equilibrium, it is noted that the volume fractions of water, ϕ_2, in the membrane are about 1−2 orders of magnitude lower than that of ethanol, ϕ_1; therefore, the plasticization coefficients ε_{12}, ε_{22} are taken as zero. We use the same set of plasticization coefficients for all three sets of experiments: ε_{11} = 5; ε_{12} = 0; ε_{21} = 12; ε_{22} = 0. The fitted values of zero-occupancy M-S diffusivities are specified in Table S4 of the Supporting Information.

Two different scenarios A and B are used to model the Nasiri and Aroujalian experiments. The continuous solid lines in Figure 2a,b are obtained using scenario A, using eq 10, along with proper evaluation of Γ_{ij} using the F-H eqs 1; there is good

DOI: 10.1021/acsomega.9b02255
ACS Omega 2019, 4, 15255−15264

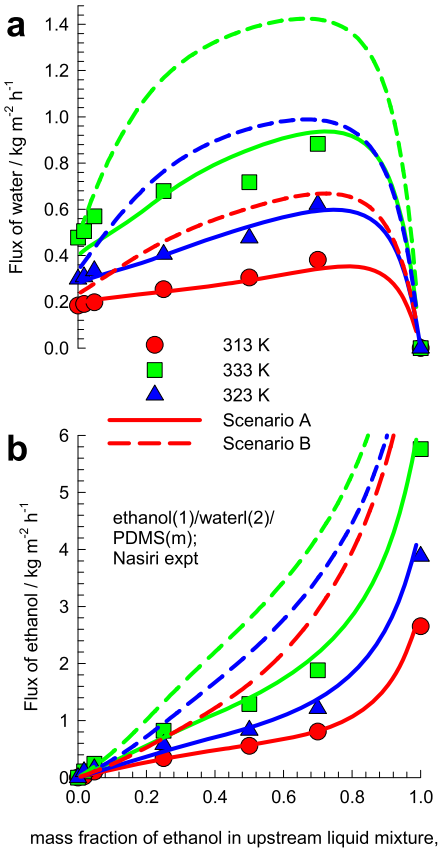

Figure 2. (a, b) Experimental data (indicated by symbols) of Nasiri and Aroujalian[4] for the mass pervaporation mass fluxes of penetrants ethanol (1) and water (2) across PDMS (m) at 313 K (red circles), 323 K (blue triangles), and 333 K (green squares), plotted as a function of the mass fraction of ethanol in the liquid feed mixture in the upstream compartment ω_1^L. The continuous solid lines are M-S model calculations (scenario A) using eqs 3, 5, and 10. The dashed lines are flux calculations in which thermodynamic correction factors are ignored (scenario B), i.e., $\Gamma_{ij} = \delta_{ij}$. The input F-H and diffusivity data are provided in Tables S2 and S4 of the Supporting Information.

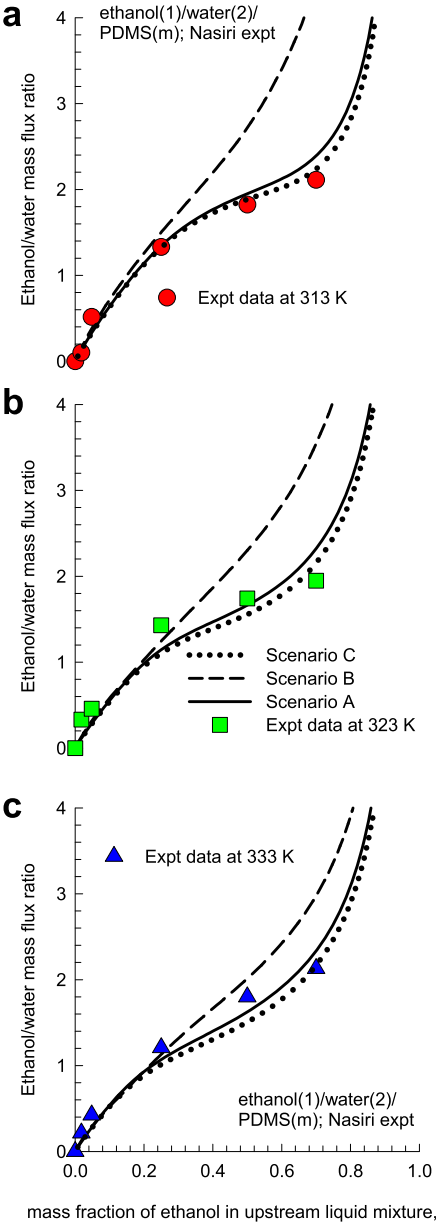

Figure 3. Ratio of the mass flux of ethanol to that of water for ethanol/water pervaporation across PDMS at (a) 313 K, (b) 323 K, and (c) 333 K, plotted as a function of the mass fraction of ethanol in the liquid feed mixture in the upstream compartment ω_1^L. Model calculations using three different scenarios A (continuous solid lines), B (dashed lines), and C (dotted lines) are compared to the experimental data (symbols) of Nasiri and Aroujalian.[4] The input diffusivity data are provided in the Supporting Information.

agreement with experimental data (indicated by the symbols). The dashed lines in Figure 2a,b are model calculations using scenario B, also using eq 10, but ignoring thermodynamic coupling contributions by invoking the assumption $\Gamma_{ij} = \delta_{ij}$, the Kronecker delta. The use of scenario B leads to overestimation of both ethanol and water fluxes. This leads us to conclude that the mutual slowing-down effects are engendered by thermodynamic coupling effects.

Further insights into the influence of negative cross-coefficients Γ_{12} and Γ_{21} are obtained by comparing the ratio of the mass fluxes of ethanol to water (see Figure 3). Ignoring thermodynamic coupling (scenario B) overestimates the ethanol/water flux ratios at all three temperatures. The influence of negative values of Γ_{12} and Γ_{21} is to suppress the flux of ethanol to a greater extent than that of water, leading to lower ethanol/water separation selectivity.

To elucidate the contribution of the correlation effects, and also the plasticization coefficients, ε_{ij}, we performed model calculations for scenario C in which (a) correlation effects are ignored, using eq 7, and (b) the influence of swelling is also ignored by setting $\varepsilon_{ij} = 0$. In scenario C, the ratio of fluxes is described by

$$\frac{N_1^V}{N_2^V} = \frac{Đ_{1m}^V(0)}{Đ_{2m}^V(0)} \frac{(\Gamma_{11}\Delta\phi_1 + \Gamma_{12}\Delta\phi_2)}{(\Gamma_{21}\Delta\phi_1 + \Gamma_{22}\Delta\phi_2)}; \quad \frac{N_1^{mass}}{N_2^{mass}} = \frac{\rho_1^L}{\rho_2^L}\frac{N_1^V}{N_2^V}; \quad \frac{N_1^{molar}}{N_2^{molar}} = \frac{N_1^V/\overline{V}_1}{N_2^V/\overline{V}_2} \tag{12}$$

Equation 12 is essentially the thermodynamically corrected driving flux ratio (cf. Figure 1b), multiplied by a constant factor. The dotted lines in Figure 3 represent model calculations of the ethanol/water mass flux ratios using eq 12. The agreement of scenario C with experiment is comparable to that of scenario A, which includes the effects

DOI: 10.1021/acsomega.9b02255
ACS Omega 2019, 4, 15255−15264

of both correlations and plasticization. Two separate conclusions can be drawn. First, correlation effects are of negligible importance for ethanol/water/PDMS permeation. Second, swelling effects do not influence permeation selectivities in the three sets of Nasiri experiments in which the ethanol mass fraction in the upstream membrane compartment was restricted to $\omega_1^L < 0.7$. Rather, swelling effects serve primarily to influence the magnitudes of the individual diffusivities $Đ_{im}^V$ and fluxes N_i^V.

Analysis of Ethanol/Water/PDMS Permeation Data of Hietaharju. Hietaharju et al.[3] report experimental data on the mass fluxes of the penetrants, N_i^{mass}, for pervaporation of ethanol/water mixtures with varying mass fractions of ethanol, ω_1^L, in the bulk liquid mixture in the upstream compartment at temperatures T = 313 and 333 K. They[3] also report experimental data for vapor permeation in which the ethanol/water vapor mixture, in equilibrium with an ethanol/water liquid-phase mixture at the corresponding dew point, is permeated across the membrane. The experimental data for the mass fluxes of ethanol and water are indicated by symbols in Figure 4a,b. The flux relations used by Hietaharju et al.[3] to model their own experiments do not account for thermodynamic coupling effects (see eqs 28 and 29 of their paper). Consequently, the match of their model predictions with experiments is extremely poor, especially for ethanol (see Figure 7 of their paper). We demonstrate that the poor match between experimental data and model is wholly ascribable to thermodynamic coupling effects.

The continuous solid lines in Figure 4a,b are model calculations using scenario A, as detailed in the foregoing section; the agreement is very good for all three data sets. We also confirmed that neglecting correlation effects and using eq 7 to calculate $[\Lambda]$ lead to nearly identical values of permeation fluxes; this leads us to conclude that the coupling effects arise solely from thermodynamic influences and not from correlated motions of penetrants in the polymer matrix.

The dashed lines in Figure 4a,b represent model calculations for scenario B in which thermodynamic coupling effects are ignored; both the fluxes of ethanol and water are higher than the estimations using scenario A. The explanation for the decrease in both fluxes is traceable to the negative off-diagonal elements Γ_{12} and Γ_{21}, as shown in Figure 1a.

Figure 5 plots the ratio of the mass fluxes of ethanol to water as a function of ω_1^L for the set of experiments at 313 K. The influence of negative values of Γ_{12} and Γ_{21} is to suppress the flux of ethanol to a greater extent, leading to lower ethanol/water separation selectivity; consequently, the flux ratios calculated using scenario A (continuous solid lines) are significantly lower than those calculated using scenario B (dashed lines). Ignoring thermodynamic coupling (scenario B) overestimates the ethanol/water flux ratios at all three temperatures.

To gauge the importance of the influence of plasticization, the dotted lines in Figure 5 present calculations for scenario C, wherein eq 12 is used to determine the flux ratios. The estimations of scenario C are slightly poorer than those for scenario A, especially for the ethanol mass fractions in the upstream membrane compartment $\omega_1^L > 0.5$. This suggests that plasticization influences the penetrant diffusivities to different extents; this influence manifests at higher penetrant occupancies in the membrane matrix.

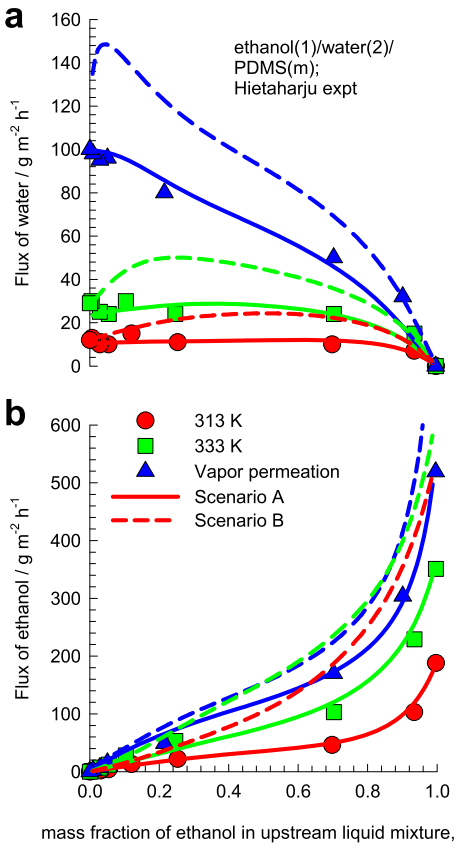

Figure 4. (a, b) Experimental data (indicated by symbols) of Hietaharju et al.[3] for the pervaporation mass fluxes of penetrants ethanol (1) and water (2) across PDMS (m) at 313 K (red circles) and 333 K (green squares), and vapor permeation (blue triangles), plotted as a function of the mass fraction of ethanol in the liquid feed mixture in the upstream compartment ω_1^L. The continuous solid lines are M-S model calculations (scenario A) using eqs 3, 5, and 10. The dashed lines are flux calculations in which thermodynamic correction factors are ignored (scenario B), i.e., $\Gamma_{ij} = \delta_{ij}$. The input F-H and diffusivity data are provided in Tables S2 and S3 of the Supporting Information.

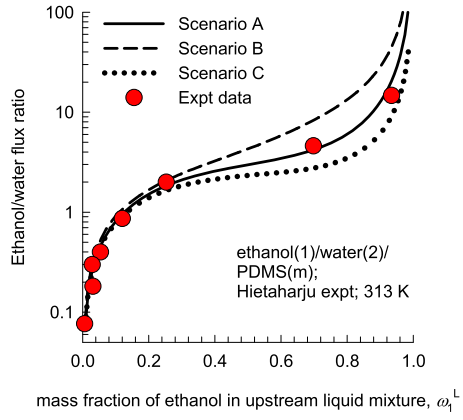

Figure 5. Ratios of the mass fluxes of ethanol to water for ethanol/water pervaporation across PDMS at 313 K plotted as a function of the mass fraction of ethanol in the liquid feed mixture in the upstream compartment ω_1^L. Model calculations using three different scenarios A (continuous solid lines), B (dashed lines), and C (dotted lines) are compared to experimental data (symbols) of Hietaharju et al.[3] The input diffusivity data are provided in Tables S2 and S3 of the Supporting Information.

DOI: 10.1021/acsomega.9b02255
ACS Omega 2019, 4, 15255−15264

Water/Ethanol Pervaporation across Hydrophilic Membranes. Figure 6a,b presents calculations of the ratios

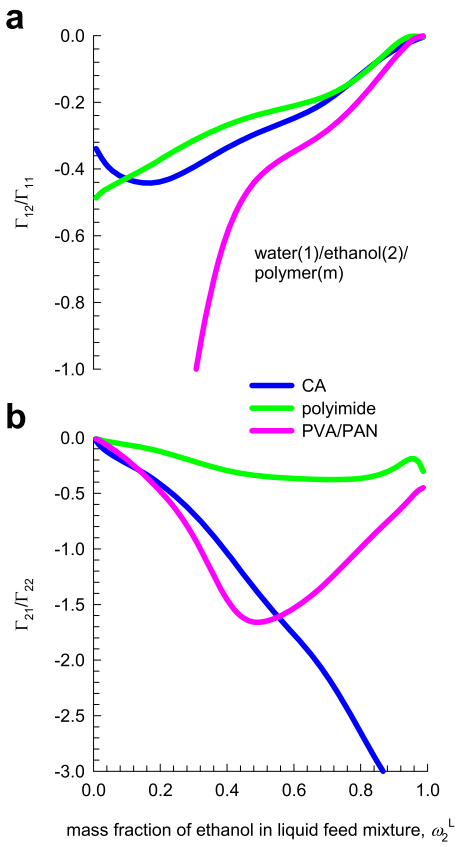

Figure 6. Flory–Huggins calculations of (a) Γ_{12}/Γ_{11} and (b) Γ_{21}/Γ_{22} for the sorption equilibrium of water (1) and ethanol (2) in CA (at 293.15 K), polyimide (at 293.15 K), and the PVA/PAN composite (at 333 K), plotted as a function of the mass fraction of ethanol in the liquid feed mixture in the upstream compartment ω_2^L. The F-H parameters and calculation details are provided in the Supporting Information.

Γ_{12}/Γ_{11} and Γ_{21}/Γ_{22} for sorption equilibrium between bulk water(1)/ethanol(2) liquid mixtures and three different hydrophilic membranes: CA, polyimide, and PVA/PAN. For all three membranes, the two ratios are negative and we should anticipate that thermodynamic coupling would engender mutual slowing-down effects. For hydrophilic membranes, correlation effects should also be expected to be of significance because the more mobile penetrant, water, also has the higher permeation flux. These two anticipated results are tested below using three case studies.

We first performed pervaporation flux calculations for water(1)/ethanol(2)/CA (m) using the F-H and M-S diffusivity data provided by Mulder et al.,[6,7] who established that swelling effects are important and the experimental data could be adequately described by choosing $\varepsilon_{11} = \varepsilon_{12} = \varepsilon_{21} = \varepsilon_{22} = 7.3$.

The continuous solid lines in Figure 7a are flux calculations using scenario A. The negative off-diagonal elements Γ_{12} and Γ_{21} cause both water and ethanol fluxes to be reduced below the values anticipated by scenario B, i.e., by invoking the simplification $\Gamma_{ij} = \delta_{ij}$.

To gauge the importance of correlation effects, Figure 7b compares the water/ethanol flux ratios for three additional

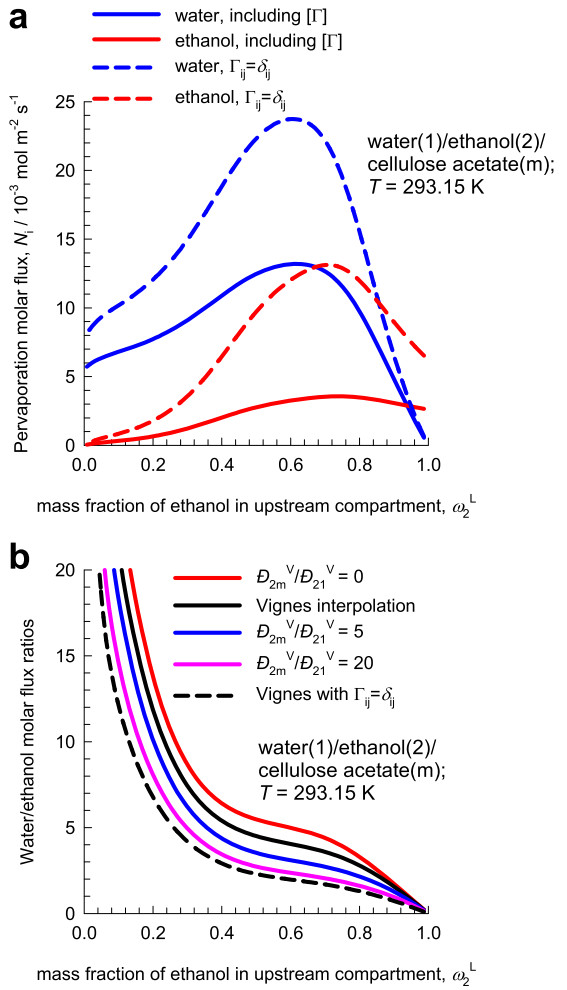

Figure 7. (a) Molar fluxes of water (1) and ethanol (2) across CA membrane as a function of the mass fraction of ethanol in the liquid feed mixture in the upstream compartment, ω_2^L. The continuous solid lines are M-S model calculations (scenario A) using eqs 3, 5, and 10. The dashed lines are flux calculations in which thermodynamic correction factors are ignored (scenario B), i.e., $\Gamma_{ij} = \Gamma_{ij}$. (b) Influence of varying degrees of correlation on the water/ethanol flux ratios. The Flory–Huggins and diffusivity data are provided in Table S5 of the Supporting Information.

scenarios to estimate the degree of correlations, $\frac{Đ_{2m}^V}{Đ_{21}^V}$, besides the Vignes interpolation formula 5: $\frac{Đ_{2m}^V}{Đ_{21}^V} = 0$, $\frac{Đ_{2m}^V}{Đ_{21}^V} = 5$, and $\frac{Đ_{2m}^V}{Đ_{21}^V} = 20$. The assertion $\frac{Đ_{2m}^V}{Đ_{21}^V} = 0$ essentially implies the use of eq 7 for flux calculations. With increasing degrees of correlation, the water/ethanol flux ratio decreases, due to increasing retardation of the mobile penetrant water. The dashed line in Figure 7b represents water/ethanol flux ratios ignoring thermodynamic coupling; this shows that the influence of the negative off-diagonal elements Γ_{12} and Γ_{21} is to reduce the flux of ethanol more than the flux of water. The reasoning for this is that the magnitude of Γ_{21}/Γ_{22} is larger than that of Γ_{12}/Γ_{11}. Consequently, we should expect thermodynamic coupling effects influence the ethanol flux to a greater extent than the water flux.

Figure 8a,b compares experimental data[11] on the molar fluxes for pervaporation of water/ethanol mixtures across PVA/PAN composite membrane at 333 K, with calculations

DOI: 10.1021/acsomega.9b02255
ACS Omega 2019, 4, 15255−15264

(indicated by the continuous solid lines) based on scenario A, in which the degree of correlations is quantified as $\frac{Đ_{2m}^{V}}{Đ_{21}^{V}} = 3$, along with the choice $\varepsilon_{11} = \varepsilon_{12} = \varepsilon_{21} = \varepsilon_{22} = 5$. If thermodynamic coupling effects are ignored and $\Gamma_{ij} = \delta_{ij}$ (scenario B calculations shown by the dashed lines), the match with experiments is significantly worse, and both water and ethanol fluxes are overestimated to a significant extent.

In Figure 8c, the experimentally determined water/ethanol fluxes ratios are compared to M-S model flux calculations using three different degrees of correlations: $\frac{Đ_{2m}^{V}}{Đ_{21}^{V}} = 0.2$, $\frac{Đ_{2m}^{V}}{Đ_{21}^{V}} = 3$, and $\frac{Đ_{2m}^{V}}{Đ_{21}^{V}} = 20$. The flux ratios reduce by more than 1 order of magnitude with increasing degree of correlations.

Figure 9a,b compares the experimental data[13] on volumetric fluxes for pervaporation of water/ethanol mixtures across a polyimide membrane with model calculations based on scenarios A and B. There is good agreement between the experimental data and scenario A in which the degree of correlations is described by $\frac{Đ_{2m}^{V}}{Đ_{21}^{V}} = 3$, along with $\varepsilon_{11} = \varepsilon_{12} = \varepsilon_{21} = \varepsilon_{22} = 2$. Use of scenario B, invoking $\Gamma_{ij} = \delta_{ij}$, leads to overestimation of both fluxes. To gauge the significance of correlations, Figure 9c compares the experimentally determined water/ethanol fluxes ratios with model calculations using scenario A to that of scenario C (using eq 12). Ignoring correlations has the effect of overestimating the water/ethanol selectivities by about an order of magnitude.

For all three cases studies on hydrophilic membranes analyzed above, the influence of swelling serves to enhance the diffusivities of either penetrant, but does not influence water/ethanol selectivities. On the other hand, the influence of thermodynamic coupling effects is to lower both water and ethanol fluxes, reducing the flux of ethanol more than the flux of water. In other words, the influence of swelling does not completely nullify the influence of thermodynamic coupling.

General Applicability of the M-S Model for Describing Membrane Permeation. In addition to the five different case studies discussed above, the applicability of the Maxwell–Stefan model eq 2 has been established for a number of other membrane permeation experimental studies.

For ethanol/water permeation across PDMS membrane, Aguilar-Valencia et al.[10] use the M-S formulation to rationalize coupling between ethanol and water fluxes observed in their experiments. Experimental data on ethanol/water pervaporation across silicone rubber membranes are amenable to quantitative modeling with the M-S formulation.[25,26] Ebneyamini et al.[5] use the M-S formulation to model their experiments for dehydration of aqueous butanol solutions using hydrophobic membranes. However, thermodynamic coupling effects are not of significant importance because the experiments were conducted with dilute aqueous solutions for which both $\Gamma_{12} \approx 0$ and $\Gamma_{21} \approx 0$. Izák et al.[27,28] establish the applicability of the M-S formulation for a near-quantitative description of the pervaporation of 1-alcohol/toluene mixtures across low-density polyethylene membranes.

Mutual slowing-down effects are not restricted to pervaporation processes; they also manifest for permeation of gaseous CO_2/C_2H_6 across a cross-linked polyethylene oxide (XLPEO) membrane.[16−18] The M-S model eq 2, with proper accounting of both thermodynamic coupling and correlation effects, is required for quantitative modeling of the experimental data;

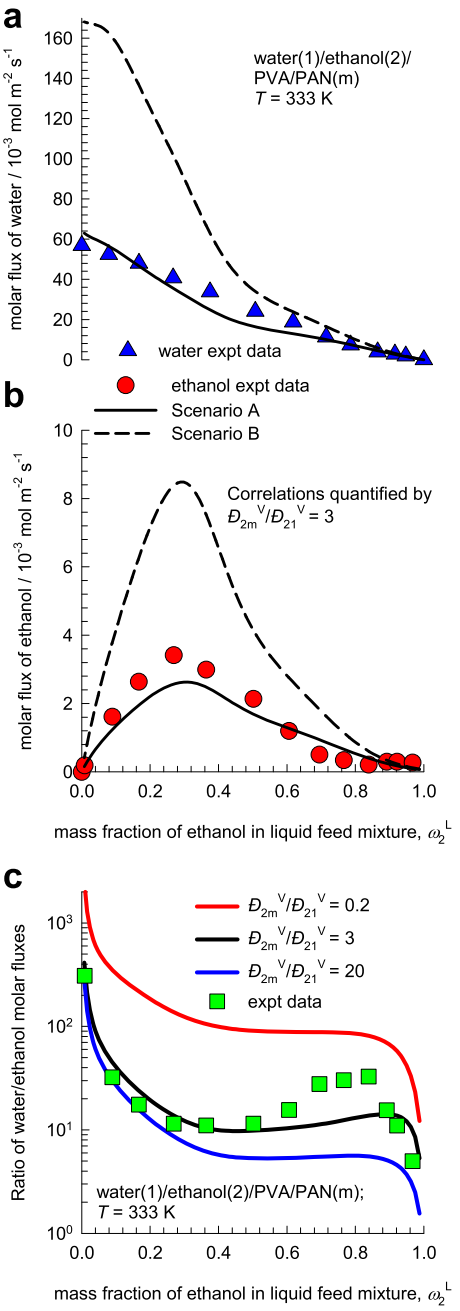

Figure 8. (a, b) Molar pervaporation fluxes for permeation of water (1)/ethanol (2) mixtures across PVA/PAN composite membrane (m) at 333 K, plotted as a function of the mass fraction of ethanol in the liquid feed mixture in the upstream compartment ω_2^L. The experimental data of Heintz and Stephan[11] (indicated by symbols) are compared to the model calculations using scenarios A and B. (c) Comparison of experimentally determined water/ethanol molar flux ratios with calculations using different degrees of correlations. The Flory–Huggins and diffusivity data are provided in Table S7 of the Supporting Information.

see Figures S14–S17 of the Supporting Information for details of analysis. Genduso et al.[29] use an analogous approach to model coupling effects in CO_2/CH_4 permeation across the XLPEO membrane.

The M-S formulation is used to describe coupling effects during water/alcohol permeation across both hydrophilic and hydrophobic zeolite membranes,[30] for which experimental

DOI: 10.1021/acsomega.9b02255
ACS Omega 2019, 4, 15255−15264

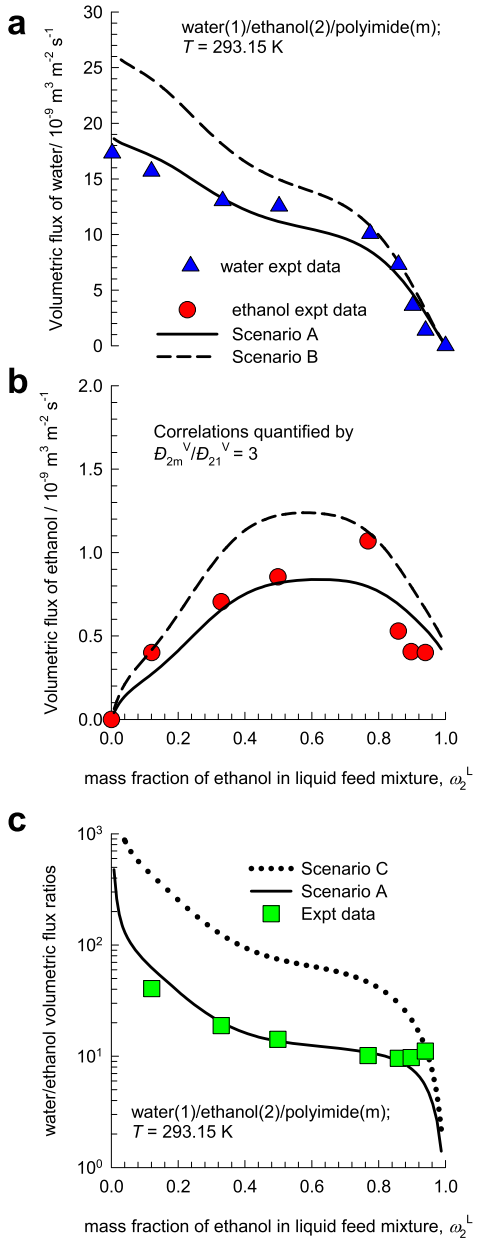

Figure 9. (a, b) Volumetric fluxes for permeation of water (1)/ethanol (2) mixtures across polyimide membrane, plotted as a function of the mass fraction of ethanol in the liquid feed mixture in the upstream compartment ω_2^L. The experimental data of Ni et al.[13] (indicated by symbols) are compared to the model calculations using scenarios A and B. (c) Comparison of experimentally determined water/ethanol volumetric flux ratios (shown by the symbols) with the model calculations using scenarios A (continuous solid lines) and C (dotted lines). The Flory–Huggins and diffusivity data are provided in Table S6 of the Supporting Information.

studies[31−33] demonstrate the occurrence of mutual slowing-down effects.

CONCLUSIONS

Published experimental data for alcohol/water pervaporation across both hydrophobic (PDMS) and hydrophilic (CA, polyimide, PVA/PAN) membranes are modeled by combining the Flory–Huggins description of sorption equilibrium with the Maxwell–Stefan diffusion formulation. For steady-state permeation, this combination results in eq 10, in which the matrices $[\Lambda]$ and $[\Gamma]$ reflect, respectively, the diffusivity and thermodynamic contributions. In general, each of these matrices contains off-diagonal contributions; as a result, the fluxes of alcohol and water are coupled to each other. The following major conclusions emerge from our analysis.

(1) For alcohol/water pervaporation across hydrophobic and hydrophilic membranes, the off-diagonal elements Γ_{12} and Γ_{21} are both negative in all of the cases examined. Consequently, the effective driving forces for penetrant transport are strongly influenced.

(2) For both hydrophobic and hydrophilic membranes, the influence of thermodynamic coupling is to suppress the flux of both penetrants, leading to mutual slowing down. For hydrophobic membranes, the flux of ethanol is reduced to a greater extent, resulting in lower ethanol/water selectivity. On the other hand, for hydrophilic membranes, the water/ethanol selectivity is enhanced by the contribution of the negative off-diagonal elements Γ_{12} and Γ_{21}.

(3) For hydrophobic PDMS membranes, correlation effects appear to be of negligible importance because more mobile water is practically excluded from the polymer matrix. In sharp contrast, for hydrophilic membranes, correlation effects serve to reduce water/ethanol selectivities to a significant extent due to retardation of water transport.

(4) While membrane swelling has the effect of influencing the magnitudes of the penetrant diffusivities, the corresponding influence on pervaporation selectivities is of minor importance for both hydrophobic and hydrophilic membranes.

(5) The distinction between swelling effects and thermodynamic coupling effects can be summarized as follows: swelling influences diffusivities, whereas the off-diagonal elements of the matrix of thermodynamic correction factors influence the driving forces for transport of penetrants.

ASSOCIATED CONTENT

Supporting Information

The Supporting Information is available free of charge on the ACS Publications website at DOI: 10.1021/acsomega.9b02255.

Detailed derivation of the Maxwell–Stefan equations, the F-H model parameters used in the phase equilibrium calculations, and input data on the M-S diffusivities (PDF)

AUTHOR INFORMATION

Corresponding Author

*E-mail: r.krishna@contact.uva.nl.

ORCID

Rajamani Krishna: 0000-0002-4784-8530

Notes

The author declares no competing financial interest.

ACKNOWLEDGMENTS

The author acknowledges the constructive remarks and suggestions of one of the reviewers.

DOI: 10.1021/acsomega.9b02255
ACS Omega 2019, 4, 15255−15264

NOMENCLATURE

Latin Alphabet

a_i activity of species i, dimensionless
$Đ_{ij}^{V}$ modified M-S diffusivity for binary penetrant pair $i-j$, $m^2\ s^{-1}$
$Đ_{im}^{V}$ modified M-S diffusivity for penetrant i in polymer m, $m^2\ s^{-1}$
M_i molar mass of species i, kg mol^{-1}
$\overline{M}$ mean molar mass of mixture, kg mol^{-1}
N_i^{molar} molar flux of species i, mol $m^{-2}\ s^{-1}$
N_i^{mass} molar flux of species i, kg $m^{-2}\ s^{-1}$
N_i^{V} volumetric flux of species i, $m^3\ m^{-2}\ s^{-1}$
R gas constant, 8.314 J $mol^{-1}\ K^{-1}$
T absolute temperature, K
$u_2 = \frac{\varphi_2}{\varphi_1+\varphi_2}$ relative volume fractions in polymer phase, dimensionless
$\overline{V}_i$ partial molar volume of species i, $m^3\ mol^{-1}$
$\overline{V}$ molar volume of mixture, $m^3\ mol^{-1}$
z distance coordinate along membrane thickness, m

Greek Alphabet

Γ_{ij}, thermodynamic factors, dimensionless
$[\Gamma]$, matrix of thermodynamic factors, dimensionless
δ, thickness of membrane, m
δ_{ij}, Kronecker delta, dimensionless
ε_{ij}, plasticization coefficient, dimensionless
$[\Lambda]$, matrix of Maxwell–Stefan diffusivities, $m^2\ s^{-1}$
μ_i, molar chemical potential, J mol^{-1}
ϕ_i, volume fraction of penetrant i in polymer, dimensionless
ϕ_m, volume fraction of polymer, dimensionless
ϕ_i^L, volume fraction in bulk liquid mixture, dimensionless
ρ_i, mass density of component i, kg m^{-3}
χ, interaction parameter in Flory–Huggins model, dimensionless
ω_i^L, mass fraction of component i in liquid-phase feed mixture, dimensionless

Subscripts

i, referring to penetrant i
m, referring to membrane
0, upstream face of membrane, $z = 0$
δ, upstream face of membrane, $z = \delta$

REFERENCES

(1) Shao, P.; Huang, R. Y. M. Polymeric membrane pervaporation. *J. Membr. Sci.* **2007**, *287*, 162–179.
(2) Yang, T.-H.; Lue, S. J. Coupled concentration-dependent diffusivities of ethanol/water mixture sthrough a polymericmembrane:Effect on pervaporative flux and diffusivity profiles. *J. Membr. Sci.* **2013**, *443*, 1–9.
(3) Hietaharju, J.; Kangas, J.; Tanskanen, J. Analysis of the permeation behavior of ethanol/water mixtures through a polydimethylsiloxane (PDMS) membrane in pervaporation and vapor permeation conditions. *Sep. Purif. Technol.* **2019**, *227*, No. 115738.
(4) Nasiri, H.; Aroujalian, A. A Novel Model Based on Cluster Formation for Pervaporation Separation of Polar Components from Aqueous Solutions. *Sep. Purif. Technol.* **2010**, *72*, 13–21.
(5) Ebneyamini, A.; Azimi, H.; Thibault, J.; Tezel, F. H. Description of butanol aqueous solution transport through commercial PDMS pervaporation membrane using extended Maxwell–Stefan model. *Separ. Sci. Technol.* **2018**, *53*, 1611–1627.
(6) Mulder, M. H. V.; Smolders, C. A. On the Mechanism of Separation of Ethanol/Water Mixtures by Pervaporation. I. Calculation of Concentration Profiles. *J. Membr. Sci.* **1984**, *17*, 289–307.
(7) Mulder, M. H. V.; Franken, A. C. M.; Smolders, C. A. On the Mechanism of Separation of Ethanol/Water Mixtures by Pervaporation. II. Experimental Concentration Profiles. *J. Membr. Sci.* **1985**, *23*, 41–58.
(8) Mulder, M. H. V.; Franken, A. C. M.; Smolders, C. A. Preferential Sorpton versus Preferential Permeability in Pervaporation. *J. Membr. Sci* **1985**, *22*, 155–178.
(9) Mulder, M. H. V.; Smolders, C. A.; et al. Ethanol-water separation by pervaporation. *J. Membr. Sci* **1983**, *16*, 269–284.
(10) Aguilar-Valencia, D. M.; Gómez-García, M. A.; Fontalvo, J. Effect of pH, CO_2, and High Glucose Concentrations on Polydimethylsiloxane Pervaporation Membranes for Ethanol Removal. *Ind. Eng. Chem. Res.* **2012**, *51*, 9328–9334.
(11) Heintz, A.; Stephan, W. A generalized solution-diffusion model of the pervaporation process through composite membranes Part II. Concentration polarization, coupled diffusion and the influence of the porous support layer. *J. Membr. Sci.* **1994**, *89*, 153–169.
(12) Heintz, A.; Stephan, W. A generalized solution-diffusion model of the pervaporation process through composite membranes Part I. Prediction of mixture solubilities in the dense active layer using the UNIQUAC model. *J. Membr. Sci.* **1994**, *89*, 143–151.
(13) Ni, X.; Sun, X.; Ceng, D.; Hua, F. Coupled Diffusion of Water and Ethanol in a Polyimide Membrane. *Polym. Eng. Sci.* **2001**, *41*, 1440–1447.
(14) Smuleac, V.; Wu, J.; Nemser, S.; Majumdar, S.; Bhattacharyya, D. Novel perfluorinated polymer-based pervaporation membranes for the separation of solvent/water mixtures. *J. Membr. Sci.* **2010**, *352*, 41–49.
(15) Tang, J.; Sirkar, K. K. Perfluoropolymer membrane behaves like a zeolite membrane in dehydration of aprotic solvents. *J. Membr. Sci.* **2012**, *421–422*, 211–216.
(16) Ribeiro, C. P.; Freeman, B. D.; Paul, D. R. Modeling of Multicomponent Mass Transfer across Polymer Films using a Thermodynamically Consistent Formulation of the Maxwell-Stefan Equations in terms of Volume Fractions. *Polymer* **2011**, *52*, 3970–3983.
(17) Krishna, R. Describing Mixture Permeation across Polymeric Membranes by a Combination of Maxwell-Stefan and Flory-Huggins Models. *Polymer* **2016**, *103*, 124–131.
(18) Krishna, R. Using the Maxwell-Stefan formulation for Highlighting the Influence of Interspecies (1-2) Friction on Binary Mixture Permeation across Microporous and Polymeric Membranes. *J. Membr. Sci.* **2017**, *540*, 261–276.
(19) Yang, T.-H.; Lue, S. J. Modeling Sorption Behavior for Ethanol/Water Mixtures in a Cross-linked Polydimethylsiloxane Membrane Using the Flory-Huggins Equation. *J. Macromol. Sci., Part B: Phys.* **2013**, *52*, 1009–1029.
(20) Ribeiro, C. P.; Freeman, B. D. Carbon Dioxide/ethane Mixed-gas Sorption and Dilation in a Cross-linked Poly(ethylene oxide) Copolymer. *Polymer* **2010**, *51*, 1156–1158.
(21) Varady, M. J.; Pearl, T. P.; Stevenson, S. M.; Mantooth, B. A. Decontamination of VX from Silicone: Characterization of Multicomponent Diffusion Effects. *Ind. Eng. Chem. Res.* **2016**, *55*, 3139–3149.
(22) Favre, E.; Schaetzel, P.; Nguygen, Q. T.; Clément, R.; Néel, J. Sorption, diffusion and vapor permeation of various penetrants through dense poly (dimethylsiloxane) membranes: a transport analysis. *J. Membr. Sci.* **1994**, *92*, 169–184.
(23) Yeom, C. K.; Huang, R. Y. M. Modelling of the pervaporation separation of ethanol-water mixtures through crosslinked poly (vinyl alcohol) membrane. *J. Membr. Sci.* **1992**, *67*, 39–55.
(24) Vignes, A. Diffusion in binary solutions. *Ind. Eng. Chem. Fundam.* **1966**, *5*, 189–199.
(25) Ghoreyshi, A. A.; Farhadpour, F. A.; Soltanieh, M. A general model for multicomponent transport in nonporous membranes based on Maxwell-Stefan formulation. *Desalination* **2002**, *144*, 93–101.
(26) Ghoreyshi, A. A.; Farhadpour, F. A.; Soltanieh, M. A general model for multicomponent transport in nonporous membranes based on Maxwell-Stefan formulation. *Chem. Eng. Commun.* **2004**, *191*, 460–499.

DOI: 10.1021/acsomega.9b02255
ACS Omega 2019, 4, 15255–15264

(27) Izák, P.; Bartovská, L.; Friess, K.; Šípek, M.; Uchytil, P. Description of binary liquid mixtures transport through non-porous membrane by modified Maxwell−Stefan equations. *J. Membr. Sci.* **2003**, *214*, 293−309.
(28) Izák, P.; Bartovská, L.; Friess, K.; Šípek, M.; Uchytil, P. Comparison of various models for transport of binary mixtures through dense polymer membrane. *Polymer* **2003**, *44*, 2679−2687.
(29) Genduso, G.; Litwiller, E.; Ma, X.; Zampini, S.; Pinnau, I. Mixed-gas sorption in polymers via a new barometric test system: sorption and diffusion of CO_2-CH_4 mixtures in polydimethylsiloxane (PDMS). *J. Membr. Sci.* **2019**, *577*, 195−204.
(30) Krishna, R.; van Baten, J. M.; Baur, R. Highlighting the Origins and Consequences of Thermodynamic Nonidealities in Mixture Separations using Zeolites and Metal-Organic Frameworks. *Microporous Mesoporous Mater.* **2018**, *267*, 274−292.
(31) Krishna, R.; van Baten, J. M. Hydrogen Bonding Effects in Adsorption of Water-alcohol Mixtures in Zeolites and the Consequences for the Characteristics of the Maxwell-Stefan Diffusivities. *Langmuir* **2010**, *26*, 10854−10867.
(32) Krishna, R.; van Baten, J. M. Highlighting Pitfalls in the Maxwell-Stefan Modeling of Water-Alcohol Mixture Permeation across Pervaporation Membranes. *J. Membr. Sci.* **2010**, *360*, 476−482.
(33) Krishna, R.; van Baten, J. M. Mutual slowing-down effects in mixture diffusion in zeolites. *J. Phys. Chem. C* **2010**, *114*, 13154−13156.

DOI: 10.1021/acsomega.9b02255
ACS Omega 2019, 4, 15255−15264

Highlighting Thermodynamic Coupling Effects in Alcohol/Water Pervaporation across Polymeric Membranes

Rajamani Krishna*

Van 't Hoff Institute for Molecular Sciences

University of Amsterdam

Science Park 904

1098 XH Amsterdam, The Netherlands

email: r.krishna@contact.uva.nl

Table of Contents

1 Preamble

The Supporting Information accompanying our article *Highlighting Thermodynamic Coupling Effects in Alcohol/Water Pervaporation across Polymeric Membranes* provides: (1) the F-H model parameters used in the phase equilibrium calculations, (2) detailed development of the M-S equations using volume fractions, and (3) input data on the M-S diffusivities.

All the calculations and simulations reported in this article were performed using MathCad 15.[1]

For ease of reading, this Supplementary material is written as a stand-alone document; as a consequence, there is some overlap of material with the main manuscript.

2 Flory-Huggins description of phase equilibrium

Polymer membranes are widely used for mixture separations; for an introduction to this topic see Wesselingh and Krishna.[2] The upstream compartment contains fluid mixtures that are either in the gaseous state at elevated pressures, or in the liquid state; see schematic in Figure S1.

2.1 The Flory-Huggins model for penetrants/polymer mixtures

The thermodynamics of sorption equilibrium of penetrants and polymer is most commonly described by the Flory-Huggins relations.[2-4] The Flory-Huggins equation in its simplest form deals with molecules that are similar chemically, but differ greatly in length. An example might be cross-linked polyethylene with the penetrant propane (C_3H_8). The Flory-Huggins model is based on the idea that the chain elements of the polymer arrange themselves randomly (but with the molecules remaining connected) on a three- dimensional lattice; see inset in Figure S1.

The Flory-Huggins model does not take effects of crystallization or other inhomogeneities into account. The resulting equation for the activity of the penetrant is a simple function of the volume fraction of the penetrant in the membrane. We use ϕ_i to denote the volume fraction of the penetrant species *i*; the volume fraction of species *i* is $\phi_i = c_i \overline{V_i}$ where c_i is the molar concentration, and $\overline{V_i}$ is the partial molar volume of the penetrant species *i*. Other concentration measures are listed in Table S1. The use of mole fractions is not convenient for description of the phase equilibrium of mixtures of penetrants in polymers, because the molar mass of the polymer chains are ill defined.[2]

The Flory-Huggins (F-H) model for binary mixture of penetrant (1) and polymer (indicated by subscript m) is

Flory-Huggins description of phase equilibrium

$$\ln a_1 = \ln(\phi_1) + (1-\phi_1) - \phi_m \frac{\overline{V_1}}{\overline{V_m}} + \chi_{1m}\phi_m^2 \qquad \phi_m = 1-\phi_1 \tag{S1}$$

Equation (S1) contains a non-ideality, or interaction parameter χ_{1m} that is assumed to be independent of the volume fraction. If $\chi_{1m} > 0$, the penetrant and polymer repel, or dislike, each other. If $\chi_{1m} < 0$, the penetrant and polymer attract each other. If $\chi_{1m} = 0$, the penetrant and polymer are similar in nature and there are no attractive or repulsive forces.

Figure S2 illustrates the influence of the interaction parameter χ_{1m} on the activity (a_1) and thermodynamic correction factor, $\Gamma = \frac{\partial \ln a_1}{\partial \ln \phi_1}$, that plays a pivotal role in diffusion (discussions on this are in the following sections). In these calculations, the ratio $\frac{\overline{V_1}}{\overline{V_m}} = 0$, i.e. the molar volume of the penetrant is negligible in comparison to the molar volume of the polymer. If χ_{1m} is positive, the solution can split into two phases for a range of volume fractions, one rich in polymer and one rich in solvent; the demixing zone is indicated in cyan in Figure S2.

If the interaction parameter χ_{1m} is dependent on the volume fractions, the F-H model for unary systems needs to be extended as follows

$$\ln a_1 = \ln(\phi_1) + (1-\phi_1) - (1-\phi_1)\frac{\overline{V_1}}{\overline{V_m}} + \chi_{1m}(1-\phi_1)^2 + \phi_1(1-\phi_1)^2 \frac{\partial \chi_{1m}}{\partial \phi_1} \tag{S2}$$

For ternary mixtures of two penetrants, 1 and 2, and the polymer (m), there are three interaction parameters in the F-H description of phase equilibrium: $\chi_{12}, \chi_{1m}, \chi_{2m}$. If each of the three interaction parameters $\chi_{12}, \chi_{1m}, \chi_{2m}$ are dependent on the volume fractions of the penetrants, ϕ_1, ϕ_2 the F-H model for the component activities a_1, a_2 of the penetrants in the polymer membrane (m) are

$$\begin{aligned}
\ln a_1 &= \ln(\phi_1) + (1-\phi_1) - \phi_2 \frac{\overline{V_1}}{\overline{V_2}} - \phi_m \frac{\overline{V_1}}{\overline{V_m}} + \left(\chi_{12}\phi_2 + \chi_{1m}\phi_m\right)\left(\phi_2 + \phi_m\right) - \chi_{2m}\frac{\overline{V_1}}{\overline{V_2}}\phi_2\phi_m - u_1u_2\phi_2\frac{\partial\chi_{12}}{\partial u_2} \\
&\quad - u_1u_2\phi_m\frac{\partial\chi_{1m}}{\partial u_2} - \phi_1\phi_m^2\frac{\partial\chi_{1m}}{\partial\phi_m} + \frac{\overline{V_1}}{\overline{V_2}}u_2^2\phi_m\frac{\partial\chi_{2m}}{\partial u_1} - \frac{\overline{V_1}}{\overline{V_2}}\phi_2\phi_m^2\frac{\partial\chi_{2m}}{\partial\phi_m} \\
\ln a_2 &= \ln(\phi_2) + (1-\phi_2) - \phi_1 \frac{\overline{V_2}}{\overline{V_1}} - \phi_m \frac{\overline{V_2}}{\overline{V_m}} + \left(\chi_{12}\phi_1\frac{\overline{V_2}}{\overline{V_1}} + \chi_{2m}\phi_m\right)\left(\phi_1 + \phi_m\right) - \chi_{1m}\frac{\overline{V_2}}{\overline{V_1}}\phi_1\phi_m + \frac{\overline{V_2}}{\overline{V_1}}u_1^2\phi_2\frac{\partial\chi_{12}}{\partial u_2} \\
&\quad + \frac{\overline{V_2}}{\overline{V_1}}u_1^2\phi_m\frac{\partial\chi_{1m}}{\partial u_2} - \frac{\overline{V_2}}{\overline{V_1}}\phi_1\phi_m^2\frac{\partial\chi_{1m}}{\partial\phi_m} - u_1u_2\phi_m\frac{\partial\chi_{2m}}{\partial u_1} - \phi_2\phi_m^2\frac{\partial\chi_{2m}}{\partial\phi_m}
\end{aligned} \tag{S3}$$

In eq (S3), we have defined $u_2 = \dfrac{\phi_2}{\phi_1+\phi_2}$; $\quad u_1 = 1-u_2 = \dfrac{\phi_1}{\phi_1+\phi_2}$; $\qquad \phi_m = 1-\left(\phi_1+\phi_2\right)$.

Equation (S3) corresponds precisely with equations (6) and (7) of Mulder et al.[5] The same set of extended equations are also given by Yang and Lue[6] and Varady et al.[7]

In the scenario in which the penetrant-membrane interaction parameters χ_{1m}, χ_{2m} are independent on the volume fractions of the penetrants, Equation (S3) simplifies to yield

$$\begin{aligned}
\ln a_1 &= \ln(\phi_1) + (1-\phi_1) - \phi_2 \frac{\overline{V_1}}{\overline{V_2}} - \phi_m \frac{\overline{V_1}}{\overline{V_m}} + \left(\chi_{12}\phi_2 + \chi_{1m}\phi_m\right)\left(\phi_2 + \phi_m\right) - \chi_{2m}\frac{\overline{V_1}}{\overline{V_2}}\phi_2\phi_m - u_1u_2\phi_2\frac{\partial\chi_{12}}{\partial u_2} \\
\ln a_2 &= \ln(\phi_2) + (1-\phi_2) - \phi_1 \frac{\overline{V_2}}{\overline{V_1}} - \phi_m \frac{\overline{V_2}}{\overline{V_m}} + \left(\chi_{12}\phi_1\frac{\overline{V_2}}{\overline{V_1}} + \chi_{2m}\phi_m\right)\left(\phi_1 + \phi_m\right) - \chi_{1m}\frac{\overline{V_2}}{\overline{V_1}}\phi_1\phi_m + \frac{\overline{V_2}}{\overline{V_1}}u_1^2\phi_2\frac{\partial\chi_{12}}{\partial u_2}
\end{aligned} \tag{S4}$$

2.2 The Flory-Huggins model for binary liquid mixtures

As a special (degenerate) case, eq (S3) can be applied to describe the component activities for binary *liquid phase* mixtures in the upstream compartment of the membrane. Let ϕ_1^L, ϕ_2^L represent the volume fractions of components 1 and 2 in the bulk liquid mixture. These volume fractions are related to the mass fractions ω_i^L in the bulk liquid mixture $\phi_i^L = \dfrac{\dfrac{\omega_i^L}{\rho_i^L}}{\displaystyle\sum_{i=1}^{n}\frac{\omega_i^L}{\rho_i^L}}$, where ρ_i^L is the liquid phase mass density of the penetrant species *i*. Other concentration measures, and inter-relations, are listed in Table S1. We also have the constraint $\phi_1^L + \phi_2^L = 1$. The component activities in the liquid mixture are obtained from

Equation (S3) by omitting terms containing χ_{1m} and χ_{2m}, and setting $\phi_m = 0$; $\phi_1^L + \phi_2^L = 1$, and $u_2^L = \frac{\phi_2^L}{\phi_1^L + \phi_2^L} = \phi_2^L$:

$$\ln a_1^L = \ln(\phi_1^L) + (1 - \frac{\overline{V_1}}{\overline{V_2}})\phi_2^L + \chi_{12}\left(\phi_2^L\right)^2 - \phi_1^L\left(\phi_2^L\right)^2 \frac{\partial \chi_{12}}{\partial \phi_2^L}$$
$$\ln a_2^L = \ln(\phi_2^L) + (1 - \frac{\overline{V_2}}{\overline{V_1}})\phi_1^L + \frac{\overline{V_2}}{\overline{V_1}}\chi_{12}\left(\phi_1^L\right)^2 + \frac{\overline{V_2}}{\overline{V_1}}\phi_2^L\left(\phi_1^L\right)^2 \frac{\partial \chi_{12}}{\partial \phi_2^L} \quad \text{(S5)}$$

Equation (S5) corresponds precisely with equations (9), and (10) of Mulder et al.[5] The χ_{12} is related to the excess Gibbs free energy

$$\chi_{12} = \frac{1}{x_1 \phi_2^L}\left[x_1 \ln(\frac{x_1}{\phi_1^L}) + x_2 \ln(\frac{x_2}{\phi_2^L}) + \frac{G^{excess}}{RT}\right]$$
$$\frac{G^{excess}}{RT} = x_1 \ln(\gamma_1) + x_2 \ln(\gamma_2) \quad \text{(S6)}$$

In Equation (S6), x_1, x_2 are liquid phase mole fractions $x_i = \frac{c_i}{c_t} = \frac{\frac{\omega_i^L}{M_i}}{\sum_{i=1}^{n}\frac{\omega_i^L}{M_i}} = \frac{\omega_i^L}{M_i}\overline{M}$, where M_i is the molar mass of component *i* (units kg mol^{-1}), and $\overline{M} = \sum_{i=1}^{n} x_i M_i$ is the mean molar mass of the mixture; see Table S1.

The interaction parameter χ_{12} for mixtures such as water/ethanol are strongly dependent on the liquid mixture composition. The excess Gibbs free energy $\frac{G^{excess}}{RT} = x_1 \ln(\gamma_1) + x_2 \ln(\gamma_2)$ can be calculated from activity coefficient models such as that of Wilson, NRTL, and UNIQUAC.[5, 6] Mulder et al.[5] have also shown that the dependence of χ_{12} on the volume fractions of components in the bulk liquid mixture can be expressed as a fourth-order polynomial in $u_2^L = \frac{\phi_2^L}{\phi_1^L + \phi_2^L} = \phi_2^L$

Flory-Huggins description of phase equilibrium

$$\chi_{12} = a + b\left(u_2^L\right) + c\left(u_2^L\right)^2 + d\left(u_2^L\right)^3 + e\left(u_2^L\right)^4; \quad \text{bulk liquid mixture}$$
$$u_2^L = \frac{\phi_2^L}{\phi_1^L + \phi_2^L} = \phi_2^L; u_1^L = \frac{\phi_1^L}{\phi_1^L + \phi_2^L} = \phi_1^L = 1 - u_2^L = 1 - \phi_2^L \quad \text{(S7)}$$

The use of the fourth-order polynomial expression is particularly convenient for the evaluation of the derivative $\frac{\partial \chi_{12}}{\partial \phi_2^L}$ in Equation (S5). The five coefficients, a, b, c, d, e can be determined by fitting of the Wilson, NRTL, and UNIQUAC models for $\frac{G^{excess}}{RT} = x_1 \ln(\gamma_1) + x_2 \ln(\gamma_2)$. For example, for ethanol/water mixtures, Hietaharju et al.[8] have determined temperature-dependent coefficients a, b, c, d, e by fitting the Wilson activity coefficient model parameters from the Aspen Plus simulation software databank (WILS-HOC, v8.8). In all the Flory-Huggins calculations presented in this article, the 4th order polynomial expressions are used to describe the volume fraction dependence of χ_{12}.

A significant contribution of Mulder et al.[5] is to demonstrate that the interaction parameter χ_{12} for the same two penetrants in the polymer membrane phase experiences the same composition dependence on the normalized volume fraction of component 2 within the membrane $u_2 = \frac{\phi_2}{\phi_1 + \phi_2}$, i.e.

$$\chi_{12} = a + b(u_2) + c(u_2)^2 + d(u_2)^3 + e(u_2)^4; \quad \text{polymer membrane phase}$$
$$u_2 = \frac{\phi_2}{\phi_1 + \phi_2}; u_1 = \frac{\phi_1}{\phi_1 + \phi_2} = 1 - u_2 \quad \text{(S8)}$$

2.3 List of Tables for Flory-Huggins description of phase equilibrium

Table S1. Concentration measures and inter-relationships.

Concentration measure	units	Inter-relation, constraint
x_i, mole fraction of species i	-	$x_i = \frac{c_i}{c_t} = \frac{\frac{\omega_i}{M_i}}{\sum_{i=1}^{n}\frac{\omega_i}{M_i}} = \frac{\omega_i}{M_i}\overline{M}; \sum_{i=1}^{n} x_i = 1$
ω_i, mole fraction of species i	-	$\omega_i = \frac{\rho_i}{\rho_t} = \frac{x_i M_i}{\sum_{i=1}^{n} x_i M_i} = \frac{x_i M_i}{\overline{M}}; \sum_{i=1}^{n} \omega_i = 1$
c_i, molar density of species i	mol m^{-3}	$c_i = \frac{\rho_i}{M_i}; \sum_{i=1}^{n} c_i = c_t = \text{mixture molar density} = \frac{1}{\overline{V}}$
ρ_i, mass density of species i	kg m^{-3}	$\rho_i = c_i M_i; \sum_{i=1}^{n} \rho_i = \rho_t = \text{mixture mass density}$
M_i, molar mass of species i	kg mol^{-1}	$\overline{M} = \sum_{i=1}^{n} x_i M_i = \text{mean molar mass of mixture}$
$\overline{V_i}$, partial molar volume of i	m^3 mol^{-1}	$\overline{V} = \sum_{i=1}^{n} x_i \overline{V_i} = \frac{1}{c_t} = \text{mean molar volume of mixture}$
ϕ_i, volume fraction of species i	-	$\phi_i = c_i \overline{V_i} = \frac{\frac{\omega_i}{\rho_i}}{\sum_{i=1}^{n}\frac{\omega_i}{\rho_i}}$

2.4 List of Figures for Flory-Huggins description of phase equilibrium

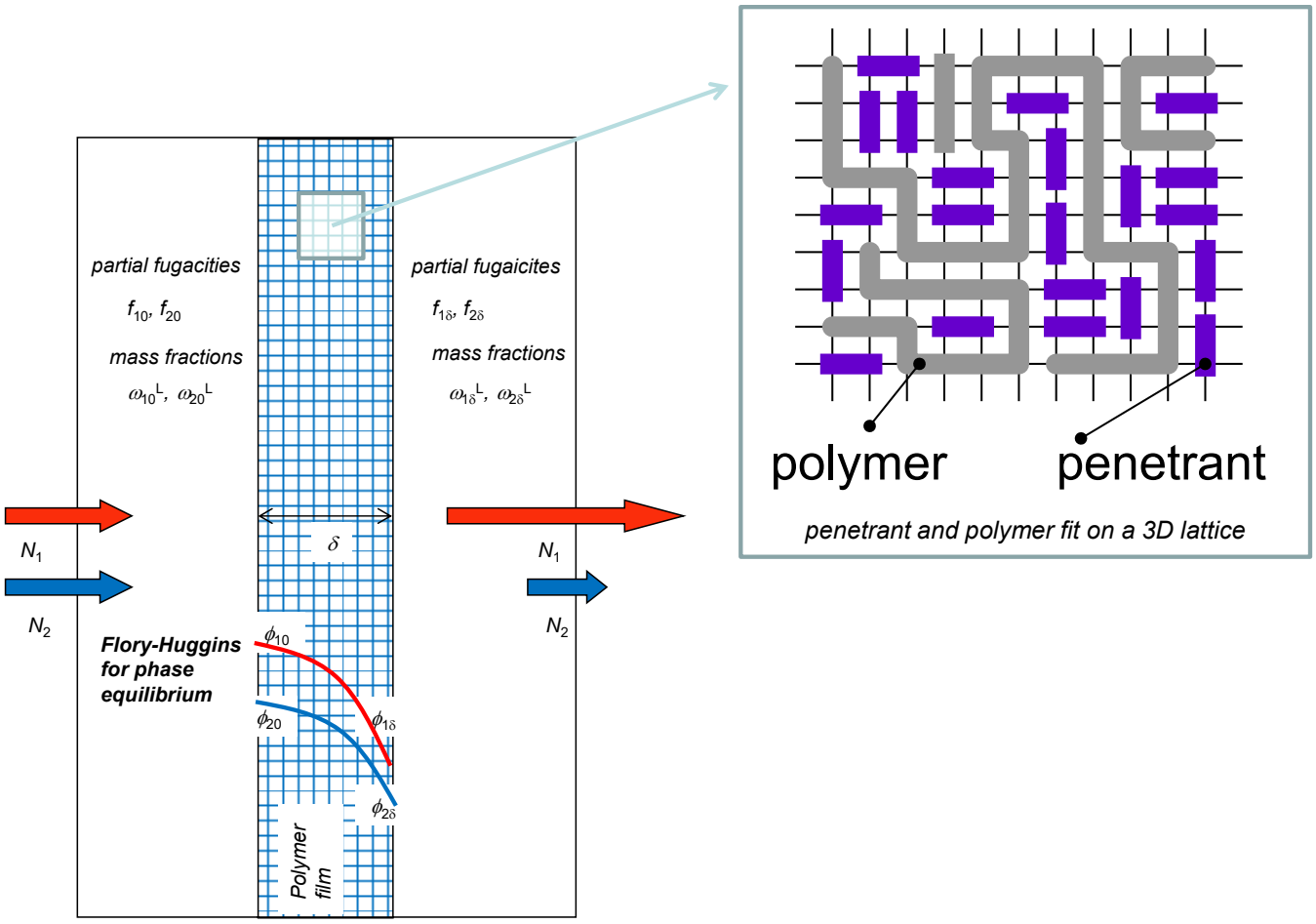

Figure S1. Schematic showing mixture permeation across polymeric membrane. The inset illustrates the Flory-Huggins lattice model.

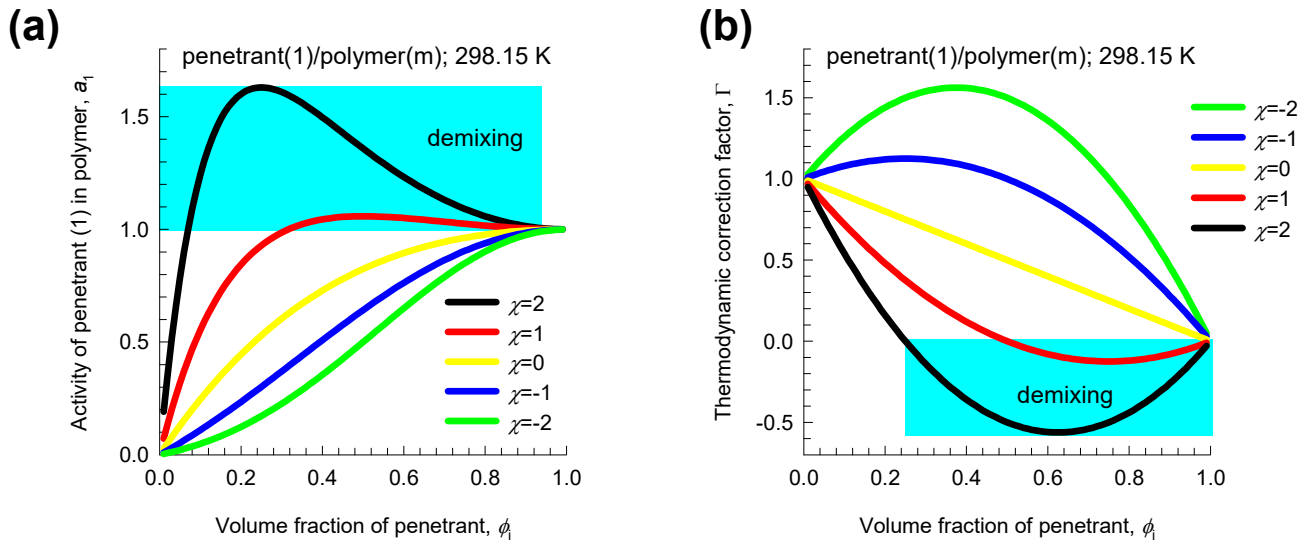

Figure S2. Influence of the interaction parameter on (a) the activity (a_1) and (b) thermodynamic correction factor, Γ. In these calculations, the ratio $\frac{\overline{V_1}}{V_m} = 0$, i.e. the molar volume of the penetrant is negligible in comparison to the molar volume of the polymer.

3 Maxwell-Stefan (M-S) diffusion formulation

3.1 The Maxwell-Stefan (M-S) description of diffusion in polymer solutions

We develop the Maxwell-Stefan (M-S) equations to describe the diffusion of *n* penetrants, 1, 2, 3,..*n* in a polymer matrix (m). The M-S equations represent a balance between the force exerted per mole of species *i* with the drag, or friction, experienced with each of the partner species in the mixture. We may expect that the frictional drag to be proportional to differences in the velocities of the diffusing species $(u_i - u_j)$, where u_i is the velocity of motion of the penetrant *i*. For diffusion in multicomponent polymer solutions such as acetone/cellulose acetate, $u_m \neq 0$, i.e. the polymer chains have a finite velocity of diffusion. For a mixture containing a total of *n* penetrants, 1, 2, 3,..*n* we write

$$
\begin{aligned}
-\frac{d\mu_1}{dz} &= \frac{RT}{Đ_{12}} X_2(u_1 - u_2) + \frac{RT}{Đ_{13}} X_3(u_1 - u_3) + \ldots + \frac{RT}{Đ_{1m}} X_m(u_1 - u_m) \\
-\frac{d\mu_2}{dz} &= \frac{RT}{Đ_{21}} X_1(u_2 - u_1) + \frac{RT}{Đ_{23}} X_3(u_2 - u_3) + \ldots + \frac{RT}{Đ_{2m}} X_m(u_2 - u_m) \\
&\cdots\cdots \\
-\frac{d\mu_n}{dz} &= \frac{RT}{Đ_{n1}} X_1(u_n - u_1) + \frac{RT}{Đ_{n2}} X_2(u_n - u_3) + \ldots + \frac{RT}{Đ_{nm}} X_m(u_n - u_m) \\
-\frac{d\mu_m}{dz} &= \frac{RT}{Đ_{m1}} X_1(u_m - u_1) + \frac{RT}{Đ_{m2}} X_2(u_m - u_3) + \ldots + \frac{RT}{Đ_{mn}} X_n(u_m - u_n)
\end{aligned}
\qquad \text{(S9)}
$$

The left members of equation (S9) are the negative of the gradients of the chemical potentials, with the units N mol^{-1}; it represents the driving force acting per mole of species 1, and 2. The subscript m refers to the polymer chain, that is regarded as the (*n*+1)*th* component in the mixture. The term $RT/Đ_{im}$ is interpreted as the drag or friction coefficient between the penetrant *i* and the polymer. The term $RT/Đ_{ij}$ is interpreted as the friction coefficient for the *i-j* pair of penetrants. The multiplier X_j in each of the right members represents a measure of the composition of component *j* in the mixture because we expect the friction to be dependent on the number of molecules of *j* relative to that of component *i*.

There are many possible choices for composition measures X_i. Written in terms of mole fractions, x_i, eqs (S9) are

$$
\begin{aligned}
-\frac{d\mu_1}{dz} &= \frac{RT}{Đ_{12}} x_2(u_1-u_2) + \frac{RT}{Đ_{13}} x_3(u_1-u_3) + \ldots + \frac{RT}{Đ_{1m}} x_m(u_1-u_m) \\
-\frac{d\mu_2}{dz} &= \frac{RT}{Đ_{21}} x_1(u_2-u_1) + \frac{RT}{Đ_{23}} x_3(u_2-u_3) + \ldots + \frac{RT}{Đ_{2m}} x_m(u_2-u_m) \\
&\cdots\cdots \\
-\frac{d\mu_n}{dz} &= \frac{RT}{Đ_{n1}} x_1(u_n-u_1) + \frac{RT}{Đ_{n2}} x_2(u_n-u_3) + \ldots + \frac{RT}{Đ_{nm}} x_m(u_n-u_m) \\
-\frac{d\mu_m}{dz} &= \frac{RT}{Đ_{m1}} x_1(u_m-u_1) + \frac{RT}{Đ_{m2}} x_2(u_m-u_3) + \ldots + \frac{RT}{Đ_{mn}} x_n(u_m-u_n)
\end{aligned}
\tag{S10}
$$

Only n of the chemical potential gradients $\frac{d\mu_i}{dz}$ are independent, because of the Gibbs-Duhem relationship

$$x_1 \frac{d\mu_1}{dz} + x_2 \frac{d\mu_2}{dz} + \cdots x_n \frac{d\mu_n}{dz} + x_m \frac{d\mu_m}{dz} = 0 \tag{S11}$$

The M-S formulation (S10) is consistent with the theory of irreversible thermodynamics. The Onsager Reciprocal Relations imply that the M-S pair diffusivities are symmetric

$$Đ_{ij} = Đ_{ji} \tag{S12}$$

3.2 Binary mixture permeation across polymer membranes

We apply the M-S formulation (S10) to describe permeation of two penetrants across a polymer membrane. We consider the polymer matrix to be stagnant, i.e. $u_m = 0$. For calculation of the chemical potential gradients, and activity gradients, using the Flory-Huggins model (i.e. eq (S3)) we need to reformulate the eq (S10) in terms of volume fractions instead of mole fractions.[7, 9, 10] Specifically for a binary mixture, we write

$$
\begin{aligned}
-\frac{1}{RT}\frac{d\mu_1}{dz} &= \frac{\phi_2(u_1-u_2)}{Đ_{12}^V} + \frac{\phi_m(u_1)}{Đ_{1m}^V} \\
-\frac{1}{RT}\frac{d\mu_2}{dz} &= \frac{\phi_1(u_2-u_1)}{Đ_{21}^V} + \frac{\phi_m(u_2)}{Đ_{2m}^V}
\end{aligned}
\tag{S13}
$$

Maxwell-Stefan (M-S) diffusion formulation

The modified M-S diffusivities $Đ_{12}^V$, $Đ_{21}^V$, $Đ_{1m}^V$, and $Đ_{2m}^V$ are related to the M-S diffusivities defined in terms of mole fractions, $Đ_{12}=Đ_{21}$, $Đ_{1m}$, $Đ_{2m}$ by $Đ_{12}^V = c_t Đ_{12}\overline{V_2} = \frac{Đ_{12}\overline{V_2}}{\overline{\overline{V}}}$, $Đ_{21}^V = c_t Đ_{21}\overline{V_1} = \frac{Đ_{21}\overline{V_1}}{\overline{\overline{V}}}$, $Đ_{1m}^V = c_t Đ_{1m}\overline{V_m} = \frac{Đ_{1m}\overline{V_m}}{\overline{\overline{V}}}$, and $Đ_{2m}^V = c_t Đ_{2m}\overline{V_m} = \frac{Đ_{2m}\overline{V_m}}{\overline{\overline{V}}}$. The symmetry constraint demanded by the Onsager Reciprocal Relations is

$$Đ_{12} = \frac{Đ_{12}^V}{\overline{\overline{V_2}}}\overline{V} = Đ_{21} = \frac{Đ_{21}^V}{\overline{\overline{V_1}}}\overline{V}; \quad \frac{Đ_{21}^V}{\overline{\overline{V_1}}} = \frac{Đ_{12}^V}{\overline{\overline{V_2}}} \tag{S14}$$

Commonly, the modified M-S diffusivities for penetrant-membrane interactions are taken to be functions of the volume fractions

$$Đ_{1m}^V = Đ_{1m}^V(0)\exp(\varepsilon_{11}\phi_1 + \varepsilon_{12}\phi_2); \quad Đ_{2m}^V = Đ_{2m}^V(0)\exp(\varepsilon_{21}\phi_1 + \varepsilon_{22}\phi_2) \tag{S15}$$

In eq (S15), the $\varepsilon_{11}, \varepsilon_{12}, \varepsilon_{21}, \varepsilon_{22}$ are termed plasticization coefficients.[8, 11]

In proceeding further, we re-write eqs (S13) by multiplying with ϕ_1, and ϕ_2, respectively,

$$\begin{aligned} -\frac{\phi_1}{RT}\frac{d\mu_1}{dz} &= \frac{\phi_1\phi_2(u_1-u_2)}{Đ_{12}^V} + \frac{\phi_1\phi_m(u_1)}{Đ_{1m}^V} \\ -\frac{\phi_2}{RT}\frac{d\mu_2}{dz} &= \frac{\phi_1\phi_2(u_2-u_1)}{Đ_{21}^V} + \frac{\phi_2\phi_m(u_2)}{Đ_{2m}^V} \end{aligned} \tag{S16}$$

Let us define the *volumetric* flux of component *i*, expressed as m^3 m^{-2} s^{-1} as $N_i^V = \phi_i u_i$. The molar flux of component *i*, expressed as mol m^{-2} s^{-1} is $N_i^{molar} = c_i u_i = \frac{\phi_i}{\overline{\overline{V_i}}}u_i = \frac{N_i^V}{\overline{\overline{V_i}}}$. The mass flux of component *i*, expressed as kg m^{-2} s^{-1} is $N_i^{mass} = \rho_i^L N_i^V = M_i N_i^{molar}$ where ρ_i^L is the liquid phase mass density of the pure component *i*. In terms of the volumetric fluxes of components,

In terms of the volumetric fluxes of components, $N_i^V = \phi_i u_i$, equation (S16) may be re-written as

Maxwell-Stefan (M-S) diffusion formulation

$$-\frac{\phi_1}{RT}\frac{d\mu_1}{dz}=\frac{\left(\phi_2 N_1^V-\phi_1 N_2^V\right)}{Đ_{12}^V}+\frac{\phi_m N_1^V}{Đ_{1m}^V}$$
$$-\frac{\phi_2}{RT}\frac{d\mu_2}{dz}=\frac{\left(\phi_1 N_2^V-\phi_2 N_1^V\right)}{Đ_{21}^V}+\frac{\phi_m N_2^V}{Đ_{2m}^V} \qquad \text{(S17)}$$

The first right members of eq (S17) quantify the contributions of 1-2 friction on the permeation fluxes.

The left members of eq (S17), containing the chemical potential gradients, may be expressed in terms of gradients in the volume fractions by introducing an 2×2 dimensional matrix of thermodynamic correction factors $[\Gamma]$:

$$\frac{\phi_i}{RT}\frac{d\mu_i}{dz}=\phi_i\frac{d\ln a_i}{dz}=\sum_{j=1}^{2}\Gamma_{ij}\frac{d\phi_j}{dz};\qquad \Gamma_{ij}=\frac{\phi_i}{\phi_j}\frac{\partial\ln a_i}{\partial\ln\phi_j};\quad i,j=1,2$$
$$\begin{bmatrix}\Gamma_{11} & \Gamma_{12}\\ \Gamma_{21} & \Gamma_{22}\end{bmatrix}=\begin{bmatrix}\phi_1\frac{\partial\ln a_1}{\partial\phi_1} & \phi_1\frac{\partial\ln a_1}{\partial\phi_2}\\ \phi_2\frac{\partial\ln a_2}{\partial\phi_1} & \phi_2\frac{\partial\ln a_2}{\partial\phi_2}\end{bmatrix} \qquad \text{(S18)}$$

The four elements $\Gamma_{11},\Gamma_{12},\Gamma_{21},\Gamma_{22}$ can be determined by analytic differentiation of eq (S3).

Furthermore, let us define a 2×2 dimensional matrix $[B]$ whose elements are given by

$$[B]=\begin{bmatrix}\frac{\phi_2}{Đ_{12}^V}+\frac{\phi_m}{Đ_{1m}^V} & -\frac{\phi_1}{Đ_{12}^V}\\ -\frac{\phi_2}{Đ_{21}^V} & \frac{\phi_1}{Đ_{21}^V}+\frac{\phi_m}{Đ_{2m}^V}\end{bmatrix}=\begin{bmatrix}B_{11} & B_{12}\\ B_{21} & B_{22}\end{bmatrix} \qquad \text{(S19)}$$

Combining eqs (S17), (S18), and (S19) we derive an explicit expression for the volumetric fluxes as functions of the gradients in the volume fractions:

$$(N^V)=-[B]^{-1}[\Gamma]\frac{d(\phi)}{dz};\quad \begin{pmatrix}N_1^V\\ N_2^V\end{pmatrix}=-\begin{bmatrix}B_{11} & B_{12}\\ B_{21} & B_{22}\end{bmatrix}^{-1}\begin{bmatrix}\phi_1\frac{\partial\ln a_1}{\partial\phi_1} & \phi_1\frac{\partial\ln a_1}{\partial\phi_2}\\ \phi_2\frac{\partial\ln a_2}{\partial\phi_1} & \phi_2\frac{\partial\ln a_2}{\partial\phi_2}\end{bmatrix}\begin{pmatrix}\frac{d\phi_1}{dz}\\ \frac{d\phi_2}{dz}\end{pmatrix} \qquad \text{(S20)}$$

Maxwell-Stefan (M-S) diffusion formulation

The matrix inversion $\begin{bmatrix} \Lambda_{11} & \Lambda_{12} \\ \Lambda_{21} & \Lambda_{22} \end{bmatrix} = \begin{bmatrix} B_{11} & B_{12} \\ B_{21} & B_{22} \end{bmatrix}^{-1}$ can be performed explicitly:

$$\begin{bmatrix} \Lambda_{11} & \Lambda_{12} \\ \Lambda_{21} & \Lambda_{22} \end{bmatrix} = \frac{\begin{bmatrix} \frac{\phi_1}{Đ_{21}^V} + \frac{\phi_m}{Đ_{2m}^V} & \frac{\phi_1}{Đ_{12}^V} \\ \frac{\phi_2}{Đ_{21}^V} & \frac{\phi_2}{Đ_{12}^V} + \frac{\phi_m}{Đ_{1m}^V} \end{bmatrix}}{\phi_m \left(\frac{\phi_1}{Đ_{21}^V Đ_{1m}^V} + \frac{\phi_2}{Đ_{12}^V Đ_{2m}^V} + \frac{\phi_m}{Đ_{1m}^V Đ_{2m}^V} \right)} = \frac{\begin{bmatrix} Đ_{1m}^V \left(\phi_m + \frac{\phi_1 Đ_{2m}^V}{Đ_{21}^V} \right) & Đ_{1m}^V \frac{\phi_1 Đ_{2m}^V}{Đ_{21}^V} \\ Đ_{2m}^V \frac{\phi_2 Đ_{1m}^V}{Đ_{12}^V} & Đ_{2m}^V \left(\phi_m + \frac{\phi_2 Đ_{1m}^V}{Đ_{12}^V} \right) \end{bmatrix}}{\phi_m \left(\frac{\phi_1 Đ_{2m}^V}{Đ_{21}^V} + \frac{\phi_2 Đ_{1m}^V}{Đ_{12}^V} + \phi_m \right)} \tag{S21}$$

The ratios $\frac{Đ_{1m}^V}{Đ_{12}^V}$, and $\frac{Đ_{2m}^V}{Đ_{21}^V}$ quantify the *degrees of correlations*; only one of these is independent because $\frac{Đ_{1m}^V}{Đ_{12}^V} = \frac{Đ_{2m}^V}{Đ_{21}^V} \frac{Đ_{1m}^V}{Đ_{2m}^V} \frac{\overline{V}_1}{\overline{\overline{V}}_2}$. Generally speaking for alcohol/water pervaporation processes, the thermodynamic coupling effects engendered by the off-diagonal elements of $\begin{bmatrix} \Gamma_{11} & \Gamma_{12} \\ \Gamma_{21} & \Gamma_{22} \end{bmatrix}$ are much stronger than the coupling effects caused by finite degrees of correlations: $\frac{Đ_{2m}^V}{Đ_{21}^V}$, $\frac{Đ_{1m}^V}{Đ_{12}^V}$.

The corresponding expression for the molar fluxes are

$$\begin{pmatrix} N_1^{molar} \\ N_2^{molar} \end{pmatrix} = -\begin{bmatrix} \frac{1}{\overline{\overline{V}}_1} & 0 \\ 0 & \frac{1}{\overline{\overline{V}}_2} \end{bmatrix} \begin{bmatrix} \Lambda_{11} & \Lambda_{12} \\ \Lambda_{21} & \Lambda_{22} \end{bmatrix} \begin{bmatrix} \phi_1 \frac{\partial \ln a_1}{\partial \phi_1} & \phi_1 \frac{\partial \ln a_1}{\partial \phi_2} \\ \phi_2 \frac{\partial \ln a_2}{\partial \phi_1} & \phi_2 \frac{\partial \ln a_2}{\partial \phi_2} \end{bmatrix} \begin{pmatrix} \frac{d\phi_1}{dz} \\ \frac{d\phi_2}{dz} \end{pmatrix} \tag{S22}$$

The corresponding expression for the mass fluxes are

$$\begin{pmatrix} N_1^{mass} \\ N_2^{mass} \end{pmatrix} = -\begin{bmatrix} \rho_1^L & 0 \\ 0 & \rho_2^L \end{bmatrix} \begin{bmatrix} \Lambda_{11} & \Lambda_{12} \\ \Lambda_{21} & \Lambda_{22} \end{bmatrix} \begin{bmatrix} \phi_1 \frac{\partial \ln a_1}{\partial \phi_1} & \phi_1 \frac{\partial \ln a_1}{\partial \phi_2} \\ \phi_2 \frac{\partial \ln a_2}{\partial \phi_1} & \phi_2 \frac{\partial \ln a_2}{\partial \phi_2} \end{bmatrix} \begin{pmatrix} \frac{d\phi_1}{dz} \\ \frac{d\phi_2}{dz} \end{pmatrix} \tag{S23}$$

3.3 Estimation 1-2 friction

We may estimate $Đ_{12}^{V}$ using the Vignes interpolation formula[12] for diffusion in binary liquid mixtures, adapted as follows[13]

$$\left(Đ_{12}^{V}/\overline{V_2}\right)=\left(Đ_{21}^{V}/\overline{V_1}\right)=\left(Đ_{1m}^{V}/\overline{V_2}\right)^{\phi_1/(\phi_1+\phi_2)}\left(Đ_{2m}^{V}/\overline{V_1}\right)^{\phi_2/(\phi_1+\phi_2)} \tag{S24}$$

with the limiting scenarios

$$\phi_2\to 0,\ Đ_{12}^{V}=Đ_{1m}^{V};\quad \phi_1\to 0,\ Đ_{21}^{V}=Đ_{2m}^{V} \tag{S25}$$

Alternatively, the degrees of correlations $\frac{Đ_{2m}^{V}}{Đ_{21}^{V}}$ may be fitted to match experimental data on mixture permeation.[14]

In the limiting scenario in which the degrees of correlations are considered to be of negligible importance, i.e. $\frac{Đ_{1m}^{V}}{Đ_{12}^{V}}\to 0;\quad \frac{Đ_{2m}^{V}}{Đ_{21}^{V}}\to 0$, the matrix $\begin{bmatrix}\Lambda_{11} & \Lambda_{12}\\ \Lambda_{21} & \Lambda_{22}\end{bmatrix}$ simplifies to yield

$$\begin{bmatrix}\Lambda_{11} & \Lambda_{12}\\ \Lambda_{21} & \Lambda_{22}\end{bmatrix}=\frac{1}{\phi_m}\begin{bmatrix}Đ_{1m}^{V} & 0\\ 0 & Đ_{2m}^{V}\end{bmatrix} \tag{S26}$$

Broadly speaking, we should expect the negligible 1-2 friction scenario to hold when the volume fractions of both penetrants in the membrane are negligibly small. Equation (S26) is used by Mulder et al.[15, 16] for modelling pervaporation of water (component 1), and ethanol (component 2) using cellulose acetate (polymer, component m) membrane.

3.4 Linearized model for binary mixture permeation across polymer membranes

In the linearized approach, we essentially assume that the volume fraction profiles for both penetrants across the membrane layer is linear. The elements of each of the two matrices $\begin{bmatrix}\Lambda_{11} & \Lambda_{12}\\ \Lambda_{21} & \Lambda_{22}\end{bmatrix}$, and $\begin{bmatrix}\Gamma_{11} & \Gamma_{12}\\ \Gamma_{21} & \Gamma_{22}\end{bmatrix}$ is evaluated by calculating the elements $Đ_{im}^{V}\left(\phi_{1,av},\phi_{2,av}\right)$, $Đ_{ij}^{V}\left(\phi_{1,av},\phi_{2,av}\right)$and $\Gamma_{ij}\left(\phi_{1,av},\phi_{2,av}\right)$ at

the arithmetic averaged volume fractions $\phi_{i,av} = \frac{(\phi_{i0} + \phi_{i\delta})}{2}$. With this assumption, the steady-state fluxes for permeation across a membrane of thickness δ are calculated explicitly using

$$\begin{pmatrix} N_1^V \\ N_2^V \end{pmatrix} = \frac{\begin{bmatrix} \Lambda_{11} & \Lambda_{12} \\ \Lambda_{21} & \Lambda_{22} \end{bmatrix}}{\delta} \begin{bmatrix} \Gamma_{11} & \Gamma_{12} \\ \Gamma_{21} & \Gamma_{22} \end{bmatrix} \begin{pmatrix} \phi_{10} - \phi_{1\delta} \\ \phi_{20} - \phi_{2\delta} \end{pmatrix}$$

$$\begin{pmatrix} N_1^{molar} \\ N_2^{molar} \end{pmatrix} = \begin{bmatrix} \frac{1}{\overline{\overline{V_1}}} & 0 \\ 0 & \frac{1}{\overline{\overline{V_2}}} \end{bmatrix} \begin{pmatrix} N_1^V \\ N_2^V \end{pmatrix} \qquad \text{(S27)}$$

$$\begin{pmatrix} N_1^{mass} \\ N_2^{mass} \end{pmatrix} = \begin{bmatrix} \rho_1^L & 0 \\ 0 & \rho_2^L \end{bmatrix} \begin{pmatrix} N_1^V \\ N_2^V \end{pmatrix}$$

The accuracy of the linearized model has been established in earlier work.[14] All the flux calculations reported in this article use the linearized eq (S27).

4 Modelling mixture permeation across polymeric membranes

4.1 Ethanol/water pervaporation across PDMS membrane

Polymeric membranes, such as polydimethylsiloxane (PDMS) membranes, have received considerable attention in the literature due to their hydrophobicity, and hence their capability to separate organics from dilute aqueous mixtures.[6, 8, 17, 18]

Below we present a re-analysis of the experimental data on pervaporation of ethanol/water mixtures reported by Hietaharju et al.[8] and Nasiri and Aroujalian,[18] with the objective of demonstrating the significant influence of thermodynamic coupling effects, embodied in the cross-coefficients of $\begin{bmatrix} \Gamma_{11} & \Gamma_{12} \\ \Gamma_{21} & \Gamma_{22} \end{bmatrix}$, on the pervaporation fluxes.

The first step is to establish the sorption equilibrium using the Flory-Huggins model. Figure S3 presents the experimental data of Yang and Lue[6] on the mass uptakes of penetrants ethanol (1) and water (2) in PDMS (m) at 298.15 K, plotted as function of the mass fraction of ethanol in the liquid feed mixture in the upstream compartment ω_1^L. The mass uptakes, expressed as kg penetrant per kg dry membrane, are related to the volume fractions ϕ_i in the membrane by

$$Uptake_i = \frac{\phi_i \rho_i^L}{\phi_m \rho_m}; \quad \phi_i = \frac{\dfrac{Uptake_i}{\rho_i^L}}{\dfrac{Uptake_1}{\rho_1^L} + \dfrac{Uptake_2}{\rho_2^L} + \dfrac{1}{\rho_m}} \tag{S28}$$

where $\rho_1^L, \rho_2^L, \rho_m$ are the densities of the liquid penetrants and membrane. The continuous solid lines are the Flory-Huggins calculations using the parameters reported by Hietaharju et al.;[8] see Table S2; The F-H calculations are in good agreement with the experimental data of Yang and Lue.[6]

Figure S4a presents calculations for the thermodynamic correction factors for the ternary mixture ethanol(1)/water(2)/PDMS(m) at 313 K, for varying mass fractions of ethanol (1) in the liquid feed

mixture in the upstream compartment ω_1^L. Particularly noteworthy are the negative values of the Γ_{12}. Figure S4b plots the ratios $\frac{\Gamma_{12}}{\Gamma_{11}}$, and $\frac{\Gamma_{21}}{\Gamma_{22}}$ as a function of the mass fraction of ethanol, ω_1^L, in the bulk liquid mixture in the upstream compartment. The large negative value of $\frac{\Gamma_{12}}{\Gamma_{11}}$ implies that the flux of ethanol is strongly influenced, i.e. suppressed, by the driving force for water transport. The value of $\frac{\Gamma_{21}}{\Gamma_{22}}$ is also negative, but smaller in magnitude than $\frac{\Gamma_{12}}{\Gamma_{11}}$.

Hietaharju et al.[8] report experimental data on the mass fluxes of the penetrants N_1^{mass}, N_2^{mass} for pervaporation of ethanol/water mixtures with varying mass fraction of ethanol, ω_1^L, in the bulk liquid mixture in the upstream compartment at temperatures T = 313 K, and 333 K. Hietaharju et al.[8] also report experimental data for vapor permeation in which the ethanol/water vapor mixture, in equilibrium with a ethanol/water liquid phase mixture at the corresponding dew point, is permeated across the PDMS membrane. For modelling their three sets of experiments, we use the linearized eq (S27), invoking the Vignes interpolation formula (S24). In the modelling procedure, eq (S15) is used to describe the penetrant-membrane interactions. For pervaporation across PDMS membranes, the volume fractions of water, ϕ_2, in the membrane are about one to two orders of magnitude lower than that of ethanol, ϕ_1, (cf. Figure S3), and therefore the plasticization coefficients $\varepsilon_{12}, \varepsilon_{22}$ are taken as zero. The fitted values of zero-occupancy M-S diffusivities, $Đ_{1m}^V(0), Đ_{2m}^V(0)$, and plasticization coefficients $\varepsilon_{11}, \varepsilon_{21}$ are specified in Table S3. It is noteworthy that we use the same set of plasticization coefficients for all three sets of experiments $\varepsilon_{11} = 5; \varepsilon_{12} = 0; \varepsilon_{21} = -18; \varepsilon_{22} = 0$. For further discussions on the interpretation and significance of negative values for ε_{21}, see Favre et al.[19] and Yang and Lue.[17]

Figure S5a,b compare the experimental mass fluxes with calculations using linearized eq (S27); the agreement is very good for all three sets. The permeation flux relations used by Hietaharju et al.[8] to model their own experiments do not account for thermodynamic coupling effects; see equations 28, and

29 of Hietaharju et al.[8] Consequently, the match of their model predictions with experiments are significantly poorer, especially for ethanol; see Figure 7 of their paper.

In order to highlight the importance of thermodynamic coupling, Figure S5c compares the mass fluxes of ethanol and water for pervaporation at 313 K, calculated using two different scenarios for $\begin{bmatrix}\Gamma_{11} & \Gamma_{12}\\ \Gamma_{21} & \Gamma_{22}\end{bmatrix}$. The continuous solid lines in Figure S5c represent model calculations using the linearized eq (S27), with proper evaluation of Γ_{ij} using the F-H eqs (S3). The dashed lines in Figure S5c represent model calculations using eq (S27) in which $\Gamma_{ij}=\delta_{ij}$, the Kronecker delta. In the scenario in which thermodynamic coupling effects are ignored, both the fluxes of ethanol and water are higher than for the scenario including thermodynamic coupling. The influence of thermodynamic coupling is essentially to reduce the permeation fluxes of both penetrants; this is akin to mutual-slowing down effects in zeolites,[20-22] engendered by molecular clustering phenomena due to hydrogen bonding between alcohol and water molecules. Figure S5d plots the ratios of the mass flux of ethanol to that of water as a function of the mass fraction of ethanol, ω_1^L, in the bulk liquid mixture in the upstream compartment. The influence of thermodynamic coupling is to suppress the flux of ethanol to a greater extent, leading to lower ethanol/water separation selectivity.

The analysis of the experimental data of Nasiri and Aroujalian[18] for pervaporation of ethanol(1)/water(2) mixtures across PDMS membrane, measured at three different temperatures T = 313 K, 323 K, and 333 K are presented in Figure S6. The fitted values of zero-occupancy M-S diffusivities, $Đ_{1m}^V(0), Đ_{2m}^V(0)$, and plasticization coefficients $\varepsilon_{11}, \varepsilon_{21}$ are specified in Table S4. It is noteworthy that we use the same set of plasticization coefficients for all three sets of experiments $\varepsilon_{11}=5; \varepsilon_{12}=0; \varepsilon_{21}=12; \varepsilon_{22}=0$. With these diffusivity data inputs, along with the F-H eqs (S3), the calculations using the linearized eq (S27) are shown by the continuous solid lines in Figure S6a,b; there is excellent agreement with the experimental data at all three temperatures.

Figure S6c compares the mass fluxes of ethanol and water for pervaporation at 313 K, calculated using two different scenarios for $\begin{bmatrix} \Gamma_{11} & \Gamma_{12} \\ \Gamma_{21} & \Gamma_{22} \end{bmatrix}$. The continuous solid lines in Figure S6c represent model calculations using the linearized eq (S27), with proper evaluation of Γ_{ij} using the F-H eqs (S3). The dashed lines in Figure S6c represent model calculations using eq (S27) in which $\Gamma_{ij} = \delta_{ij}$, the Kronecker delta. In the scenario in which thermodynamic coupling effects are ignored, both the fluxes of ethanol and water are higher than for the scenario including thermodynamic coupling. The influence of thermodynamic coupling is essentially to reduce the permeation fluxes of both penetrants; this is akin to mutual-slowing down effects in zeolites,[20-22] engendered by molecular clustering phenomena due hydrogen bonding between alcohol and water molecules. Figure S6d plots the ratios of the mass flux of ethanol to that of water as a function of the mass fraction of ethanol, ω_1^L, in the bulk liquid mixture in the upstream compartment. The influence of thermodynamic coupling is to suppress the flux of ethanol to a greater extent, leading to lower ethanol/water separation selectivity.

In eqs 19, and 20 of Nasiri and Aroujalian,[18] used to model their own experiments, the M-S diffusivities are modified in the following manner in order to explicitly account cluster formation leading to mutual slowing-down:

$$\begin{aligned} Đ_{1m}^V &= Đ_{1m}^V(0)\exp(\varepsilon_{11}\phi_1)\exp\left(-b_{11}\phi_1^2 - b_{12}\phi_1\phi_2\right); \\ Đ_{2m}^V &= Đ_{2m}^V(0)\exp(\varepsilon_{21}\phi_1)\exp\left(-b_{22}\phi_2^2 - b_{21}\phi_1\phi_2\right) \end{aligned} \tag{S29}$$

The set of plasticization, and clustering, coefficients, along with the zero-occupancy diffusivities are fitted for each of the three experiments sets; see Table 2 of their paper.

4.2 Water/ethanol pervaporation across cellulose acetate membrane

Cellulose acetate membranes are hydrophilic, and preferentially adsorb water from water/ethanol bulk liquid mixtures. The upstream face of the membrane is in equilibrium with water/ethanol liquid mixture of varying mass fractions. Figure S7a presents calculations of the volume fractions of penetrants water (1), ethanol (2) in a cellulose acetate (polymer, component m) at 293.15 K using the Flory-Huggins

parameters from Mulder et al.,[15, 16] the input data are specified in Table S5. The *x*-axis is the mass fraction of ethanol, ω_2^L, in the bulk liquid mixture in the upstream compartment.

Figure S7b presents calculations for the thermodynamic correction factors for the ternary mixture consisting of water (component 1), ethanol (component 2) and cellulose acetate (polymer, component m). Particularly noteworthy are the large negative values of the Γ_{12}. Figure S7c plots the ratios $\frac{\Gamma_{12}}{\Gamma_{11}}$, and $\frac{\Gamma_{21}}{\Gamma_{22}}$ as a function of the mass fraction of ethanol, ω_2^L, in the bulk liquid mixture in the upstream compartment. The large negative value of $\frac{\Gamma_{21}}{\Gamma_{22}}$ implies that the flux of ethanol is strongly influenced, i.e. suppressed, by the driving force for water transport. The value of $\frac{\Gamma_{12}}{\Gamma_{11}}$ is also negative, but smaller in magnitude than $\frac{\Gamma_{21}}{\Gamma_{22}}$.

In order to illustrate the influence of thermodynamic coupling on the pervaporation fluxes, we perform calculations using the input diffusivity data from Mulder et al;[15] see data in Table S5.

Following, Mulder et al.,[15] the modified M-S diffusivities for penetrant-membrane interactions are taken to be functions of the volume fractions

$$\begin{aligned} &Đ_{1m}^V = Đ_{1m}^V(0)\exp\left(\varepsilon_{11}\phi_1 + \varepsilon_{12}\phi_2\right); \quad Đ_{2m}^V = Đ_{2m}^V(0)\exp\left(\varepsilon_{21}\phi_1 + \varepsilon_{22}\phi_2\right); \\ &\varepsilon_{11} = \varepsilon_{12} = \varepsilon_{21} = \varepsilon_{22} = 7.3 \end{aligned} \tag{S30}$$

The molar fluxes are calculated using eq (S27), with the assumption that the volume fractions at the downstream face of the membrane are vanishingly small, $\phi_{1\delta} \approx 0; \phi_{2\delta} \approx 0$. The elements of each of the two matrices $\begin{bmatrix} \Lambda_{11} & \Lambda_{12} \\ \Lambda_{21} & \Lambda_{22} \end{bmatrix}$, and $\begin{bmatrix} \Gamma_{11} & \Gamma_{12} \\ \Gamma_{21} & \Gamma_{22} \end{bmatrix}$ is evaluated by calculating the elements $Đ_{im}^V\left(\phi_{1,av}, \phi_{2,av}\right)$, $Đ_{ij}^V\left(\phi_{1,av}, \phi_{2,av}\right)$and $\Gamma_{ij}\left(\phi_{1,av}, \phi_{2,av}\right)$ at the arithmetic averaged volume fractions $\phi_{i,av} = \frac{\left(\phi_{i0} + \phi_{i\delta}\right)}{2} \approx \frac{\phi_{i0}}{2}$. The Vignes interpolation formula (S24) is used for estimation of the degrees of correlation.

The continuous solid lines in Figure S8a are the calculations of the permeation fluxes using eq (S27) as function of the mass fraction of ethanol (2) in the liquid feed mixture in the upstream compartment, ω_2^L. The dashed lines in Figure S8a represent calculations of the permeation fluxes assuming a scenario in which the thermodynamic coupling effects are ignored and we assume which $\Gamma_{ij} = \delta_{ij}$, the Kronecker delta. The influence of thermodynamic coupling is that both water and ethanol fluxes are suppressed due to the transport of partners in the mixture.

In Figure S8b, the ratio of the molar flux of water to that of ethanol is plotted as function of the mass fraction of ethanol (2) in the liquid feed mixture in the upstream compartment, ω_2^L. Ignoring thermodynamic coupling leads to lower water/ethanol fluxes. The large negative value of $\frac{\Gamma_{21}}{\Gamma_{22}}$ implies that the flux of ethanol is more strongly influenced, i.e. suppressed, by the driving force for water transport.

For pervaporation of water/ethanol mixtures across the hydrophilic CA membrane, correlation effects are important, and serve to retard the transport of water, the more mobile partner in the mixture. In order to gauge the importance of correlation effects, Figure S8c compares the water/ethanol flux ratios for three additional scenarios for estimating the degrees of correlation, $\frac{Đ_{2m}^V}{Đ_{21}^V}$ besides the Vignes interpolation formula (S24): $\frac{Đ_{2m}^V}{Đ_{21}^V} = 0$, $\frac{Đ_{2m}^V}{Đ_{21}^V} = 5$, and $\frac{Đ_{2m}^V}{Đ_{21}^V} = 20$. Please note that the value $\frac{Đ_{1m}^V}{Đ_{12}^V}$ is calculable from $\frac{Đ_{1m}^V}{Đ_{12}^V} = \frac{Đ_{2m}^V}{Đ_{21}^V}\frac{Đ_{1m}^V}{Đ_{2m}^V}\frac{\overline{V_1}}{\overline{V_2}}$. The assertion $\frac{Đ_{2m}^V}{Đ_{21}^V} = 0$ essentially implies the use of eq (S31):

$$\begin{pmatrix} N_1^{molar} \\ N_2^{molar} \end{pmatrix} = -\begin{bmatrix} \frac{1}{\overline{V_1}} & 0 \\ 0 & \frac{1}{\overline{V_2}} \end{bmatrix} \frac{1}{(1-\phi_1-\phi_2)} \begin{bmatrix} Đ_{1m}^V & 0 \\ 0 & Đ_{2m}^V \end{bmatrix} \begin{bmatrix} \Gamma_{11} & \Gamma_{12} \\ \Gamma_{21} & \Gamma_{22} \end{bmatrix} \frac{\begin{pmatrix} \phi_{10}-\phi_{1\delta} \\ \phi_{20}-\phi_{2\delta} \end{pmatrix}}{\delta} \tag{S31}$$

With increasing degrees of correlation, the water/ethanol flux ratio decreases, as is to be expected.

4.3 Water/ethanol pervaporation across polyimide membrane

Figure S9a,b present calculations of the compositions of penetrants water (component 1), ethanol (component 2) in polyimide membrane (polymer, component m) at 293.15 K. The upstream face of the membrane is in equilibrium with water/ethanol liquid mixture of varying mass fractions. The Flory-Huggins model calculations are in good agreement with the experimental sorption data of Ni et al.,[23] as presented in Figures 1, and 2 of their paper. Water is preferentially sorbed in the polyimide membrane.

Figure S10a shows calculations of the elements of $[\Gamma]$ as function of the mass fraction of ethanol (2) in the liquid feed mixture in the upstream compartment, ω_2^L. The negative values of the off-diagonal elements Γ_{12}, Γ_{21} are particularly noteworthy. These negative values imply that the fluxes of both water and ethanol are negatively influenced by transport of the partners in the mixture.

Figure S10b plots the ratios of the elements of thermodynamic correction factors, $\frac{\Gamma_{12}}{\Gamma_{11}}, \frac{\Gamma_{21}}{\Gamma_{22}}$ as function of the mass fraction of ethanol (2) in the liquid feed mixture in the upstream compartment ω_2^L. The off-diagonal elements are significant fractions of the corresponding diagonal elements. Clearly, thermodynamic coupling should be expected to exert a significant influence on the permeation fluxes.

In order to underscore the significance of thermodynamic coupling we consider the experimental data of Ni et al.[23] on the volumetric fluxes of water, and ethanol, plotted in Figure S11a,b (indicated by symbols). For modeling purposes, the modified M-S diffusivities for penetrant-membrane interactions are taken to be functions of the volume fractions

$$\begin{aligned} &Đ_{1m}^V = Đ_{1m}^V(0)\exp\left(\varepsilon_{11}\phi_1 + \varepsilon_{12}\phi_2\right); \quad Đ_{2m}^V = Đ_{2m}^V(0)\exp\left(\varepsilon_{21}\phi_1 + \varepsilon_{22}\phi_2\right); \\ &\varepsilon_{11} = \varepsilon_{12} = \varepsilon_{21} = \varepsilon_{22} = 2 \end{aligned} \tag{S32}$$

The M-S diffusivities at zero volume fractions for penetrant-membrane interactions used in the calculations are the same as reported in Table 1 of Ni et al.[23]

$Đ_{1m}^V(0) = 25.5\times10^{-13}$ m^2 s^{-1}; $Đ_{2m}^V(0) = 2.1\times10^{-13}$ m^2 s^{-1}.

The continuous solid line in Figure S11a,b represent the estimates of the permeation fluxes using the linearized eq (S27). The best agreement with experiments is obtained the choice of the degree of correlaton $\frac{Đ^V_{2m}}{Đ^V_{21}} = 3; \quad Đ^V_{12} = Đ^V_{21}\frac{\overline{V_2}}{\overline{V_1}}$. Ni et al.[23] have also concluded that correlation effects cannot be ignored.

The dashed lines in Figure S11a,b represent calculations of the permeation fluxes assuming a scenario in which the thermodynamic coupling effects are ignored and we assume and $\Gamma_{ij} = \delta_{ij}$. The influence of thermodynamic coupling is that both water and ethanol fluxes are suppressed due to the transport of their partners in the mixture.

4.4 Water/ethanol pervaporation across PVA/PAN membrane

Figure S12a shows the experimental data (symbols) of Heintz and Stephan[24] for binary sorption of water/ethanol mixtures across a poly (vinyl alcohol) /poly (acrylonitrile) (PVA/PAN) composite membrane. The *x*-axis is the mass fraction of ethanol(2) in the liquid feed mixture in the upstream compartment ω_2^L. The continuous solid lines are the F-H model calculations using the input data in Table S7. There is very good agreement between the experimental sorption data and the F-H calculations.

Figure S12b presents calculations of the thermodynamic correction factors, Γ_{ij}, plotted as function of the mass fraction of ethanol(2) in the liquid feed mixture in the upstream compartment ω_2^L. The negative values of the off-diagonal elements Γ_{12}, Γ_{21} are particularly noteworthy. These negative values imply that the fluxes of both water and ethanol are negatively influenced by transport of the partners in the mixture. Figure S12c plots the ratios of the elements of thermodynamic correction factors, $\frac{\Gamma_{12}}{\Gamma_{11}}, \frac{\Gamma_{21}}{\Gamma_{22}}$ as function of the mass fraction of ethanol (2) in the liquid feed mixture in the upstream compartment ω_2^L. The large negative value of $\frac{\Gamma_{12}}{\Gamma_{11}}$ implies that the flux of water is strongly influenced, i.e.

suppressed, by the driving force for ethanol transport. The value of $\frac{\Gamma_{21}}{\Gamma_{22}}$ is also negative, but smaller in magnitude than $\frac{\Gamma_{12}}{\Gamma_{11}}$.

Figure S13a,b present calculations of the pervaporation fluxes for permeation of water(1)/ethanol(2) mixtures across PVA/PAN composite membrane (m) at 333 K. The continuous solid lines are flux calculations based on the linearized eq (S27); wherein the 1-2 friction is described by $\frac{Đ_{2m}^{V}}{Đ_{21}^{V}} = 4$, following previous work.[14] There is excellent agreement between the experimental data of Heintz and Stephan[25] (indicated by symbols) and the model calculations. The dashed lines are flux calculations in which thermodynamic correction factors are ignored, i.e. $\Gamma_{ij} = \delta_{ij}$. The influence of thermodynamic coupling is that both water and ethanol fluxes are suppressed due to the transport of their partners in the mixture.

4.5 CO_2/C_2H_6 permeation across XLPEO membrane

Figure S14a,b,c,d present calculations of the volume fractions of penetrants (a) CO_2 (1) and (b) C_2H_6 (2) in a cross-linked polyethylene oxide (XLPEO) membrane (m) at (a,b) 298.15 K, and (c, d) 263.15. The upstream face of the membrane is in equilibrium with CO_2/C_2H_6 mixtures of five different compositions. The F-H model calculations, indicated by the continuous solid lines, are in excellent agreement with the experimental data of Ribeiro and Freeman.[26] This is to be expected because the three interaction parameters $\chi_{12}, \chi_{1m}, \chi_{2m}$ were determined by fitting of the experimental data.

In order to highlight the importance of thermodynamic coupling effects, Figure S15a,b present the calculations of the four elements of the matrix of thermodynamic factors Γ_{ij}. In these calculations, the upstream face of the membrane is in equilibrium with 70% CO_2 gas mixture. Particularly noteworthy is the significant negative values of Γ_{12} for sorption at 263.15 K.

Figure S16a,b,c,d show the experimental data of Ribeiro et al.[27] for permeabilities of (a, c) CO_2 (1) and (b, d) C_2H_6 (2) for temperatures (a, b) 263.15 K, and (c, d) 293.15 K. The *x*-axis represents the partial fugacity of the permeants in the bulk gas phase in the upstream compartment. Five different mixture compositions are considered. We note that the permeability of C_2H_6 is strongly influenced (increased) by increasing proportion of CO_2 in the bulk gas phase mixture in the upstream compartment. On the other hand, the permeability of CO_2 is influenced to a much reduced extent by the feed mixture composition. The linearized solution to the M-S equation, eq (S27), wherein the 1-2 friction is described by $\frac{Đ_{2m}^{V}}{Đ_{21}^{V}} = 4$ following previous work,[14] are shown by the continuous solid lines. In this case thethermodynamic correction factors, Γ_{ij}, are calculated using the F-H eqs (S3). The M-S model captures, quantitatively, all the essential features of the composition dependence of the permeabilities of CO_2 and C_2H_6, for all feed mixture compositions at either temperature; see comparisons in

In order to highlight the importance of thermodynamic coupling on the permeation fluxes, Figure S17 presents parity plots of experimentally determined permeabilities with model predictions using two different scenarios for calculation of the thermodynamic correction factors, Γ_{ij}. In the first scenario (indicated by red circles), the Γ_{ij} are calculated using the F-H eqs (S3); in the second scenario (indicated by open squares), the thermodynamic coupling effects are ignored and $\Gamma_{ij} = \delta_{ij}$, the Kronecker delta. Ignoring thermodynamic coupling leads to overestimation of the permeabilities of both penetrants. In other words, thermodynamic coupling leads to mutual slowing down of the penetrants.

4.6 List of Tables for Modelling mixture permeation across polymeric membranes

Table S2. Flory-Huggins parameters for ethanol(1)/water(2)/PDMS(m).

The T-dependent coefficients a,b,c,d,e in the fourth-order polynomial expression $\chi_{12} = a + b(u_2) + c(u_2)^2 + d(u_2)^3 + e(u_2)^4$; $u_2 = \frac{\phi_2}{\phi_1 + \phi_2}\chi_{12}$ are provided in Table S2 of Hietaharju et al.[8] The penetrant-membrane parameters χ_{1m}, χ_{2m} are described using the model of Yang and Lue:[6] $\chi_{1m} = a_{1m}(T) + \frac{b_{1m}(T)}{(1 + c_{1m}(T)\phi_m)^2}$; $\chi_{2m} = a_{2m}(T) + \frac{b_{2m}(T)}{(1 + c_{2m}(T)\phi_m)^2}$. The T-dependent coefficients are provided in Table 1 of Hietaharju et al.[8]

The mass densities and molar volumes used in the F-H calculations are

$\overline{V_1} = 58.69 \times 10^{-6}$ m^3 mol^{-1}; $\overline{V_2} = 18 \times 10^{-6}$ m^3 mol^{-1}

$\frac{\overline{V_1}}{V_m} \approx 0; \frac{\overline{V_2}}{V_m} \approx 0; \rho_{1L} = 785; \rho_{2L} = 997; \rho_m = 965$ kg m^{-3}

Membrane thickness: $\delta = 1.3 \times 10^{-7}$ m.

Table S3. Diffusivity data for modelling of Hietaharju experiments for ethanol(1)/water(2)/PDMS(m).

Hietaharju et al.[8] report three sets of experimental data for pervaporation of ethanol(1)/water(2) mixtures across PDMS membrane of thickness $\delta = 80\times10^{-6}$ m.

The inputs used for the Maxwell-Stefan diffusivities and plasticization coefficients

$Đ_{1m}^{V} = Đ_{1m}^{V}(0)\exp(\varepsilon_{11}\phi_1 + \varepsilon_{12}\phi_2)$; $Đ_{2m}^{V} = Đ_{2m}^{V}(0)\exp(\varepsilon_{21}\phi_1 + \varepsilon_{22}\phi_2)$ for the three sets are as follows.

Set I: Pervaporation with liquid ethanol(1)/water(2) mixture in upstream compartment at T = 313 K

$Đ_{1m}^{V}(0) = 1.3\times10^{-10}$ m^2 s^{-1}; $Đ_{2m}^{V}(0) = 2.0\times10^{-10}$ m^2 s^{-1}

Set II: Pervaporation with liquid ethanol(1)/water(2) mixture in upstream compartment at T = 333 K

$Đ_{1m}^{V}(0) = 0.75\times10^{-10}$ m^2 s^{-1}; $Đ_{2m}^{V}(0) = 3.8\times10^{-10}$ m^2 s^{-1}

Set III: Vapor phase permeation of ethanol(1)/water(2) mixture

$Đ_{1m}^{V}(0) = 3\times10^{-11}$ m^2 s^{-1}; $Đ_{2m}^{V}(0) = 12\times10^{-10}$ m^2 s^{-1}

For all three sets of experiments the same set of plasticization coefficients were used:

$\varepsilon_{11} = 5; \varepsilon_{12} = 0; \varepsilon_{21} = -18; \varepsilon_{22} = 0$

Table S4. Diffusivity data for modelling of Nasiri experiments for ethanol(1)/water(2)/PDMS(m).

Nasiri and Aroujalian[18] report three sets of experimental data for pervaporation of ethanol(1)/water(2) mixtures across PDMS membrane of thickness $\delta = 40\times10^{-6}$ m. The inputs used for the Maxwell-Stefan diffusivities and plasticization coefficients

$Đ_{1m}^{V} = Đ_{1m}^{V}(0)\exp(\varepsilon_{11}\phi_1 + \varepsilon_{12}\phi_2)$; $Đ_{2m}^{V} = Đ_{2m}^{V}(0)\exp(\varepsilon_{21}\phi_1 + \varepsilon_{22}\phi_2)$ for the three sets are as follows.

Set I: Pervaporation with liquid ethanol(1)/water(2) mixture in upstream compartment at T = 313 K

$Đ_{1m}^{V}(0) = 1.0\times10^{-9}$ m^2 s^{-1}; $Đ_{2m}^{V}(0) = 1.9\times10^{-9}$ m^2 s^{-1}

Set II: Pervaporation with liquid ethanol(1)/water(2) mixture in upstream compartment at T = 323 K

$Đ_{1m}^{V}(0) = 0.75\times10^{-9}$ m^2 s^{-1}; $Đ_{2m}^{V}(0) = 2.5\times10^{-9}$ m^2 s^{-1}

Set III: Pervaporation with liquid ethanol(1)/water(2) mixture in upstream compartment at T = 323 K

$Đ_{1m}^{V}(0) = 0.65\times10^{-9}$ m^2 s^{-1}; $Đ_{2m}^{V}(0) = 3.3\times10^{-9}$ m^2 s^{-1}

For all three sets of experiments the same set of plasticization coefficients were used:

$\varepsilon_{11} = 5; \varepsilon_{12} = 0; \varepsilon_{21} = 12; \varepsilon_{22} = 0$

Table S5. Thermodynamics and diffusion data for water/ethanol/cellulose acetate.

The Flory-Huggins parameters for penetrants water (component 1) and ethanol (Component 2) in cellulose acetate (CA) membrane (indicated by subscript m) at T = 293.15 K. The data are taken from Mulder et al.:[5, 15, 16]

$$\chi_{12} = a + b(u_2) + c(u_2)^2 + d(u_2)^3 + e(u_2)^4; \quad u_2 = \frac{\phi_2}{\phi_1 + \phi_2}$$

$$a = 0.9820; b = -1.3483; c = 4.15; d = -3.3116; e = 0.8897;$$

$$\chi_{1m} = 1.4; \chi_{2m} = 1.1;$$

$$\overline{V_1} = 18 \times 10^{-6} \text{ m}^3 \text{ mol}^{-1}$$

$$\frac{\overline{V_1}}{\overline{V_2}} = 0.309; \frac{\overline{V_1}}{\overline{V_m}} = 0.002; \frac{\overline{V_2}}{\overline{V_m}} = 0.00647;$$

Modified Maxwell-Stefan diffusivities for permeation of penetrants water (component 1) and ethanol (Component 2) across a cellulose acetate (CA) membrane (indicated by subscript m) at T = 293.15 K. The data are taken from the legend to Figure 5 of Mulder and Smolders.[15]

$$Đ_{1m}^{V}(0) = 8.8 \times 10^{-12} \text{ m}^2 \text{ s}^{-1}$$

$$Đ_{2m}^{V} = 6 \times 10^{-12} \text{ m}^2 \text{ s}^{-1}$$

$$\delta = 20 \times 10^{-6} \quad \text{m}$$

$$\varepsilon_{11} = \varepsilon_{12} = \varepsilon_{21} = \varepsilon_{22} = 7.3$$

Table S6. Thermodynamics and diffusion data for water/ethanol/polyimide.

The Flory-Huggins parameters for penetrants water (1) and ethanol (2) in Polyimide membrane (indicated by subscript m) at T = 293.15 K. The data are based on the information provided from Ni et al.[23] The χ_{12} parameters are taken to be the same as for water/ethanol/CA.

$$\chi_{12} = a + b(u_2) + c(u_2)^2 + d(u_2)^3 + e(u_2)^4; \quad u_2 = \frac{\phi_2}{\phi_1 + \phi_2}$$

$$a = 0.9820; b = -1.3483; c = 4.15; d = -3.3116; e = 0.8897;$$

$$\chi_{1m} = 1.4; \chi_{2m} = 2.2 + 0.7\left(\frac{\phi_1}{\phi_1 + \phi_2}\right);$$

$$\overline{V_1} = 18 \times 10^{-6} \text{ m}^3 \text{ mol}^{-1}$$

$$\frac{\overline{V_1}}{\overline{V_2}} = 0.309; \frac{\overline{V_1}}{V_m} \approx 0.002; \frac{\overline{V_2}}{V_m} = 0.00649;$$

Membrane thickness: $\delta = 20 \times 10^{-6}$ m .

Modified Maxwell-Stefan diffusivities for permeation of penetrants water (component 1) and ethanol (Component 2) across the polyimide membrane (indicated by subscript m) at T = 293.15 K. The data on modified M-S diffusivities at zero volume fractions are taken from Table 1 of Ni et al.[23]. The exponential model is used to describe the variation of the modified M-S diffusivities on the volume fractions $Đ_{1m}^{V}(0) = 25.5 \times 10^{-13}$ m^2 s^{-1} $Đ_{2m}^{V}(0) = 1.5 \times 10^{-13}$ m^2 s^{-1} . The 1-2 friction is described by $\frac{Đ_{2m}^{V}}{Đ_{21}^{V}} = 3$.

$$\varepsilon_{11} = \varepsilon_{12} = \varepsilon_{21} = \varepsilon_{22} = 5$$

Table S7. Thermodynamics and diffusion data for water/ethanol/PVA/PAN.

Flory-Huggins parameters for permeation of penetrants water (1) and ethanol (2) across a poly (vinyl alcohol) /poly (acrylonitrile) (PVA/PAN) composite membrane (indicated by subscript m) at T = 333 K. The χ_{12} parameters were taken to be the same as for water/ethanol/CA. The values of χ_{1m}, χ_{2m} were chosen to match the experimental sorption data presented in Figure 2 of Heintz and Stephan.[24]

$$\chi_{12} = a + b(u_2) + c(u_2)^2 + d(u_2)^3 + e(u_2)^4; \quad u_2 = \frac{\phi_2}{\phi_1 + \phi_2}$$

$$a = 0.9820; b = -1.3483; c = 4.15; d = -3.3116; e = 0.8897;$$

$$\chi_{1m} = 0.65; \chi_{2m} = 1.75$$

$$\overline{V_1} = 18 \times 10^{-6} \text{ m}^3 \text{ mol}^{-1}; \overline{V_2} = 58.4 \times 10^{-6} \text{ m}^3 \text{ mol}^{-1}$$

$$\frac{\overline{V_1}}{V_m} \approx 0; \frac{\overline{V_2}}{V_m} \approx 0; \rho_{1L} = 1000; \rho_{2L} = 789; \rho_m = 1200 \quad \text{kg m}^{-3}$$

Membrane thickness: $\delta = 1.3 \times 10^{-7}$ m.

Modified Maxwell-Stefan diffusivities for permeation of penetrants water (1) and ethanol (2) across the PVA/PAN (indicated by subscript m) at T = 333 K. The M-S diffusivities for water and ethanol penetrants are assumed to follow an exponential dependence on the volume fractions

$Đ_{1m}^{V}(0) = 7.5 \times 10^{-14}$ m^2 s^{-1}

$Đ_{2m}^{V}(0) = 0.35 \times 10^{-14}$ m^2 s^{-1}. The 1-2 friction is quantified by $\frac{Đ_{2m}^{V}}{Đ_{21}^{V}} = 3$.

$\varepsilon_{11} = \varepsilon_{12} = \varepsilon_{21} = \varepsilon_{22} = 2$

Table S8. Thermodynamics and diffusion data for CO_2/C_2H_6/XLPEO at 263.15 K.

Flory-Huggins parameters for permeation of penetrants CO_2 (1) and C_2H_6 (2) across a cross-linked polyethylene oxide (XLPEO) membrane (indicated by subscript m) at T = 263.15 K. The input parameters are based on calculations using the information presented in Appendix A of Ribeiro et al.[9] In the Supplementary material of the paper by Krishna,[13] detailed comparison of experimental phase equilibrium data with predictions of the F-H equations are provided.

$f_{1,sat} = 21\times10^5$ Pa; $f_{2,sat} = 14.5\times10^5$ Pa

$\chi_{12} = -28.2 - \frac{44.3}{\ln(\phi_1)}$; $\chi_{1m} = 1.0421 + 12.3\phi_2$; $\chi_{2m} = 2.421 + 4.76\sqrt{\phi_1}$

$\overline{V_1} = 3.31\times10^{-5}$ m^3 mol^{-1}; $\overline{V_2} = 4.14\times10^{-5}$ m^3 mol^{-1}

Modified Maxwell-Stefan diffusivities for permeation of penetrants CO_2 (component 1) and C_2H_6 (Component 2) across a cross-linked polyethylene oxide (XLPEO) membrane (indicated by subscript m) at T = 263.15 K.

Input data for diffusivities used in the mixture permeability calculations:

$Đ_{1m}^V = 100\times10^{-12}\exp(8(\phi_1+\phi_2))$ m^2 s^{-1}
$Đ_{2m}^V = 38\times10^{-12}\exp(9(\phi_1+\phi_2))$ m^2 s^{-1}. The magnitude of 1-2 friction is described by $\frac{Đ_{2m}^V}{Đ_{21}^V} = 4$, following previous work.[14]

Table S9. Thermodynamics and diffusion data for CO_2/C_2H_6/XLPEO at 298.15 K.

Flory-Huggins parameters for permeation of penetrants CO_2 (1) and C_2H_6 (2) across a cross-linked polyethylene oxide (XLPEO) membrane (indicated by subscript m) at T = 298.15 K. The input parameters are based on calculations using the information presented in Appendix A of Ribeiro et al.[9] In the Supplementary material of the paper by Krishna,[13] detailed comparison of experimental phase equilibrium data with predictions of the F-H equations are provided.

$f_{1,sat} = 43\times10^5$ Pa; $f_{2,sat} = 28\times10^5$ Pa

$\chi_{12} = 1.52$; $\chi_{1m} = 0.9085$; $\chi_{2m} = 2.0804$

$\overline{V_1} = 4.174\times10^{-5}$ m^3 mol^{-1}; $\overline{V_2} = 6.04\times10^{-5}$ m^3 mol^{-1}

Modified Maxwell-Stefan diffusivities for permeation of penetrants CO_2 (component 1) and C_2H_6 (Component 2) across a cross-linked polyethylene oxide (XLPEO) membrane (indicated by subscript m) at T = 298.15 K.

Input data for diffusivities used in the mixture permeability calculations:

$Đ_{1m}^V = 100\times10^{-12}\exp(8(\phi_1+\phi_2))$ m^2 s^{-1}

$Đ_{2m}^V = 38\times10^{-12}\exp(9(\phi_1+\phi_2))$ m^2 s^{-1}. The magnitude of 1-2 friction is described by $\frac{Đ_{2m}^V}{Đ_{21}^V} = 4$, following previous work.[14]

4.7 List of Figures for Modelling mixture permeation across polymeric membranes

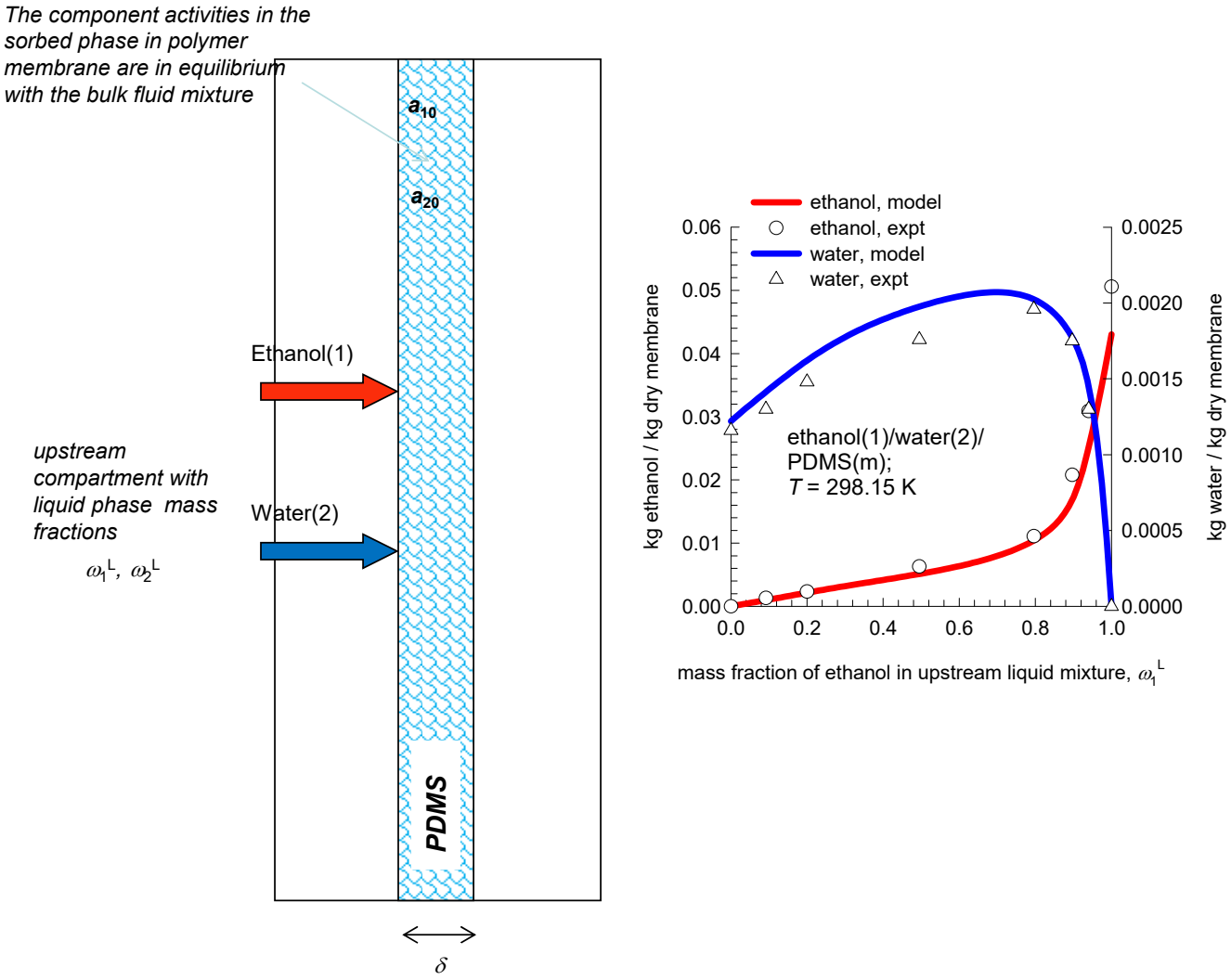

Figure S3. Experimental data (indicated by symbols) of Yang and Lue[6] of the mass uptakes of penetrants ethanol (1) and water (2) in PDMS (m) at 298.15 K, plotted as function of the mass fraction of ethanol in the liquid feed mixture in the upstream compartment ω_1^L. The continuous solid lines are the Flory-Huggins calculations using the input parameters provided in Table S2.

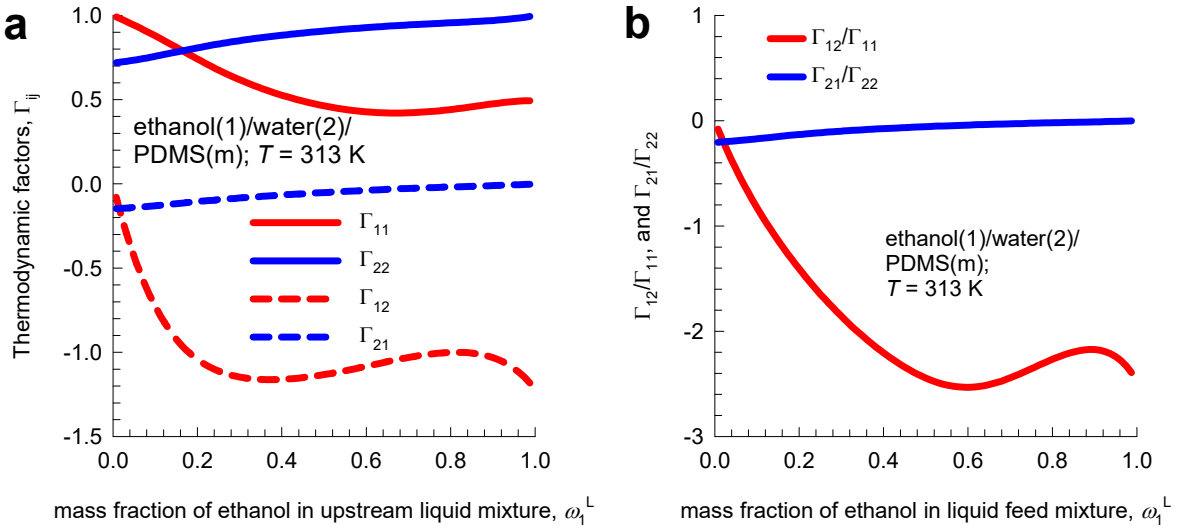

Figure S4. Flory-Huggins calculations of (a) the thermodynamic correction factors, Γ_{ij} and (b) ratios of the elements of thermodynamic correction factors, $\Gamma_{12}/\Gamma_{11}, \Gamma_{21}/\Gamma_{22}$ for sorption equilibrium of ethanol (1) and water (2) in PDMS (m) at 313 K, plotted as function of the mass fraction of ethanol in the liquid feed mixture in the upstream compartment ω_1^L. The F-H parameters are provided in Table S2.

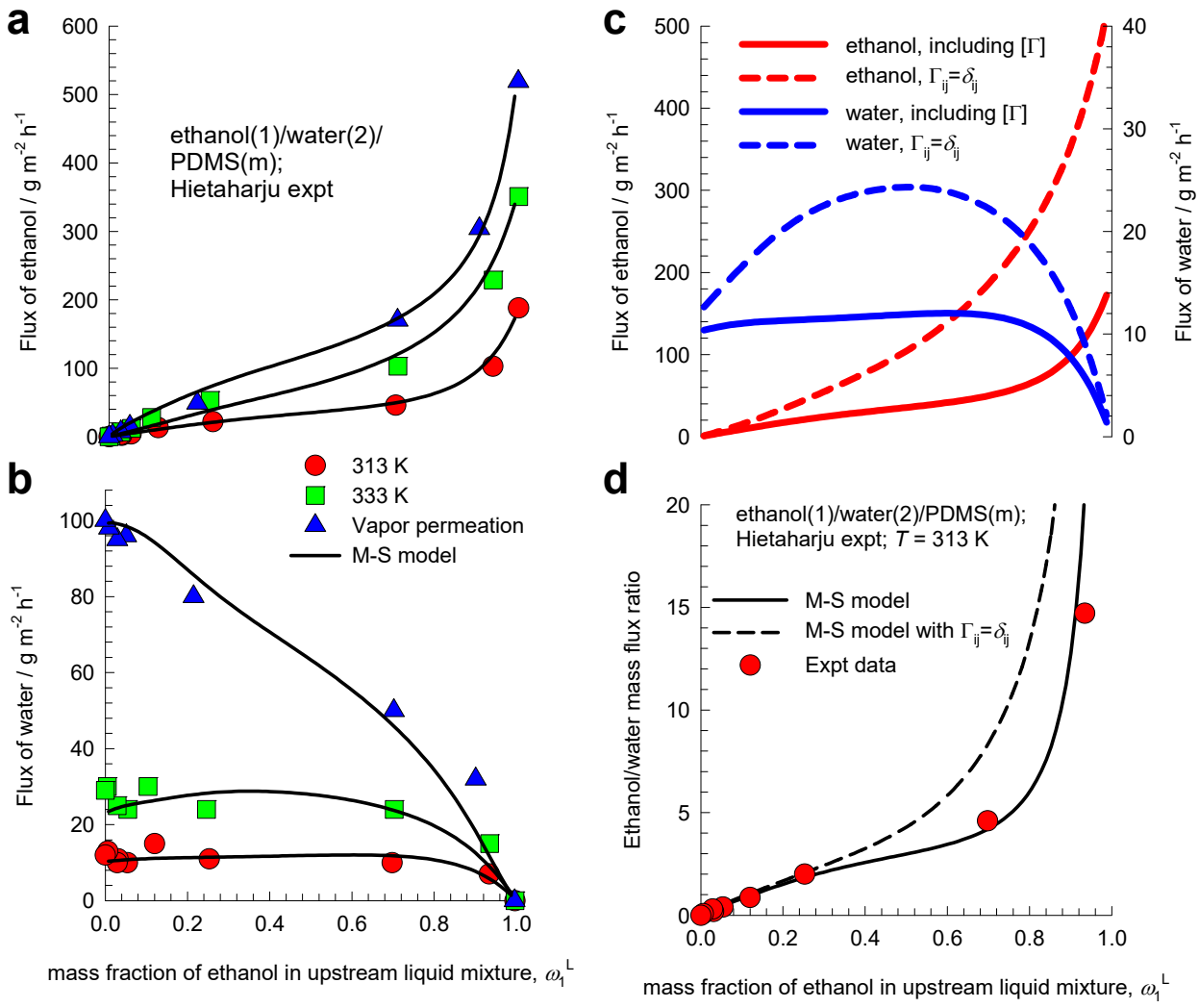

Figure S5. (a, b) Experimental data (indicated by symbols) of Hietaharju et al.[8] for the pervaporation mass fluxes of penetrants ethanol (1) and water (2) across PDMS (m) at 313 K, and 333 K, and vapor permeation, plotted as function of the mass fraction of ethanol in the liquid feed mixture in the upstream compartment ω_1^L. (c) Comparison of the fluxes of ethanol and water at 313 K. (d) Comparison of the ethanol/water mass flux ratios. The continuous solid lines are flux calculations based on eq (S27). The dashed lines are flux calculations in which thermodynamic correction factors are ignored, i.e. $\Gamma_{ij} = \delta_{ij}$. The input diffusivity data are provided in Table S3.

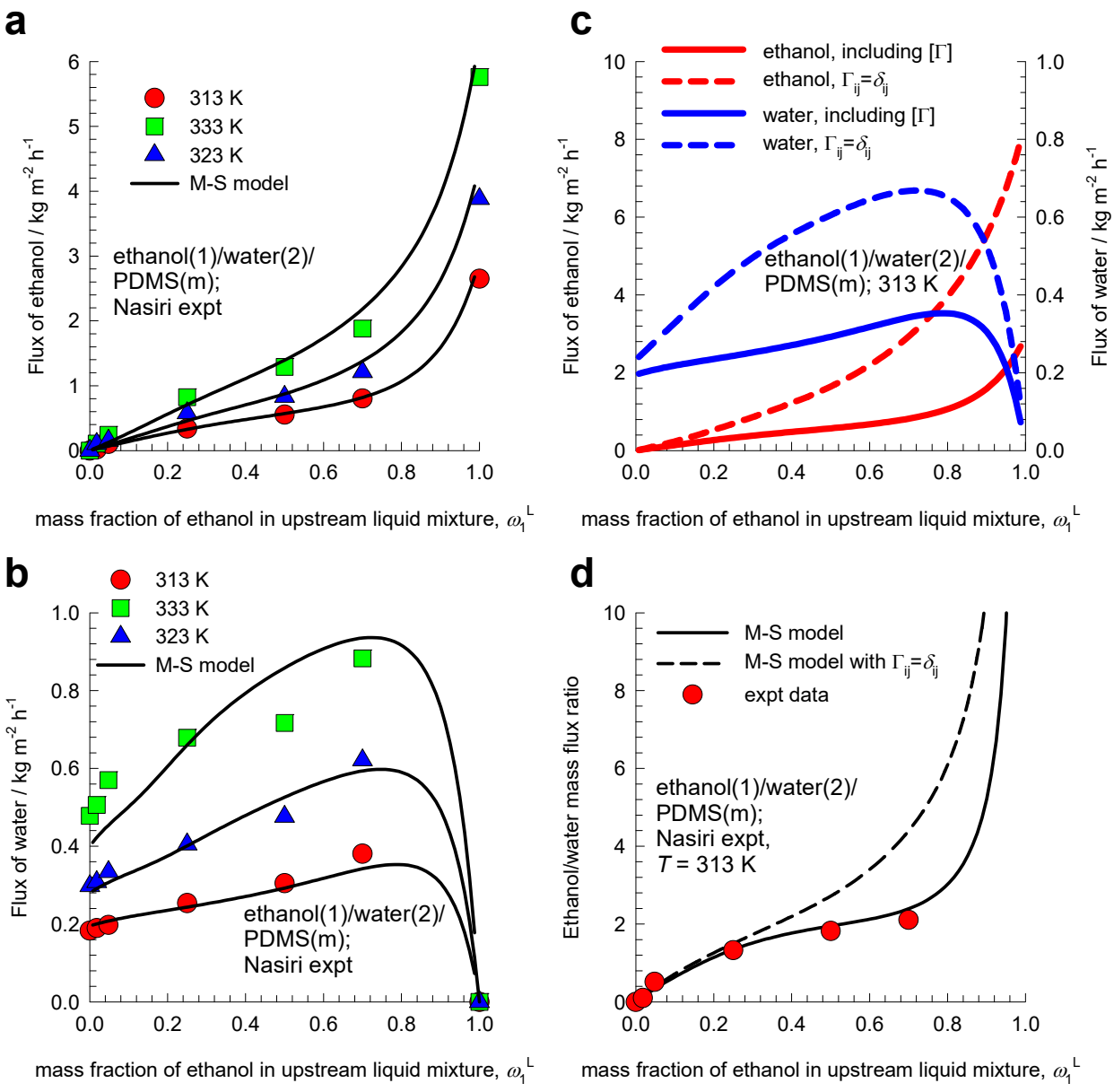

Figure S6. (a, b) Experimental data (indicated by symbols) of Nasiri and Aroujalian,[18] for the mass pervaporation mass fluxes of penetrants ethanol (1) and water (2) across PDMS (m) at 313 K, 323 K, and 333 K, plotted as function of the mass fraction of ethanol in the liquid feed mixture in the upstream compartment ω_1^L. (c) Comparison of the fluxes of ethanol and water at 313 K. . (d) Comparison of the ethanol/water mass flux ratios. The continuous solid lines are flux calculations based on eq (S27). The dashed lines are flux calculations in which thermodynamic correction factors are ignored, i.e. $\Gamma_{ij} = \delta_{ij}$. The input diffusivity data are provided in Table S4.

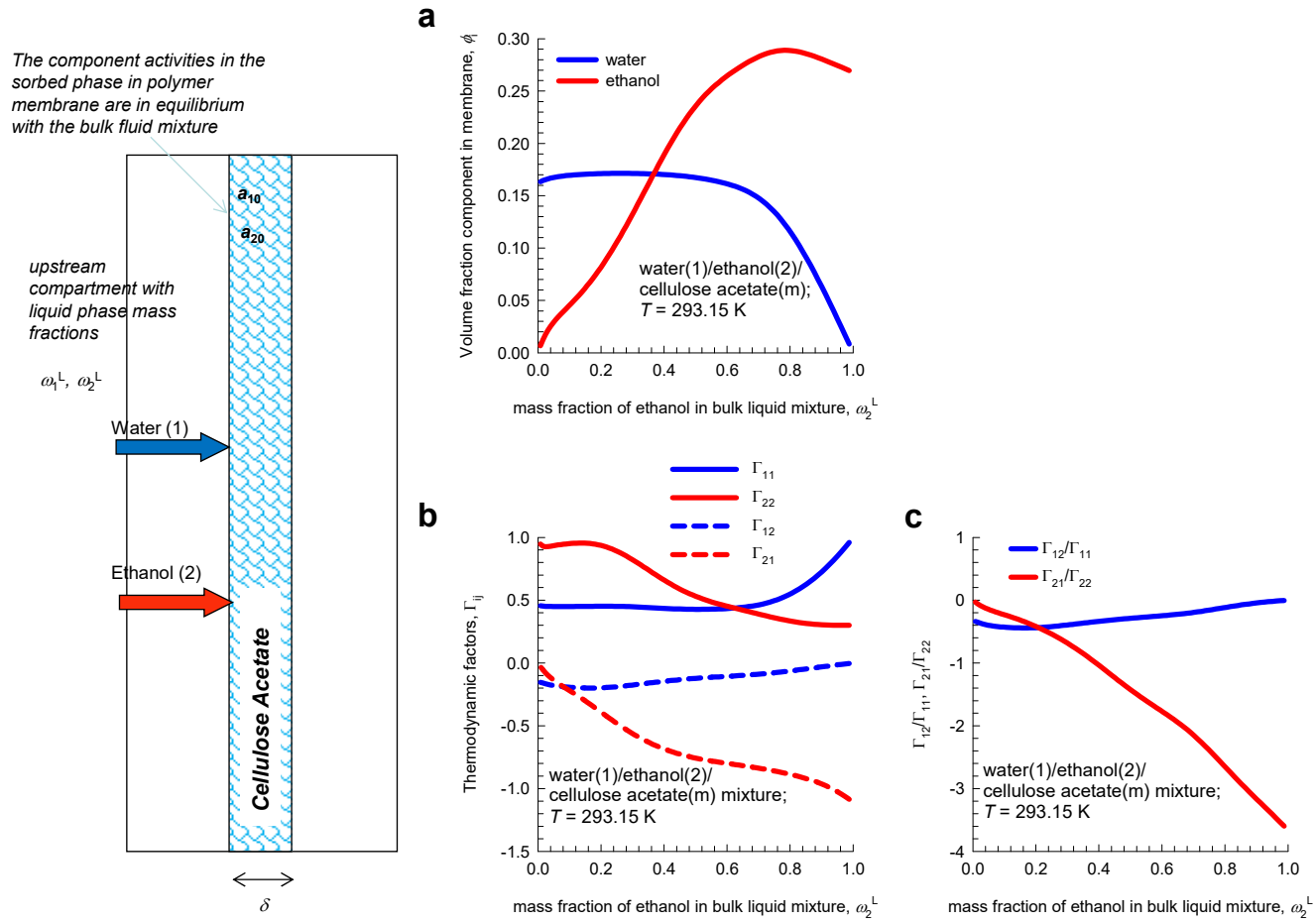

Figure S7. (a) Calculations of the volume fractions of penetrants water (1), ethanol (2) in a cellulose acetate membrane (m) at 293.15 K, plotted as function of the mass fraction of ethanol in the liquid feed mixture in the upstream compartment ω_2^L. (b) Thermodynamic correction factors, Γ_{ij}. (c) Ratios of the elements of thermodynamic correction factors, $\Gamma_{12}/\Gamma_{11}, \Gamma_{21}/\Gamma_{22}$. The Flory-Huggins parameters are specified in Table S5.

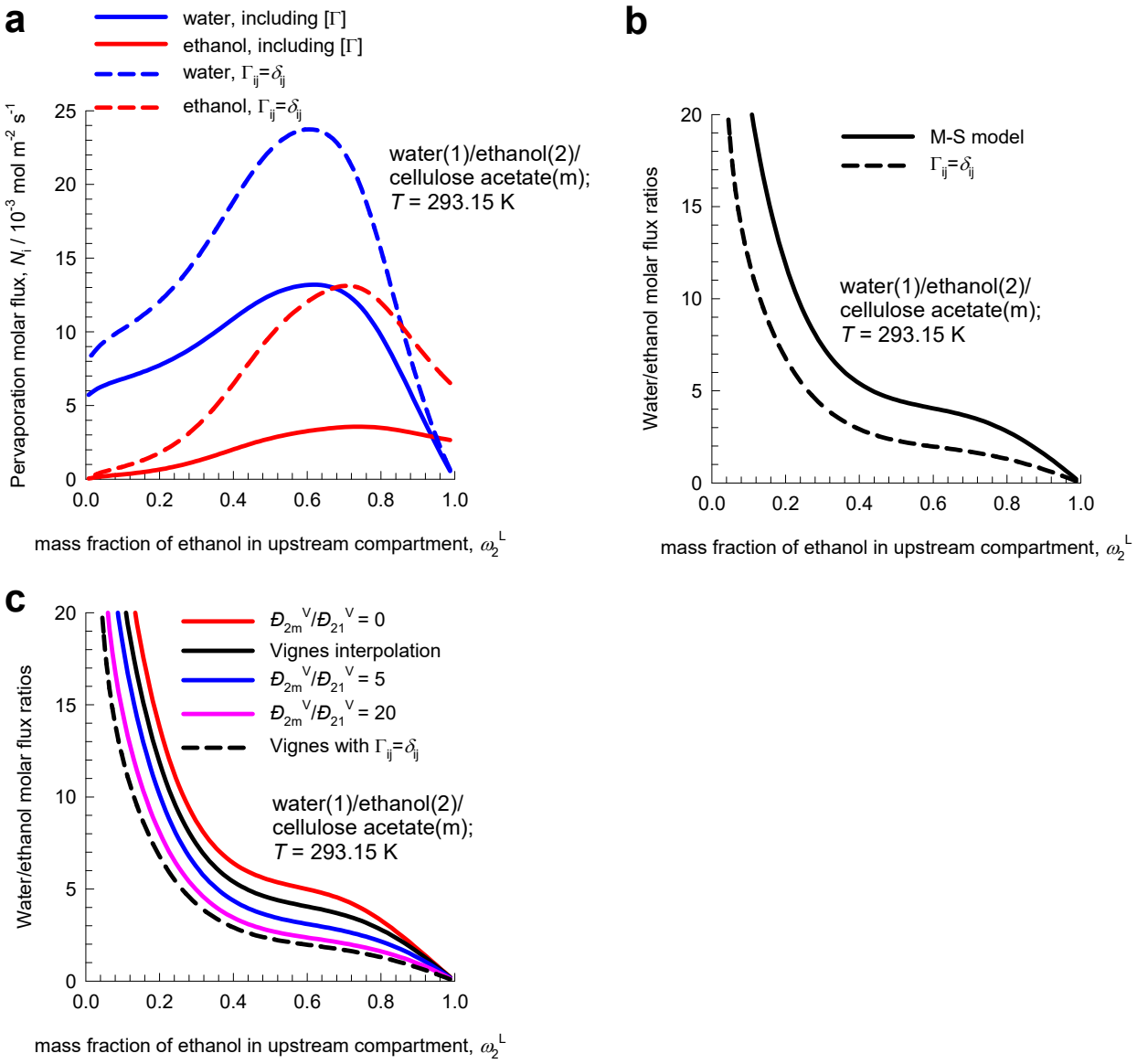

Figure S8. (a) Molar fluxes of water, and ethanol across CA membrane, as function of the mass fraction of ethanol in the liquid feed mixture in the upstream compartment, ω_2^L. (b) Ratio of molar flux of water to that of ethanol, as function of the mass fraction of ethanol in the liquid feed mixture in the upstream compartment, ω_2^L. The continuous solid lines are flux calculations based on eq (S27). The dashed lines are flux calculations in which thermodynamic correction factors are ignored, i.e. $\Gamma_{ij} = \delta_{ij}$. (c) Influence of varying degrees of correlation on the water/ethanol flux ratios. The Flory-Huggins and diffusivity data are specified in Table S5.

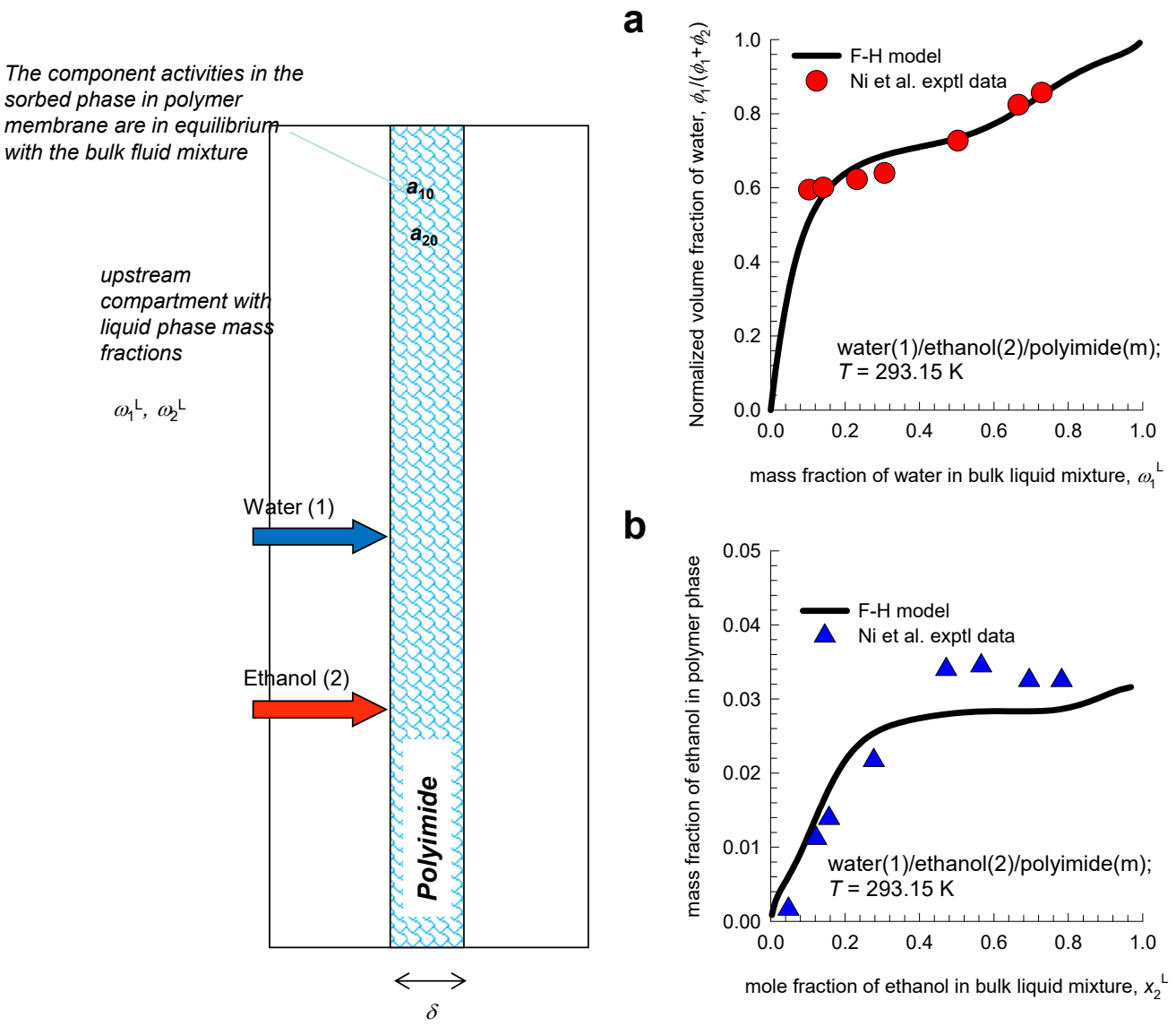

Figure S9. (a, b) Flory-Huggins calculations (continuous solid lines) of the compositions of penetrants (a) water (1), (b) ethanol (2) in polyimide membrane (m) at 293.15 K as a function of the composition of the liquid feed mixture in the upstream compartment. The experimental data (shown by the symbols) are taken from Figure 1 (for ethanol) and Figure 2 (for water) of Ni et al.[23]. The Flory-Huggins parameters are specified in Table S6.

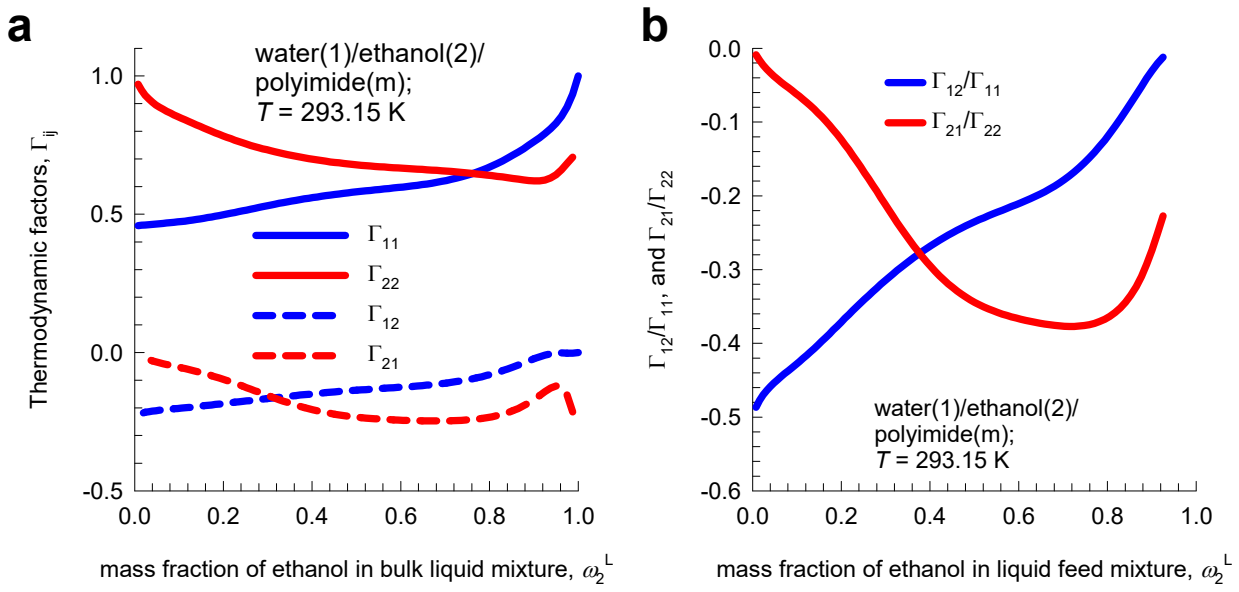

Figure S10. (a) Thermodynamic correction factors factors, Γ_{ij}, for the ternary mixture consisting of water(1), ethanol(2) and polyimide (m), plotted as function of the mass fraction of ethanol (2) in the liquid feed mixture in the upstream compartment ω_2^L. (b) Ratios of the elements of thermodynamic correction factors, $\Gamma_{12}/\Gamma_{11}, \Gamma_{21}/\Gamma_{22}$ as function of the mass fraction of ethanol (2) in the liquid feed mixture in the upstream compartment ω_2^L. The Flory-Huggins parameters are specified in Table S6.

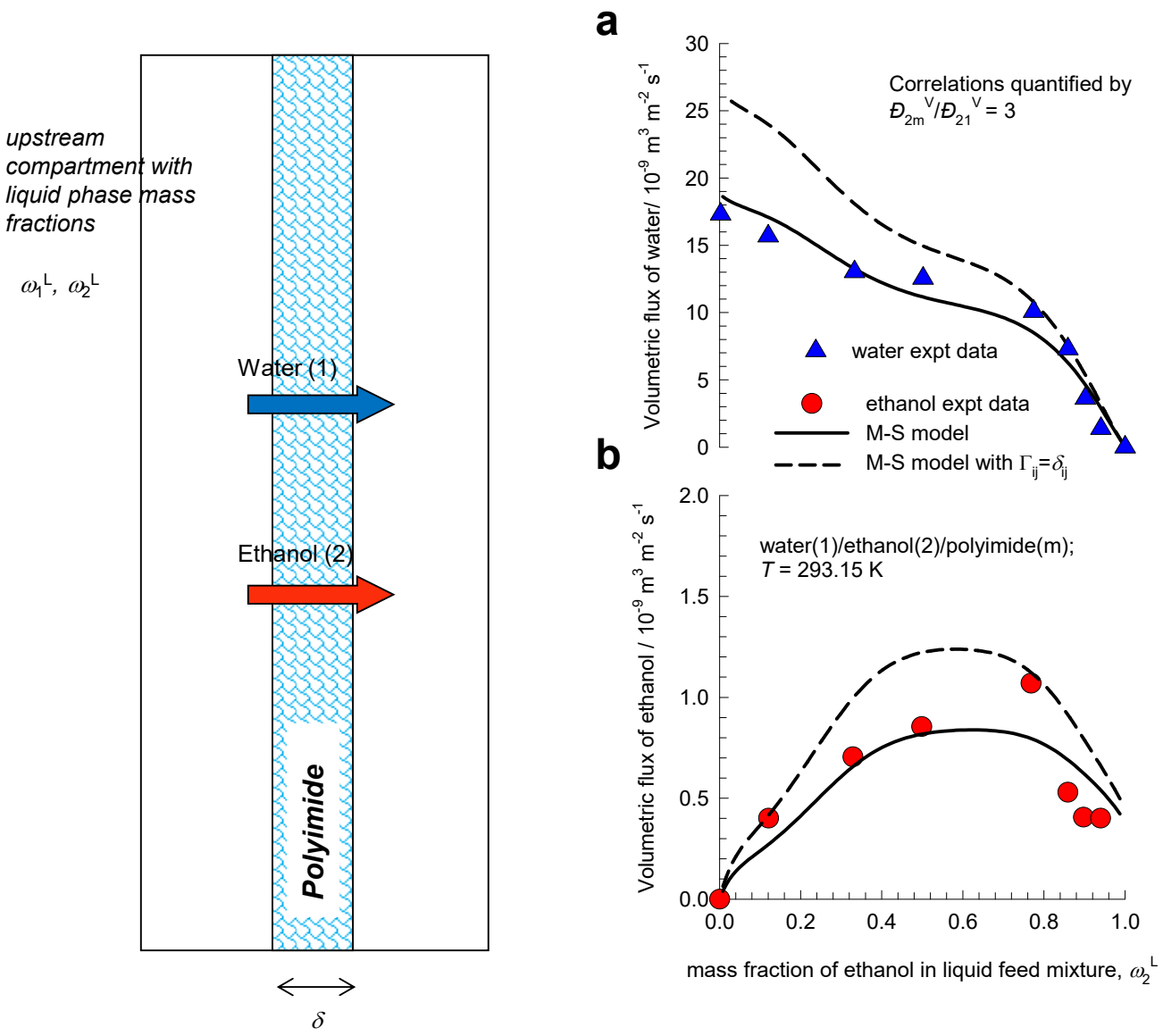

Figure S11. (a, b) Volumetric fluxes of (a) water, and (b) ethanol across polyimide membrane at 293.15 K. The experimental data (shown by the symbols) are taken from Ni et al.[23] The continuous solid lines are flux calculations based on eq (S27); wherein the 1-2 friction is described by $Đ_{2m}^V / Đ_{21}^V = 3$. The dashed lines are flux calculations in which thermodynamic correction factors are ignored, i.e. $\Gamma_{ij} = \delta_{ij}$. The Flory-Huggins and diffusivity data are specified in Table S6.

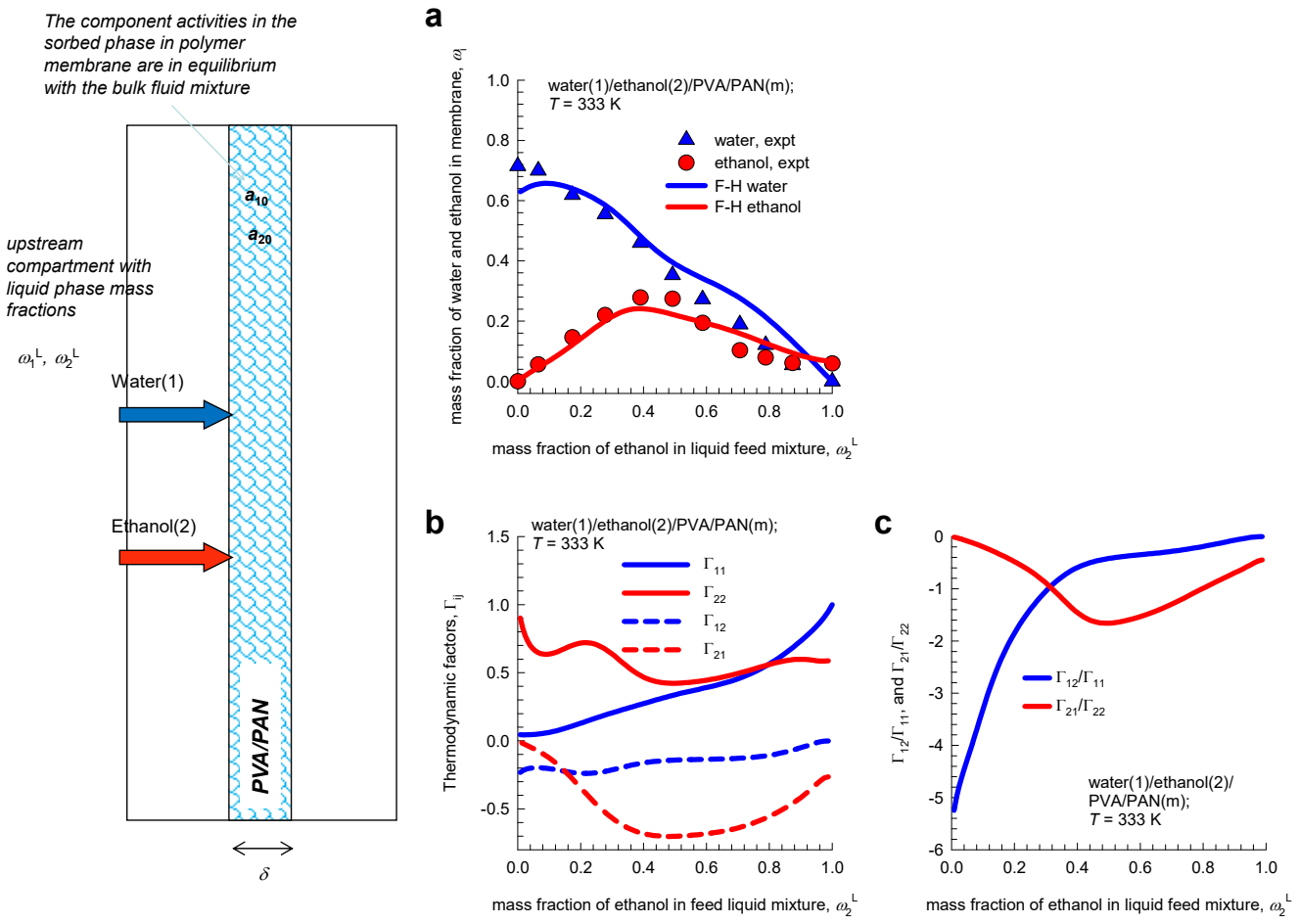

Figure S12. (a) Experimental data (symbols) of Heintz and Stephan[24] for binary sorption of water(1)/ethanol(2) mixtures in poly (vinyl alcohol) /poly (acrylonitrile) (PVA/PAN) composite membrane at 333 K. The *x*-axis is the mass fraction of ethanol(2) in the liquid feed mixture in the upstream compartment ω_2^L. The continuous solid lines are the F-H model calculations using the input data in Table S7. (b) Thermodynamic correction factors factors, Γ_{ij}, plotted as function of the mass fraction of ethanol(2) in the liquid feed mixture in the upstream compartment ω_2^L. (c) Ratios of the elements of thermodynamic correction factors, $\Gamma_{12}/\Gamma_{11}, \Gamma_{21}/\Gamma_{22}$ as function of the mass fraction of ethanol (2) in the liquid feed mixture in the upstream compartment ω_2^L.

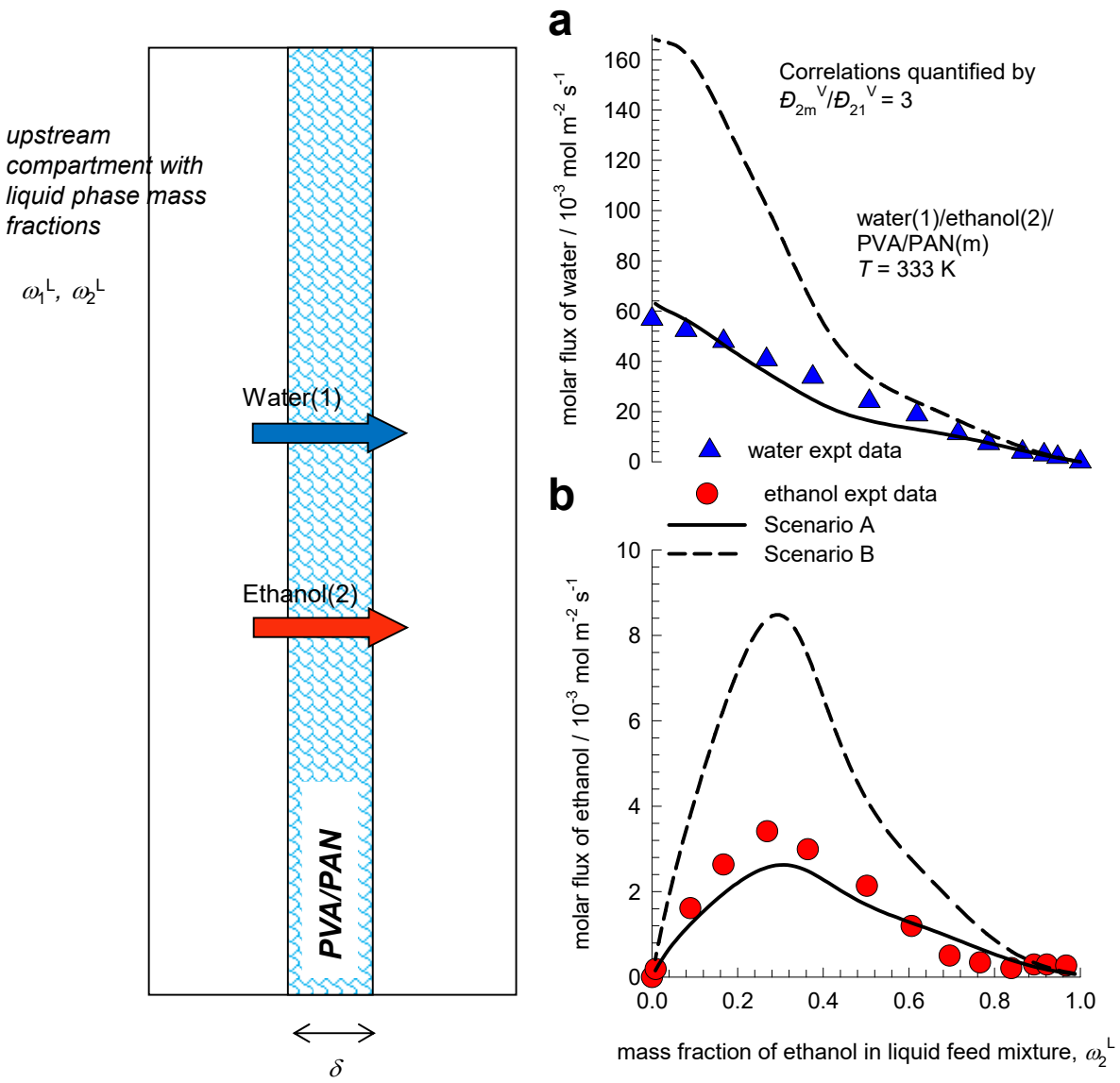

Figure S13. (a, b) Pervaporation fluxes for permeation of water(1)/ethanol(2) mixtures across PVA/PAN composite membrane (m) at 333 K. The experimental data of Heintz and Stephan[25] are indicated by symbols. The continuous solid lines are flux calculations based on eq (S27); wherein the 1-2 friction is described by $Đ_{2m}^V / Đ_{21}^V = 3$. The dashed lines are flux calculations in which thermodynamic correction factors are ignored, i.e. $\Gamma_{ij} = \delta_{ij}$. The Flory-Huggins and diffusivity data are specified in Table S7.

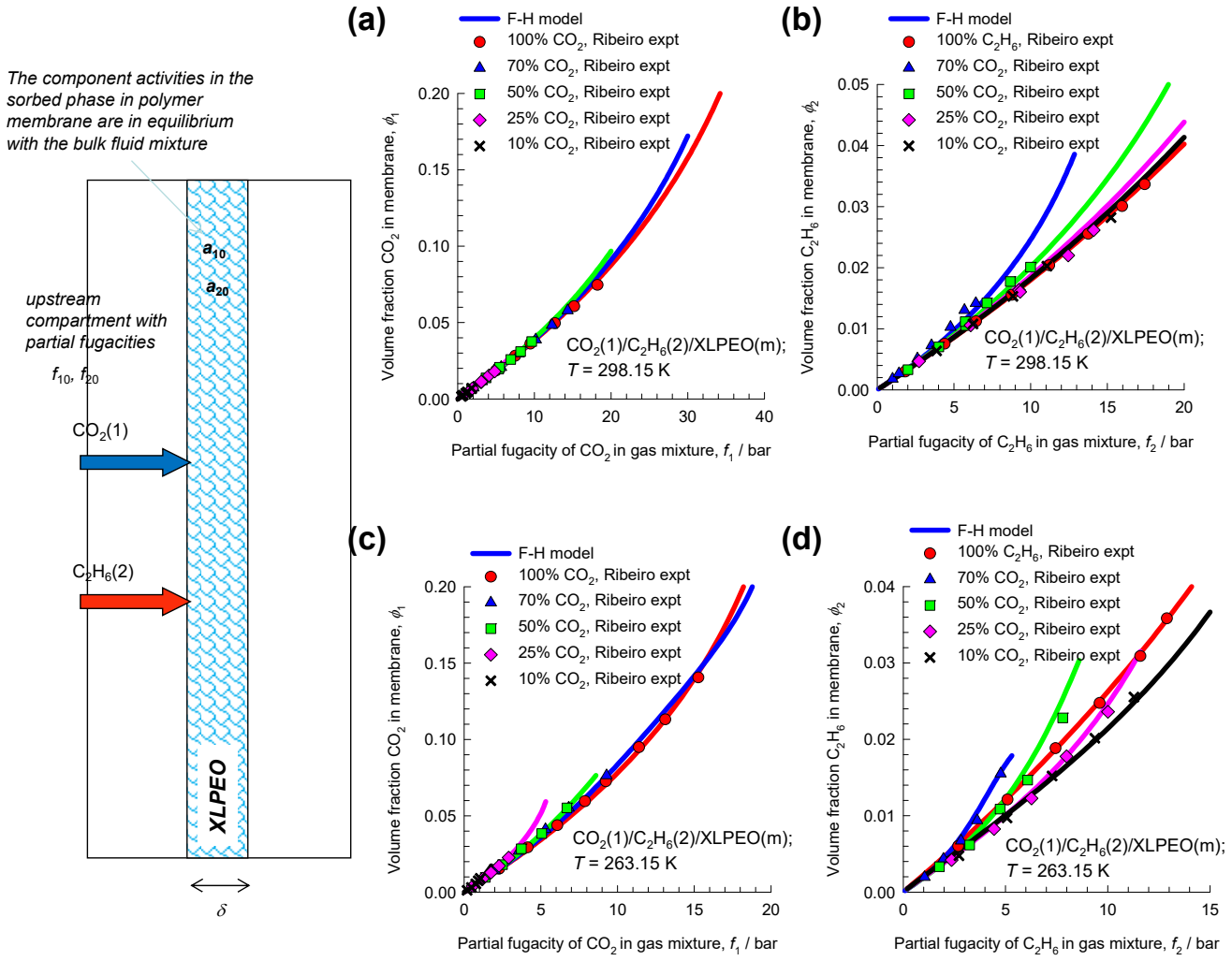

Figure S14. Calculations of the volume fractions of penetrants (a) CO_2 (1) and (b) C_2H_6 (2) in a cross-linked polyethylene oxide (XLPEO) membrane (m) at (a, b) 298.15 K, and (c, d) 263.15. The upstream face of the membrane is in equilibrium with CO_2/C_2H_6 mixtures of five different compositions. The experimental data (symbols) on mixed-gas sorption are those presented in Figures 5 and 6 of Ribeiro and Freeman.[26] The F-H data are summarized in Table S8, and Table S9. In these calculations, the ratio $\frac{\overline{V_1}}{V_m} = 0$, i.e. the molar volume of the penetrant is negligible in comparison to the molar volume of the polymer.

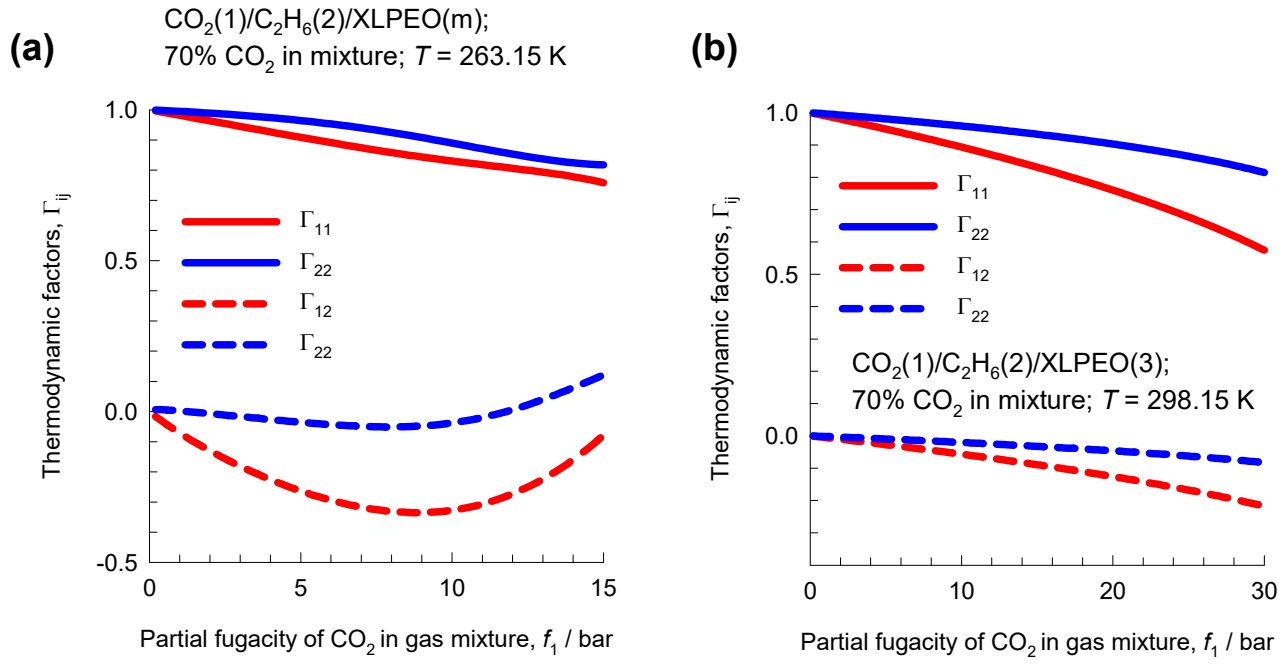

Figure S15. (a, b) Calculations of the elements of the matrix of thermodynamic factors for penetrants CO_2 (component 1) and C_2H_6 (Component 2) in a cross-linked polyethylene oxide (XLPEO) membrane (indicated by subscript m) at (a) 263.15 K, and (b) 298.15 K. The F-H data are summarized in Table S8, and Table S9.

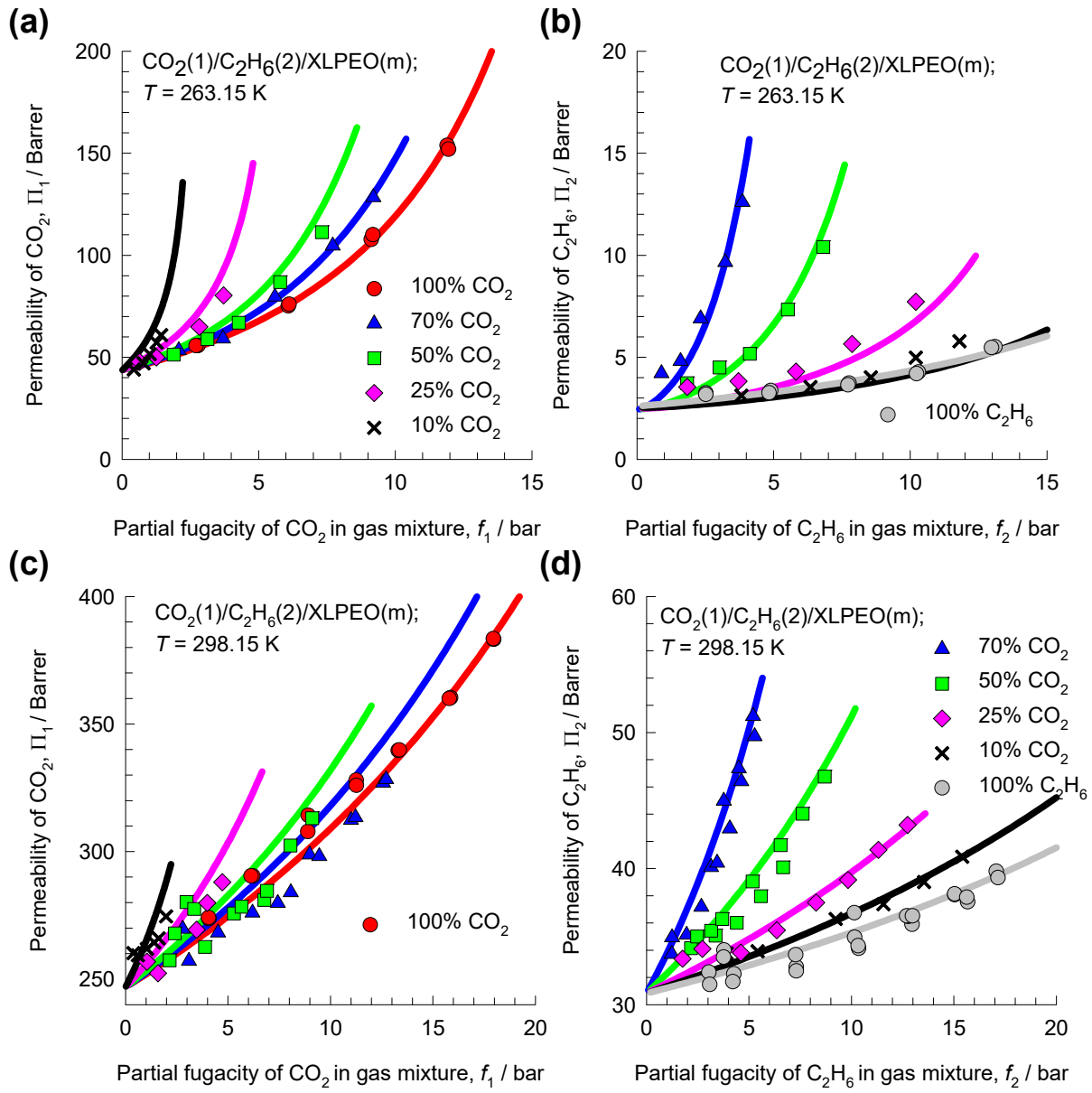

Figure S16. Membrane permeabilities, expressed in Barrers, of (a, c) $CO_2(1)$, and (b, d) $C_2H_6(2)$ for binary $CO_2(1)/C_2H_6(2)$ mixture permeation across a cross-linked polyethylene oxide (XLPEO) membrane at (a, b) 263.15 K, (c, d) 298.15 K. The *x*-axis represents the partial fugacity of (a, c) $CO_2(1)$, and (b, d) $C_2H_6(2)$ in the bulk gas phase in the upstream compartment. The experimental data (symbols) on component permeabilities are those presented in Figures 2, 4, and 5 of Ribeiro et al.[27] The continuous solid lines are the the linearized M-S model predications in which the 1-2 friction is described by $Đ_{2m}^{V} / Đ_{21}^{V} = 4$. The F-H and diffusivity data are summarized in Table S8, and Table S9.

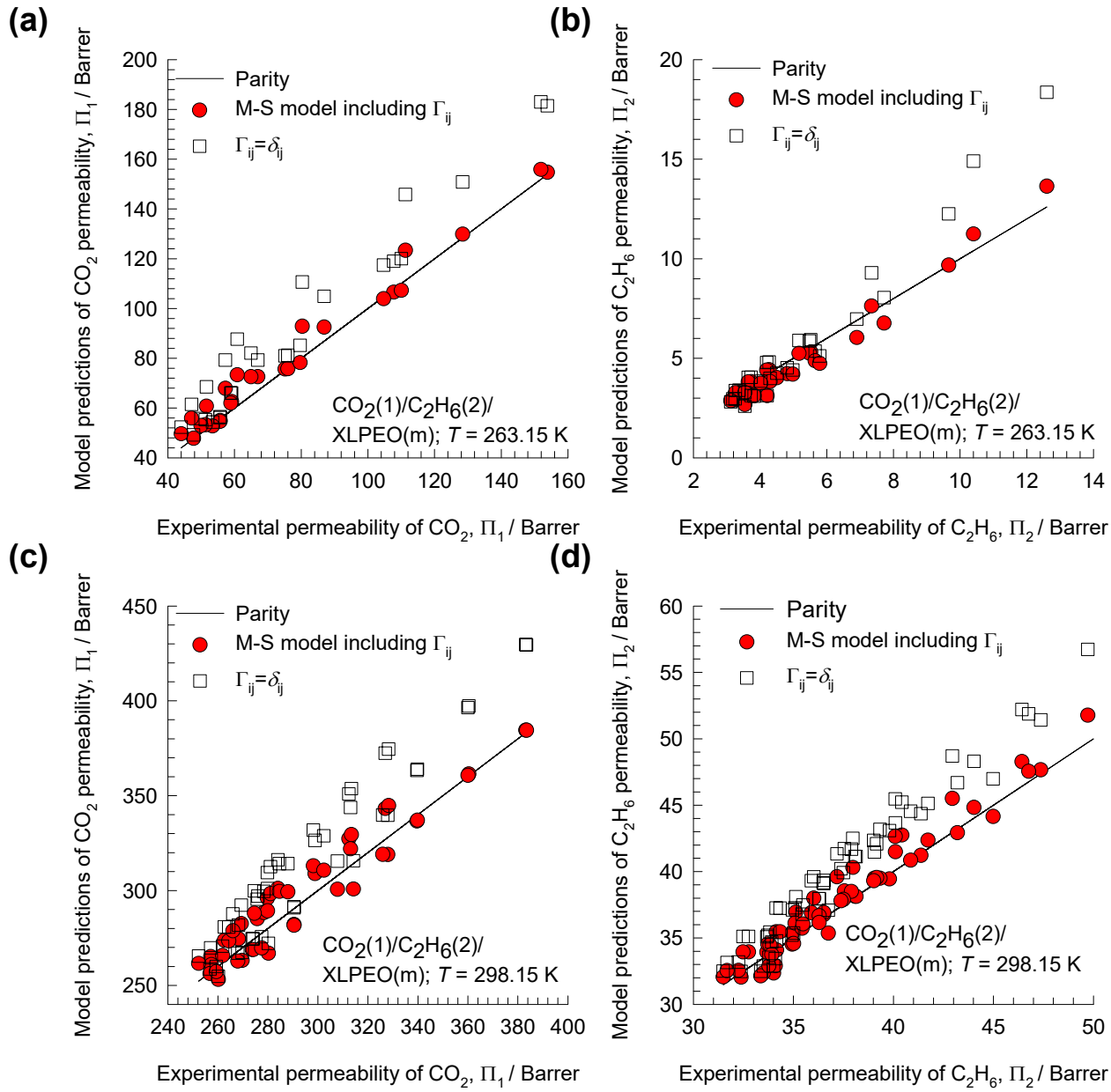

Figure S17. Parity plots comparisons of the experimental data on membrane permeabilities reported by Ribeiro et al.[27] of (a, c) CO_2, and (b, d) C_2H_6 for binary CO_2/C_2H_6 mixture permeation across cross-linked polyethylene oxide (XLPEO) membrane at (a, b) 263.15 K, (c, d) 298.15 K with the model predictions using the linearized M-S model (indicated by red circles) in which the 1-2 friction is described by $Đ_{2m}^{V}/Đ_{21}^{V}=4$. The open squares are the M-S calculations in which the thermodynamic correction factors are ignored, i.e. i.e. $\Gamma_{ij}=\delta_{ij}$. The F-H and diffusivity data are summarized in Table S8, and Table S9.

5 Nomenclature

Latin alphabet

a_i	activity of species *i*, dimensionless
$[B]$	Square matrix containing M-S diffusivities, m^{-2} s
c_i	molar concentration of species *i*, mol m^{-3}
$Đ_{ij}$	M-S diffusivity for binary pair *i-j*, m^2 s^{-1}
$Đ_{ij}^V$	modified M-S diffusivity for binary penetrant pair *i-j*, m^2 s^{-1}
$Đ_{im}^V$	modified M-S diffusivity for penetrant *i* in polymer m, m^2 s^{-1}
f_i	partial fugacity of species *i*, Pa
$f_{i,sat}$	saturation fugacity of species *i*, Pa
$[I]$	Identity matrix with elements δ_{ij}, dimensionless
m	refers to polymer membrane (= species n+1), dimensionless
M_i	molar mass of species *i*, kg mol^{-1}
$\overline{M}$	mean molar mass of mixture, kg mol^{-1}
N_i^{molar}	molar flux of species *i*, mol m^{-2} s^{-1}
N_i^{mass}	molar flux of species *i*, kg m^{-2} s^{-1}
N_i^V	volumetric flux of species *i*, m^3 m^{-2} s^{-1}
n	number of penetrants, dimensionless
p_i	partial pressure of species *i*, Pa
R	gas constant, 8.314 J mol^{-1} K^{-1}
T	absolute temperature, K
$u_2^L = \frac{\phi_2^L}{\phi_1^L + \phi_2^L}$	relative volume fractions in bulk liquid mixture, dimensionless

Nomenclature

$u_2 = \frac{\phi_2}{\phi_1 + \phi_2}$ relative volume fractions in polymer phase, dimensionless

u_i velocity of motion of *i*, m s^{-1}

$\overline{V_i}$ partial molar volume of species *i,* m^3 mol^{-1}

$\overline{V}$ molar volume of mixture*,* m^3 mol^{-1}

z distance coordinate along membrane thickness, m

Greek alphabet

Γ_{ij} thermodynamic factors, dimensionless

$[\Gamma]$ matrix of thermodynamic factors, dimensionless

δ thickness of membrane, m

δ_{ij} Kronecker delta, dimensionless

ε_{ij} plasticization coefficient, dimensionless

$[\Lambda]$ matrix of Maxwell-Stefan diffusivities, m^2 s^{-1}

μ_i molar chemical potential, J mol^{-1}

ϕ_i volume fraction of penetrant *i* in polymer, dimensionless

ϕ_i^L volume fraction in bulk liquid mixture, dimensionless

Π_i permeability of species *i* for polymer membrane, mol m m^{-2} s^{-1} Pa^{-1}

ρ_i mass density of component *i*, kg m^{-3}

χ interaction parameter in Flory-Huggins model, dimensionless

ω_i mass fraction of component *i*, dimensionless

ω_i^L mass fraction of component *i* in liquid phase feed mixture, dimensionless

Subscripts

Nomenclature

i	referring to penetrant *i*
m	referring to membrane
0	upstream face of membrane, $z = 0$
δ	upstream face of membrane, $z = \delta$

Superscripts

V	referring to use of volume fractions

6 References

(1) PTC MathCad 15.0. http://www.ptc.com/, PTC Corporate Headquarters, Needham, 3 November 2015.

(2) Wesselingh, J. A.; Krishna, R. *Mass transfer in multicomponent mixtures*. VSSD: Delft, 2000.

(3) Ribeiro, C. P.; Freeman, B. D. Sorption, Dilation, and Partial Molar Volumes of Carbon Dioxide and Ethane in Cross-Linked Poly(ethylene oxide). *Macromolecules* **2008**, *41*, 9458-9468.

(4) Ribeiro, C. P.; Freeman, B. D. Solubility and Partial Molar Volume of Carbon Dioxide and Ethane in Crosslinked Poly(ethylene oxide) Copolymer. *J. Polym. Sci.: Part B: Polym. Phys.* **2010**, *41*, 9458-9468.

(5) Mulder, M. H. V.; Franken, A. C. M.; Smolders, C. A. Preferential Sorpton versus Preferential Permeability in Pervaporation. *J. Membr. Sci.* **1985**, *22*, 155-178.

(6) Yang, T.-H.; Lue, S. J. Modeling Sorption Behavior for Ethanol/Water Mixtures in a Cross-linked Polydimethylsiloxane Membrane Using the Flory-Huggins Equation. *J. Macromol. Sci., Part B: Phys* **2013**, *52*, 1009-1029.

(7) Varady, M. J.; Pearl, T. P.; Stevenson, S. M.; Mantooth, B. A. Decontamination of VX from Silicone: Characterization of Multicomponent Diffusion Effects. *Ind. Eng. Chem. Res.* **2016**, *55*, 3139-3149.

(8) Hietaharju, J.; Kangas, J.; Tanskanen, J. Analysis of the permeation behavior of ethanol/water mixtures through a polydimethylsiloxane (PDMS) membrane in pervaporation and vapor permeation conditions. *Sep. Purif. Technol.* **2019**, *227*, 115738. https://doi.org/10.1016/j.seppur.2019.115738.

(9) Ribeiro, C. P.; Freeman, B. D.; Paul, D. R. Modeling of Multicomponent Mass Transfer across Polymer Films using a Thermodynamically Consistent Formulation of the Maxwell-Stefan Equations in terms of Volume Fractions. *Polymer* **2011**, *52*, 3970-3983.

(10) Fornasiero, F.; Prausnitz, J. M.; Radke, C. J. Multicomponent Diffusion in Highly Asymmetric Systems. An Extended Maxwell-Stefan Model for Starkly Different-Sized, Segment-Accessible Chain Molecules. *Macromolecules* **2005**, *38*, 1364-1370.

(11) Shao, P.; Huang, R. Y. M. Polymeric membrane pervaporation. *J. Membr. Sci.* **2007**, *287*, 162-179. https://doi.org/10.1016/j.memsci.2006.10.043.

(12) Vignes, A. Diffusion in binary solutions. *Ind. Eng. Chem. Fundamentals* **1966**, *5*, 189-199.

(13) Krishna, R. Describing Mixture Permeation across Polymeric Membranes by a Combination of Maxwell-Stefan and Flory-Huggins Models. *Polymer* **2016**, *103*, 124-131.

(14) Krishna, R. Using the Maxwell-Stefan formulation for Highlighting the Influence of Interspecies (1-2) Friction on Binary Mixture Permeation across Microporous and Polymeric Membranes. *J. Membr. Sci.* **2017**, *540*, 261-276. https://doi.org/10.1016/j.memsci.2017.06.062.

(15) Mulder, M. H. V.; Smolders, C. A. On the Mechanism of Separation of Ethanol/Water Mixtures by Pervaporation. I. Calculation of Concentration Profiles *J. Membr. Sci.* **1984**, *17*, 289-307.

(16) Mulder, M. H. V.; Franken, A. C. M.; Smolders, C. A. On the Mechanism of Separation of Ethanol/Water Mixtures by Pervaporation. II. Experimental Concentration Profiles *J. Membr. Sci.* **1985**, *22*, 41-58.

References

(17) Yang, T.-H.; Lue, S. J. Coupled concentration-dependent diffusivities of ethanol/water mixture sthrough a polymericmembrane:Effect on pervaporative flux and diffusivity profiles. *J. Membr. Sci.* **2013**, *443*, 1-9. https://doi.org/10.1016/j.memsci.2013.05.002.

(18) Nasiri, H.; Aroujalian, A. A Novel Model Based on Cluster Formation for Pervaporation Separation of Polar Components from Aqueous Solutions. *Sep. Purif. Technol.* **2010**, *72*, 13-21.

(19) Favre, E.; Schaetzel, P.; Nguygen, Q. T.; Clément, R.; Néel, J. Sorption, diffusion and vapor permeation of various penetrants through dense poly (dimethylsiloxane) membranes: a transport analysis. *J. Membr. Sci.* **1994**, *92*, 169-184.

(20) Krishna, R.; van Baten, J. M. Hydrogen Bonding Effects in Adsorption of Water-alcohol Mixtures in Zeolites and the Consequences for the Characteristics of the Maxwell-Stefan Diffusivities. *Langmuir* **2010**, *26*, 10854-10867.

(21) Krishna, R.; van Baten, J. M. Highlighting Pitfalls in the Maxwell-Stefan Modeling of Water-Alcohol Mixture Permeation across Pervaporation Membranes. *J. Membr. Sci.* **2010**, *360*, 476-482.

(22) Krishna, R.; van Baten, J. M. Mutual slowing-down effects in mixture diffusion in zeolites. *J. Phys. Chem. C* **2010**, *114*, 13154-13156.

(23) Ni, X.; Sun, X.; Ceng, D. Coupled Diffusion of Water and Ethanol in a Polyimide Membrane. *Polymer Eng. Sci.* **2001**, *41*, 1440-1447.

(24) Heintz, A.; Stephan, W. A generalized solution-diffusion model of the pervaporation process through composite membranes Part I. Prediction of mixture solubilities in the dense active layer using the UNIQUAC model. *J. Membr. Sci.* **1994**, *89*, 143-151.

(25) Heintz, A.; Stephan, W. A generalized solution-diffusion model of the pervaporation process through composite membranes Part II. Concentration polarization, coupled diffusion and the influence of the porous support layer. *J. Membr. Sci.* **1994**, *89*, 153-169.

(26) Ribeiro, C. P.; Freeman, B. D. Carbon Dioxide/ethane Mixed-gas Sorption and Dilation in a Cross-linked Poly(ethylene oxide) Copolymer. *Polymer* **2010**, *51*, 1156-1158.

(27) Ribeiro, C. P.; Freeman, B. D.; Paul, D. R. Pure- and Mixed-Gas Carbon Dioxide/Ethane Permeability and Diffusivity in a Cross-linked Poly(ethylene oxide) Copolymer. *J. Membr. Sci.* **2011**, *377*, 110-123.